

**EFFECTS ON RHEOLOGY AND HYDRATION OF THE ADDITION OF  
CELLULOSE NANOCRYSTALS (CNC) IN PORTLAND CEMENT  
PASTES**

by

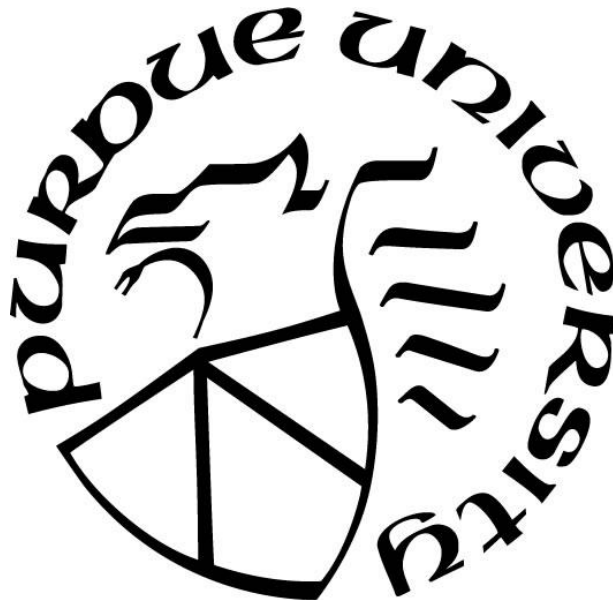
**Francisco Javier Montes Montejo**

**A Dissertation**

*Submitted to the Faculty of Purdue University*

*In Partial Fulfillment of the Requirements for the degree of*

**Doctor of Philosophy**



School of Materials Engineering

West Lafayette, Indiana

May 2019

**THE PURDUE UNIVERSITY GRADUATE SCHOOL**  
**STATEMENT OF COMMITTEE APPROVAL**

Prof. Jeffrey P. Youngblood, Chair

School of Materials Engineering

Prof. Kendra A. Erk

School of Materials Engineering

Prof. Carlos J. Martinez

School of Materials Engineering

Prof. Kevin P. Trumble

School of Materials Engineering

**Approved by:**

Prof. David F. Bahr

Head of the Graduate Program

*On the brink of her 100th birthday, I dedicate this work to my  
grandmother as a small token of gratitude to all those  
cheerful moments, life lessons, shows of character, and all  
the love a human being is capable to give.*

*Gracias por todo Lita.*

## ACKNOWLEDGMENTS

I would like to thank my advisor, Prof. Jeffrey Youngblood, my professors Kendra Erk, Rodney Trice, Kevin Trumble, Carlos Martinez, John Howarter, Carol Handwerker, David Bahr, and my colleagues Reaz Choudhury, Shikha Shrestha, Yvette Valadez, Miran Mavlan, Reza Moini. I also want to thank my collaborators Tengfei Fu, Jason Weiss, Sean McAlpine and Alan Rudie.

This work would not have been possible without the support of my professors, and staff from the School of Materials Science and Engineering. I appreciate all your guidance, all your patience, kindness and the timely scolding.

This work was funded by diverse projects, the US Endowment for Forestry and Communities Grant P3-1, the National Science Foundation Scalable Nanomanufacturing program under award CMMI-1449358, and the National Council of Science and Technology from Mexico through the scholarship No. 382254.

And last but not least, I'd like to express my most sincere gratitude to my family and friends, and specially to my girlfriend Bere, my confident, my shenanigans partner, my crying pillow, my driving force.

## TABLE OF CONTENTS

LIST OF TABLES .....	8
LIST OF FIGURES .....	9
ABSTRACT .....	13
1. INTRODUCTION .....	15
1.1 Cellulose as a Sustainable Additive .....	16
1.2 CNC-Cement Interactions. Mechanism of the Observed Effects. ....	17
1.2.1 Rheological Behavior .....	18
1.2.2 Hydration Improvement and Delay .....	20
1.3 This Work Contributions .....	20
1.3.1 Workability .....	21
1.3.2 Impurities detection and purification.....	22
1.3.3 Effects on Cement Hydration of Washed CNC .....	23
1.4 Orphan Results .....	24
2. RHEOLOGICAL IMPACT OF USING CELLULOSE NANOCRYSTALS (CNCS) IN CEMENT PASTES.....	25
2.1 Introduction.....	25
2.2 Materials and Experimental methods .....	26
2.2.1 Materials .....	26
2.2.2 Paste Preparation .....	30
2.2.3 Rheometer Setup, Procedure and Analysis .....	31
2.3 Results and Discussion .....	35
2.3.1 Rheometry of Type V cement at w/c 0.35 .....	35
2.3.2 Rheometry of CNC1 with Type I/II and Type V cement .....	40
2.3.2.1 Overall Yield Stress .....	47
2.3.2.2 Maximum yield stress reduction .....	49
2.3.2.3 Yield stress increases at high dosages .....	50
2.3.3 Using CNC as a cement additive.....	51
2.4 Conclusions.....	54

3. THE PRESENCE OF OLIGOSACCHARIDES AND DERIVATIVE IMPURITIES IN CELLULOSE NANOCRYSTALS.....	56
3.1 Introduction.....	56
3.2 Experiments and materials.....	58
3.2.1 CNC Materials.....	58
3.2.2 Experiments.....	60
3.2.2.1 Ultrafiltration.....	60
3.2.2.2 Cyclic Voltammetry.....	60
3.2.2.3 Anthrone Assay.....	60
3.2.2.4 Bicinchoninic Acid Assay.....	61
3.2.2.5 HPLC Analysis.....	61
3.2.2.6 MALDI-MS and TOF.....	62
3.3 Results and Discussion.....	62
3.3.1 Reducing ends.....	62
3.3.2 Total amount of foreign sugar- like species in CNC samples.....	63
3.3.3 The amount of reducing sugars in CNC samples.....	66
3.3.4 Identification of different types of sugar molecules.....	69
3.3.5 How washable are the impurities.....	74
3.3.6 What can we know about the impurities in CNC slurries.....	76
3.4 Conclusions.....	78
4. RETARDATION EFFECTS OF CELLULOSE NANOCRYSTALS (CNC) IN PORTLAND CEMENT PASTES.....	79
4.1 Introduction.....	79
4.2 Experimental and Materials.....	80
4.2.1 CNC and Cement.....	80
4.2.2 Experiments.....	81
4.2.2.1 Ultra-filtration and sugar detection.....	81
4.2.2.2 Paste Preparation.....	82
4.2.2.3 Isothermal Calorimetry.....	82
4.3 Results and Discussion.....	83
4.3.1 Anthrone Assays.....	83

4.3.2 Isothermal Calorimetry .....	84
4.4 Conclusions .....	94
5. CELLULOSE NANOCRYSTALS CHARACTERIZATION .....	96
5.1.1 Size Distributions .....	96
5.1.2 Turbidity .....	106
5.1.3 Crystallinity .....	107
APPENDIX .....	115
REFERENCES .....	127
VITA .....	136

## LIST OF TABLES

Table 2-1. Ordinary Portland Cements Oxide Contents and Chemical Compositions .....	26
Table 2-2. CNC average length and aspect ratio (Length/Diameter), and Zeta potential at pH of 13 .....	28
Table 2-3. Cement pastes with CNC1 addition maximum stress reduction dosages and magnitudes. ....	47
Table 3-1. Results of the BCA reducing end analysis. Values in the last columns were calculated under the assumption that every reducing end detected, is from a monosaccharide. ..	67
Table 3-2. Information obtained in this work.....	77
Table 4-1. New CNC wt% of the washed slurries. ....	88
Table 4-2. Resulting dosages from purified slurries (when used as the original wt% to get a 1% by volume of cement). ....	88
Table 4-3. Heat release peak retardation of pastes made with 0.36 w/c and CNC. Values in Delayed column are from neat paste for Unwashed materials and from the Unwashed CNC for the washed ones. Bold blue numbers are the calculated delay increments using the values from Table 4-2 and the trend calculated in Figure 4-4.....	92
Table 4-4. Heat release peak retardation of pastes made with 0.35 w/c and CNC. Values in Delayed column are from neat paste for Unwashed materials and from the Unwashed CNC for the washed ones.....	94
Table 5-1. Crystallinity index of CNC films. ....	109
Table A-1. Total heat of hydration by the end of the isothermal calorimetry measurements. ....	126

## LIST OF FIGURES

Figure 1-1. Representation of the four stages of the addition of CNC to cement paste: a) No CNC added (original yield stress), b) Positive regions CNC saturated (minimum yield stress), c) CNC start forming aggregates of their own (yield stress increases), and d) Excessive CNC (abrupt yield stress increment).....	19
Figure 2-1. Sample of all the TEM micrographs of all nine CNCs used in this study. ....	29
Figure 2-2. Scaled representation of cement particles and CNC. ....	30
Figure 2-3. 3D Illustration of the rheometer serrated parallel plates, rotary plate 40mm diameter, ABS cover and inner sponge to preserve humidity, 1mm gap. ....	31
Figure 2-4. Stress strain measurements showing different slope changes at different CNC dosages. Blue markers are within minimum and maximum shear rates (0.1 – 100 s <sup>-1</sup> ), range considered for the linear regression (red line) to determine Yield Stress...34	34
Figure 2-5. Changes in yield stress of Type V paste at a w/c of 0.35 with different CNCs. The values are normalized by the yield stress of plain paste (control, at unit value in vertical axis). Yield stress values of the control mixture had an average of 26 Pa with a standard deviation of 9.4 Pa. ....	36
Figure 2-6. The minimum yield stress achieved by each CNC in Type V pastes at a w/c of 0.35 as a function of (a) CNC zeta potential at pH 13, (b) Average CNC length, (c) Average crystal aspect ratio, and (d) Zeta potential divided by CNC length. Linear regressions are shown along with each coefficient of determination (R <sup>2</sup> ).....	38
Figure 2-7. Average yield stress of Type I/II cement pastes at different w/c versus CNC dosages. ....	41
Figure 2-8. Average yield stress of Type V cement pastes at different w/c versus CNC dosages	42
Figure 2-9. Yield stress changes of 0.30 w/c mixtures in a) absolute values and b) changes normalized by the control sample (0 % CNC).....	44
Figure 2-10. Yield stress changes of 0.35 w/c mixtures in a) absolute values and b) changes normalized by the control sample (0 % CNC).....	45
Figure 2-11. Yield stress changes of 0.4 w/c mixtures in a) absolute values and b) changes normalized by the control sample (0 % CNC).....	46

Figure 2-12. Zeta potential measurements of cement pastes diluted in DI water at a dilution factor of 300.....	48
Figure 2-13. Maximum normalized yield stress reduction obtained at each w/c. ....	50
Figure 2-14. Yield stresses of pastes made using Types a) I/II and b) V cement at different CNC1 dosages and three w/c.....	52
Figure 3-1. Four different scan rates to determine the Cyclic Voltammetry response of CNC1 filtrate. ....	63
Figure 3-2. Standard calibration for anthrone analysis. ....	64
Figure 3-3. Anthrone assay response of filtrates diluted at a dilution factor of 10. Sugar concentration are calculated using the base line form Figure 3-2.....	65
Figure 3-4. Sugar concentration measured by anthrone assay are compared with the Glucose concentration assumed by the BCA results. Dashed line fits the proportion of the total sugar rings detected and the sugar rings with a reducing end. Solid red line represents the 1:1 proportion of sugar rings and reducing ends. ....	68
Figure 3-5. Selected HPLC Results of CNC filtrates. Peaks with retention times similar to known molecules are indicated. Standard molecules and retention times are shown at the bottom right corner.....	71
Figure 3-6. MALDI results of all filtrates. Horizontal Lines signal common oligosaccharides molecular weights. Common ions are highlighted.....	72
Figure 3-7 MS/MS. Result from selected MALDI Ions. Dextrose is pointed out to show the proximity of the detected fragments to a single ring saccharide.....	73
Figure 3-8. Sugars detected by anthrone assay in CNCs washed 5 times with ultrasonication before every filtration. ....	75
Figure 4-1. Sugars detected by anthrone assay of 5 consecutive washes of CNC slurries. Samples were ultrasonicated and vortexed before every filtration. ....	84
Figure 4-2. Heat release rate of Type V cement pastes with CNC1 addition. Pastes made using 0.36 w/c and 1% by volume CNC as acquired, washed 1 time and washed 5 times. 86	
Figure 4-3. Heat release rate of Type V cement pastes with CNC2 addition. Pastes made using 0.36 w/c and 1% by volume CNC as acquired, washed 1 time and washed 5 times. 87	
Figure 4-4. Relationship between CNC1 dosage and hydration peak delay, from the work of Fu et al.[33].....	89

Figure 4-5. Heat release rate of Type V cement pastes with CNC3 addition. Pastes made using 0.36 w/c and 1% by volume CNC as acquired, washed 1 time and washed 5 times.	90
Figure 4-6. Heat release rate of Type V cement pastes with CNC3 addition. Pastes made using 0.36 w/c and 0.2% by volume CNC as acquired, washed 1 time and washed 5 times. .....	91
Figure 4-7. Heat release rate of Type V cement pastes with CNC3 and CNC4 addition. Pastes made using 0.35 w/c and 0.2% by volume CNC4 as acquired, washed 1 time and washed 5 times. ....	93
Figure 5-1. TEM image of CNC1. ....	97
Figure 5-2. Length distribution of CNC1. Average Length of $92.7 \pm 48.3$ nm, average width of $7.1 \pm 4$ nm, for an aspect ratio of $13 \pm 5.9$ .....	97
Figure 5-3. TEM image of CNC2. ....	98
Figure 5-4. Length distribution of CNC2. Average Length of $127.4 \pm 34.4$ nm, average width of $9.5 \pm 2.6$ nm, for an aspect ratio of $14.5 \pm 6$ .....	98
Figure 5-5. TEM image of CNC3. ....	99
Figure 5-6. . Length distribution of CNC3. Average Length of $964.5 \pm 381.8$ nm, average width of $28.5 \pm 9.5$ nm, for an aspect ratio of $46 \pm 48.2$ .....	99
Figure 5-7. TEM image of CNC4 .....	100
Figure 5-8 . Length distribution of CNC4. Average Length of $97.2 \pm 48.3$ nm, average width of $6.7 \pm 3.2$ nm, for an aspect ratio of $15 \pm 4.7$ .....	100
Figure 5-9. TEM image of CNC5. ....	101
Figure 5-10 . Length distribution of CNC5. Average Length of $83.4 \pm 28.4$ nm, average width of $7.6 \pm 2.4$ nm, for an aspect ratio of $12.3 \pm 6.1$ .....	101
Figure 5-11. TEM image of CNC6. ....	102
Figure 5-12 . Length distribution of CNC6. Average Length of $89 \pm 26.7$ nm, average width of $8.2 \pm 2.7$ nm, for an aspect ratio of $11.8 \pm 6.8$ .....	102
Figure 5-13. TEM image of CNC7. ....	103
Figure 5-14 . Length distribution of CNC7. Average Length of $84.8 \pm 22.6$ nm, average width of $8.5 \pm 2.3$ nm, for an aspect ratio of $10.7 \pm 4.5$ .....	103
Figure 5-15. TEM image of CNC8. ....	104

Figure 5-16 . Length distribution of CNC8. Average Length of $184 \pm 51.7$ nm, average width of $13.8 \pm 4.6$ nm, for an aspect ratio of $15 \pm 6.7$ .	104
Figure 5-17. TEM image of CNC9.	105
Figure 5-18 . Length distribution of CNC9. Average Length of $155.9 \pm 39.9$ nm, average width of $10.1 \pm 1.7$ nm, for an aspect ratio of $16.4 \pm 5.5$ .	105
Figure 5-19. CNC lengths and widths with error bars.	106
Figure 5-20. Turbidity of CNC 2wt% aqueous suspensions measured by transmittance %.	107
Figure 5-21. X-ray diffraction of CNC1 film.	110
Figure 5-22. X-ray diffraction of CNC2 film.	110
Figure 5-23. X-ray diffraction of CNC3 film.	111
Figure 5-24. X-ray diffraction of CNC4 film.	111
Figure 5-25. X-ray diffraction of CNC5 film.	112
Figure 5-26. X-ray diffraction of CNC6 film.	112
Figure 5-27. X-ray diffraction of CNC7 film.	113
Figure 5-28. X-ray diffraction of CNC8 film.	113
Figure 5-29. X-ray diffraction of CNC9 film.	114
Figure A-1. Yield stresses of cement pastes made using Type V cement at a 0.24 w/c at different additions of Plasticizers.	118
Figure A-2. Yield Stresses of Pastes made using Type V cement at a 0.24 w/c, CNC addition and Plasticizer.	119
Figure A-3. Yield Stresses of Pastes made using Type I/II cement at a 0.36 w/c, CNC addition and 144 mL/100 kg of Plasticizer.	120
Figure A-4. Yield Stresses of Pastes made using Type III cement at a 0.36 w/c, CNC addition and 144 mL/100 kg plasticizer.	121
Figure A-5. HPLC results from CNC1 and CNC4 filtrates	122
Figure A-6. HPLC results from CNC3 and CNC5 filtrates	123
Figure A-7. HPLC results from CNC6 and CNC8 filtrates	124
Figure A-8. HPLC results from CNC7 and CNC9 filtrates	125

## ABSTRACT

Author: Montes Montejó, Francisco Javier. PhD  
Institution: Purdue University  
Degree Received: May 2019  
Title: Effects on Rheology and Hydration of the Addition of Cellulose Nanocrystals (CNC) in Portland Cement Pastes.  
Committee Chair: Prof. Jeffrey Youngblood

Cellulose Nanocrystals have been used in a wide range of applications including cement composites as a strength enhancer. This work analyses the use of CNC from several sources and production methods, and their effects on rheology and hydration of pastes made using different cement types with different compositions. Cement Types I/II and V were used to prepare pastes with different water to cement ratios (w/c) and measure the changes in rheology upon CNC addition. The presence of tricalcium aluminate (cement chemistry denotes as  $C_3A$ ) made a difference in the magnitude of CNC effects. At dosages under 0.5vol% to dry cement, CNC reduced the yield stress up to 50% the control value. Pastes with more  $C_3A$  reduced yield stress over a wider range of CNC dosages. CNC also increased yield stress of pastes with dosages above 0.5%, twice the control value for pastes with high  $C_3A$  content at 1.5% CNC and up to 20 times for pastes without  $C_3A$  at the same dosage.

All the CNCs used were characterized in length, aspect ratio, and zeta potential to identify a definitive factor that governs the effect in the rheology of cement pastes. However, no definitive evidence was found that any of these characteristics dominated the measured effects.

The CNC dosage at which the maximum yield stress reduction occurred increased with the amount of water used in the paste preparation, which provides evidence of the dominance of the water to cement ratio in the rheological impact of CNC.

Isothermal calorimetry showed that CNC cause concerning retardation effects in cement hydration. CNC slurries were then tested for sugars and other carbohydrates that could cause the aforementioned effect, then slurries were filtered, and impurities were detected in the filtrate, these impurities were quantified and characterized, however, the retardation appeared to be unaffected by the amount of the species detected, suggesting that the crystal chemistry, which is a consequence of the production method, is responsible of this retardation.

This work explores the benefits and drawbacks of the use of CNC in cement composites by individually approaching rheology and heat of hydration on a range of physical and chemical tests to build a better understanding of the observed effects.

Understanding the effect of CNCs on cement paste rheology can provide insights for future work of CNCs applications in cement composites.

## 1. INTRODUCTION

The performance of hydrated cement depends greatly on the water to cement ratio (w/c) used to make the paste, better properties of the final product like shrinkage, strength, impermeability and durability are mainly governed by the reduction of that parameter. However, using low w/c has a known drawback, which is the decrease in workability. As labor could be the most expensive part of cement and concrete projects and low workability can be a placement impediment, chemical admixtures are used to improve workability of low w/c ratios. Water Reducing Admixtures (WRA), or Plasticizers (PC), are defined by ASTM C125-18b[1] as a material that provides better flow performance to cement paste and concrete mixtures. Depending on the cement type and composition (pure Portland cement and with substituents), the effect of WRAs changes because the different interaction with the constituents [2], [3].

Cement particles are finely ground crystalline minerals, and thus attractive forces exist between surfaces, edges and corners, these forces are responsible of cement flocculation, flocs that entrain considerable amounts of water. Most commercial WRA are comb-like copolymers, negative charged polyacrylic acid (PAA) or polymethyl methacrylate (PMMA) backbones with grafted polyethylene oxide (PEO) chains[4], [5]. When WRAs are added to cement paste, because the mentioned attraction forces, the backbone chains are adsorbed to the cement particles surface, then grafted chains extend their hydroxide ends into the pore solution. By better dispersing the cement particles, more water is available in the cement mixture, increasing workability [3], [4], [6]–[8].

## 1.1 Cellulose as a Sustainable Additive

In the recent years, sustainability in the form of green solutions has been studied and developed for many applications, becoming a glamorous competitive advantage because of its lower environmental impact.

Cellulose the most abundant biodegradable and renewable biopolymer. Cellulose Nanocrystals (CNCs), or Nanocrystals from Cellulose (NCCs), are high aspect ratio (3-20 nm in width, 50-500 nm in length) needle-shaped whiskers of crystalline cellulose. CNCs have high stiffness[9], high strength[10], high thermal conductivity[11], low thermal expansion[12], and are nontoxic and renewable[10]. CNC are increasingly being used in a wide range of applications including nanocomposites[13], [14], metallic particle suspension[15], Pickering emulsion surfactants[16], and biological applications[17].

CNC are present in wood, plants, algae, and in bacterial[10]. To isolate CNC from the raw material, selective degradation of the amorphous compositions is performed by different methods (*e.g.*, acid hydrolysis)[10]. Size and aspect ratio strongly depend on the precursor used, and depending on the acid employed and the reaction parameters, the surface chemistry of the final product is affected by branches of the same acid nature[18]–[26].

For cementitious materials, cellulose based high molecular mass polymers (hydropropyl methylcellulose) had been studied as Viscosity Modifier Admixtures (VMA) along with traditional high range water reducing admixtures (polynaphthalene sulfonate and a polymelamine sulfonate) for cement grout, this combination showed to be not as convenient as HRWR alone in terms of grout workability, nor in the final product strength, porosity and speed of hydration[27]. Other cellulose based materials have been used as cement additives, such as VMAs [28], strengthening

admixtures [29], water retention admixtures [30] and water reducing admixtures [31], and set retarders[32].

Cao *et al.*[19] introduced nano-engineered cellulose as an additive to replace synthetic polymers as chemical admixtures for cement, showing advantages in workability[19] and strength[8]. Cao *et al.* [19] also reported the reduction of the yield stress of fresh paste, with a minimum yield stress at a dosage of 0.04 % CNC by volume of cement. In a subsequent study by Cao *et al.*[8], it showed that beyond a dosage of 1.35 %, the CNCs agglomerated in the cement paste, increasing the yield stress of the mixture. Recent studies, by Fu *et al.* [33], point to CNCs having a potential reinforcing effect in cement applications. Proper interaction between CNCs and cement particles can reduce micro-cracking and improves the degree of hydration [33], thereby significantly improving the mechanical properties of the system. Addition of as little as 0.2% CNC by volume of cement, can improve flexural strength up to 30% [33]. Moreover, the addition of CNC into cement mixtures improves the degree of hydration[33].

## **1.2 CNC-Cement Interactions. Mechanism of the Observed Effects.**

Cao *et al.*[19] used a combination of steric stabilization and short circuit diffusion mechanisms to respectively explain the increments in workability and hydration of cement paste, *i.e.* CNC would adhere to the cement surfaces and improve workability through the mitigation of electrostatic interactions between cement particles, and later, due their hydrophilic functionality, CNC would improve the transport of water through the high density CSH shell formed around the unhydrated cement.

Although Fu *et al.*[33] only made observations about the loss of workability at high dosages, the increments in hydration (and therefore strength) of cement pastes were explained through the CNC saturation of Aluminate phases (ettringite and monosulfate), as isothermal calorimetry revealed that, for dosages <1% CNC by volume of Type I/II cement, the increments in their hydration peaks were higher than those for the silicate phases. Also, at the highest dosages (2% CNC), the excess CNC could be adsorbed to the silicate phases, which yielded a higher hydration (portlandite content) at later ages. Both authors pointed out the delaying effect of CNC in the hydration of cement paste, and related the similar effect as with some commercial WRAs.

### **1.2.1 Rheological Behavior**

The interaction of cement pastes and different dosages of CNC could be explained from the observations made by Cao *et al.*[19] and Fu *et al.*[33] about the CNC being adsorbed to the surface of the cement particles. Figure 1-1 shows four different stages of CNC additions. In Figure 1-1(a) no CNC had been added, so the interactions between the negative (clear) and the positive (black) regions is not inhibited whatsoever, and at the volume fractions at which cement paste is usually prepared ( $>0.5$ ), the electrostatic interaction and the surface tension of the ground minerals will favor flocculation[34]. After CNC is added (Figure 1-1(b)), they start being adsorbed to the positive regions of the cement particle surface, thus reducing the strength of the cement surface interaction and favoring dispersivity. If CNC keep been added, they will keep adsorbing to the rest of the cement surface and even form aggregates of their own (Figure 1-1(c)), and the mixture will gradually lose the previously achieved workability. Beyond the dosage at which all cement surfaces are saturated (Figure 1-1 (d)), the CNC will form groups with themselves and even, aided

by the ionic content of the pore solution, could form gels[35], retaining water from the mixture and hindering its workability, just as it has been described by Cao *et al.*[19] and Fu *et al.*[33].

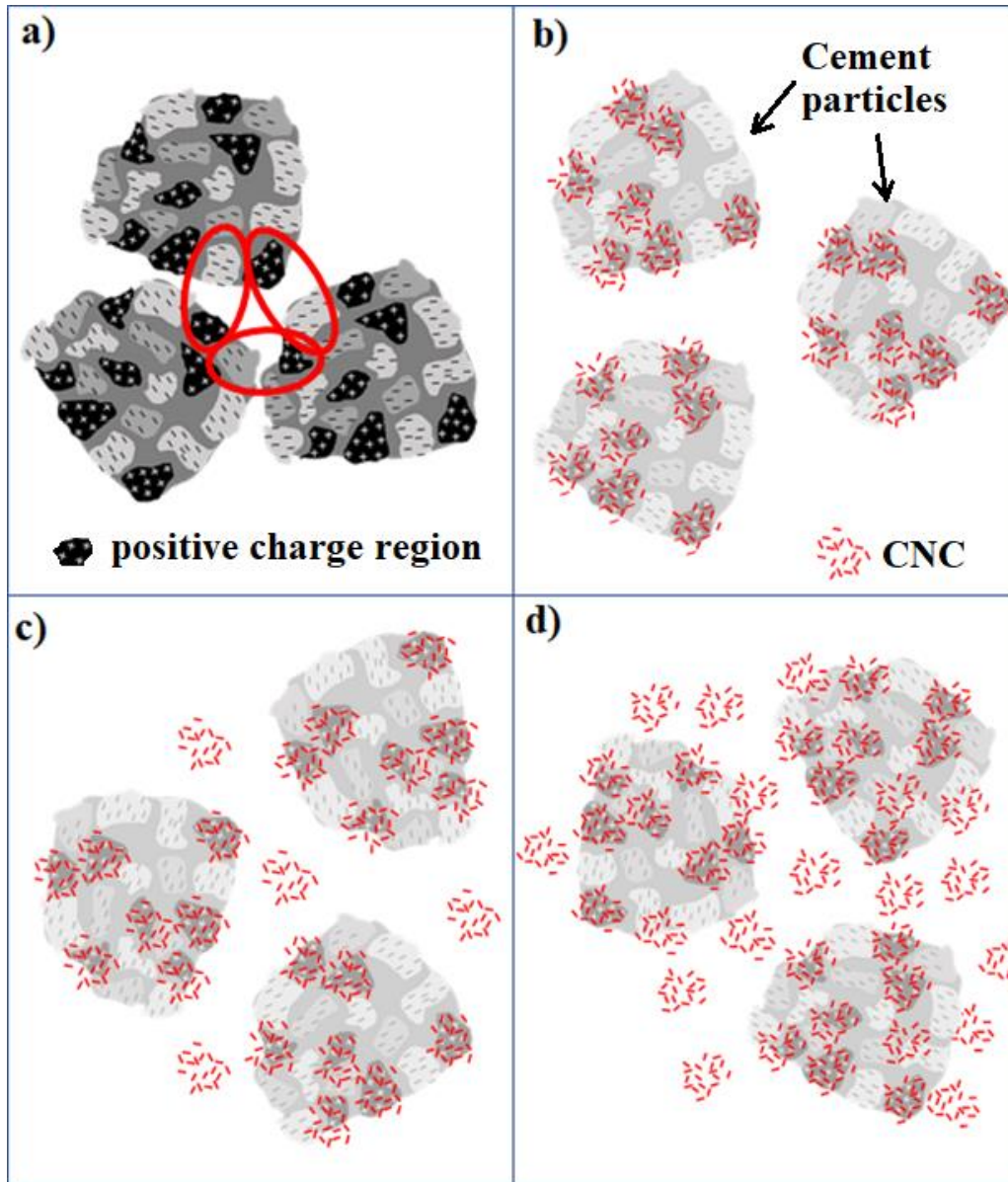


Figure 1-1. Representation of the four stages of the addition of CNC to cement paste: a) No CNC added (original yield stress), b) Positive regions CNC saturated (minimum yield stress), c) CNC start forming aggregates of their own (yield stress increases), and d) Excessive CNC (abrupt yield stress increment).

### **1.2.2 Hydration Improvement and Delay**

The other main observable effect described by the previously mentioned authors, is the improvement of the Degree of Hydration, which was measured by both, measuring the total heat of hydration using isothermal calorimetry, and the amount of portlandite (calcium hydroxide) in the cured paste using thermogravimetric analysis. It was previously mentioned how, through short circuit diffusion, CNC increase the degree of hydration. But even though the longer dormant period (hydration delay) was mentioned, it was only pointed out its similarity to the effects of a commercial WRA. Some cement components (aluminates and aluminoferrites) start hydrating at the very instant that come in contact with water, this is called the rapid heat release stage, followed by the dormant period, which takes from 2 to 5 hours. Almost no reactions occur during this period, but it is the preamble to the main stage of the hydration heat release, the accelerating stage[36]. There are different opinions of the purpose of the dormant period[37], but it is clear that its duration is extended when CNC are added. Similar effects have been documented when adding carbohydrates[38] and organic acids[39], and the presented explanation involves these components "poisoning" the nucleation of calcium silicate hydrates (CSH), which prevents (delays) the beginning of the accelerating stage[38], [40], [41].

### **1.3 This Work Contributions**

The conclusions of this work, will help to take better informed decisions while using CNC as cement additives, regarding: (1) the type of CNC to be used, (2) the amount of CNC to be added depending on the desired effect, and (3) the test and treatments to perform to the CNC slurry before being added to the cement paste.

The use of CNCs as a cement additive will prove to have more than one purpose, as well as drawbacks. In addition to the already described benefits in cement hydration, it was found that although small dosages of most CNCs can reduce the yield stress of cement pastes (like WRAs do), at the dosages at which FU *et al.*[33] found benefits in strength and hydration, CNC acted more like a VMA, which is also a desirable effect due its water retention capabilities[30], [42], [43].

Several techniques were used to characterize CNCs from different sources and manufacturers, and to understand the observed effects of the addition of CNC to cement pastes. These effects were mainly related to the rheological performance and the heat of hydration of the resulting cement pastes. The purity of the CNC slurries was also studied, and different aspects of the detected impurities, as well as methods proposed to quantify and evaluate them, as well as the practical impact of purifying the CNC.

Three drawbacks of using CNC as cement additives are also described: (1) The loss of workability at high CNC dosages ( $>0.5\%$ ), (2) the concerning delays that the use of certain CNC could have in the cement paste hydration, and (3) the improbability of identifying the exact type of sugar-like impurities in the slurries, which are also disregarded by the producers' purification methods and quality controls.

### **1.3.1 Workability**

The first chapter takes up the works of Cao *et al.*[19] and the materials used by Fu *et al.*[33]. All 9 different CNC were characterized and used as a rheological admixture. The addition of different CNCs to Type V cement paste, resulted in differences in the performance of the paste.

The characteristics of all the CNC were compared with their performance as rheological admixtures, but no strong evidence was found that suggested that any of the measured quantities were the governing factor. The CNC with the best performance was then added to cement pastes made using both cement Types V and I/II at three different water to cement ratios (w/c), and the rheological differences were compared. The w/c proved to be proportional to the CNC dosage at which the maximum yield stress reduction was observed for both cement types. Based on fundamental particle interactions. This work provides mechanistic explanations of the observed effects.

### **1.3.2 Impurities detection and purification**

In the following chapter, free sugars in the CNC slurries, as the impurities suspected of being the cause of the hydration delay effects observed by Fu et al.[33], were detected, quantified, and characterized. The amount of detected impurities could not be related to the time of hydration delay, however, they could be related to age and purification methods of different CNC batches. A series of mass analysis methods and results databases were used to narrow down the identity and nature of the impurities detected. Although a comprehensive characterization path was offered in order to detect a specific compound that could be of interest for the desired application, the obtained MS results of the impurities in the selected materials, yielded countless options of molecules, so the exact identification of them was not possible. Even so, ultra-sonication, ultrafiltration and anthrone assay were proposed as a quick and cheap technique to incorporate to the CNC production method in order to measure and reduce detect the amount of free sugars in the slurries.

### 1.3.3 Effects on Cement Hydration of Washed CNC

In order to evaluate the benefits of the purification method described, the following chapter analyzes, through Isothermal Calorimetry, the effects of washed CNC slurries on the hydration heat release of Type V cement paste. Four different CNCs were selected to be washed up to 5 times before being used at similar dosages as in the work of Fu *et al.*[33]. As concluded in the previous chapter, the results confirmed that the amount of detected impurities were not entirely responsible for the observed hydration delay. Out of the four CNC selected, two of them (the ones fabricated through acid hydrolysis), when used at a 1 % dosage, the delay in heat release was increased by minutes. It is believed that this difference is due the higher content of CNC in the slurry (as impurities were washed away).

The other two CNCs were selected because of being produced through oxidative degradation. One of these materials was the one that posed a concerning delay (In the work of Fu *et al.*[33]) on the hydration of Type V cement paste. These CNC, when used at a 0.2 % dosage, presented the opposite effect than the ones produced through acid hydrolysis as, when used after being washed 1 and 5 times, the hydration peak delay was reduced by hours. Nonetheless, when used at a 1 % dosage (unwashed, or washed), the paste still didn't set after a week. The oxidative process through which these two materials were produced, could most likely result in free carboxylic acids[10]. And for the yellowish look of one of them, residual lignin is also suspected. Both byproducts are known cement hydration retarders [44]–[47].

## 1.4 Orphan Results

During the time that this work was done, numerous techniques were used to characterize the CNCs by themselves and in related applications. And although some results did not fit into the chapters compiled here, this information has proven useful for other authors[48]. That is why the last chapter gathers these results along with some of the open-ended problems that they yielded, with the intention that they could be used in future work.

## 2. RHEOLOGICAL IMPACT OF USING CELLULOSE NANOCRYSTALS (CNCS) IN CEMENT PASTES

This work was made in collaboration with Drs. Tengfei Fu, Jason Weiss and Jeffrey Youngblood. My contributions were all the experimentation and first versions writing, the document was then edited collaboratively.

### 2.1 Introduction

This section focuses in expanding the existing knowledge on the effects of CNC in the rheological properties of cement pastes. It is already known, from the work of Cao *et al.*[19], that a particular CNC can be used as a cement plasticizer. However, the studies by Cao *et al.*[8] were performed using a CNC made from a single source of CNC at a fixed w/c. Little is known of the effects of CNC made using different raw material sources or different processing techniques. Further, little is known on how the cement composition impacts the performance of the fresh paste.

In this study, nine different CNCs and two types of cement powder were tested. The first part of this study uses the same w/c and cement type as that used by Cao *et al.*[19] to study the impact of nine different CNCs acquired from different manufacturers. These experiments are useful to identify how CNC characteristics influence cement paste rheology. The second part of this study consists of experiments conducted with one CNC added to Type V and Type I/II cement pastes at three different w/c (0.30, 0.35, and, 0.40) to assess the influence of cement and paste composition. Finally, one CNC was selected to be tested for a range of dosages (control-0%, 0.023%, 0.052%, 0.12%, 0.275%, 0.631%, 1.445%, and, 3.311%). The main questions that this work will seek to answer are:

- Will the CNC manufacturing process and source impact cement paste rheology?
- What characteristics of CNC have the most significant impact on cement paste rheology?
- How does the cement composition influences performance of cement paste with CNC?
- How does the change in w/c affect the rheological behavior?

## 2.2 Materials and Experimental methods

### 2.2.1 Materials

One Type V cement and one Type I/II ordinary portland cement were used. The oxide contents and chemical composition are shown in Table 2-1.

Table 2-1. Ordinary Portland Cements Oxide Contents and Chemical Compositions

Components	Percent by mass (%)	
	Type I/II	Type V
SiO <sub>2</sub>	20.1	21.3
Al <sub>2</sub> O <sub>3</sub>	4.7	2.8
Fe <sub>2</sub> O <sub>3</sub>	3.5	4.5
CaO	63.7	64.3
MgO	0.7	2.4
SO <sub>3</sub>	3.1	2.9
Loss on Ignition	2.6	0.85
Free Lime	4	0.51
Insoluble Residue	0.3	0.15
Equivalent Alkali (NaEq%)	0.51	0.19
C <sub>3</sub> S	53	64
C <sub>2</sub> S	18	13
C <sub>3</sub> A	7	0
C <sub>4</sub> AF	11	13
Blaine Fineness (m <sup>2</sup> /kg)	386	305

Nine different CNCs were studied, These CNCs were acquired from various producers with proprietary manufacturing processes and different raw material sources. The majority of the

CNCs were in aqueous suspension except for CNC6 and CNC7 which were received in dry powder form. Although not all processes information is publicly disclosed, general descriptions of the source material and manufacturing processes are as follows: CNC1, CNC2 and CNC3 were acquired from the same provider, they were extracted from the raw material using sulfuric acid hydrolysis at 45°C for 1 hour. The primary difference between these three CNC types is the raw material source, being wood pulp, cotton and algae (*Cladophora*), respectively. CNC4 and CNC5 were acquired from another provider, and they were both extracted by oxidative methods from acetate grade dissolving pulp (*Western Hemlock*). These manufacturing processes were reported as transition metal catalyzed oxidation, using copper and sodium hypochlorite for CNC4, and iron and hydrogen peroxide for CNC5. CNC6 was produced by a pilot scale plant from softwood dissolving pulp, by degrading the amorphous regions through sulfuric acid hydrolysis at a controlled temperature for 2 hours. CNC7 was made from bleached Kraft pulp by sulfuric acid hydrolysis. CNC8 was produced from woodchips, resulting in a product with a medium range of weak acid groups. CNC9 was extracted from paper and pulp industry sludge by acid hydrolysis. A more detailed description of these materials can be found in previous work (Fu *et al.*[33]). Detailed manufacturing processes can be found in the works of Nelson & Retsina[48], and in the benchmark published by Reid *et al.* [49].

Zeta potential was measured for all CNC using a Zetasizer Nano ZS equipment (Malvern Instruments Ltd). To match the approximate pH of fresh cement pore solution, CNC slurries were diluted in a NaOH solution at a pH of 13. All CNC tested have negative charges in a range of magnitudes from 20 to 60 mV. This negative charge is attributed to the chemistry and the grafting density of the functional groups on the CNC surface as consequence of the manufacturing processes[10]. For pastes, one gram of cement paste was diluted in 300 mL of DI water and

manually mixed before following the same measurement procedure as for CNC suspensions for zeta potential.

The CNC dimensions were measured manually by ImageJ using TEM (Philips CM-100 operated at 100 kV) micrographs (as shown in Figure 2-1). Except for CNC3, at least 200 single crystals from each CNC were measured in length and width to calculate length and aspect ratio averages. A scale bar of 200 nm is provided for all images in Figure 2-1, except for CNC3 due to much larger crystal size (it should be noted that CNC3 is not a typical CNC, this material was specially made for this study because of its atypical longer dimensions). Measurements of CNC3 were fewer as there were less crystals in the micrographs. Zeta potential, average particle length, and average aspect ratio of all nine CNCs are listed in Table 2-2, Detailed TEM micrographs and Length distributions can be found in Section 5.1.1. A scaled size comparison of all CNC and the two cement types is presented in Figure 2-2 , the size of the cement particles was approximated from the Blaine fineness, neglecting porosity.

Table 2-2. CNC average length and aspect ratio (Length/Diameter), and Zeta potential at pH of 13.

CNC	Zeta potential [mV]	Average Length [nm]	Average Aspect Ratio
CNC1	-44	93 ±48	13 ±6
CNC2	-47	127 ±34	14 ±6
CNC3	-42	966 ±382	46 ±48
CNC4	-39	97 ±48	15 ±5
CNC5	-34	83 ±28	12 ±6
CNC6	-49	90 ±27	12 ±7
CNC7	-55	85 ±23	11 ±5
CNC8	-21	184 ±52	15 ±7
CNC9	-53	156 ±40	17 ±6

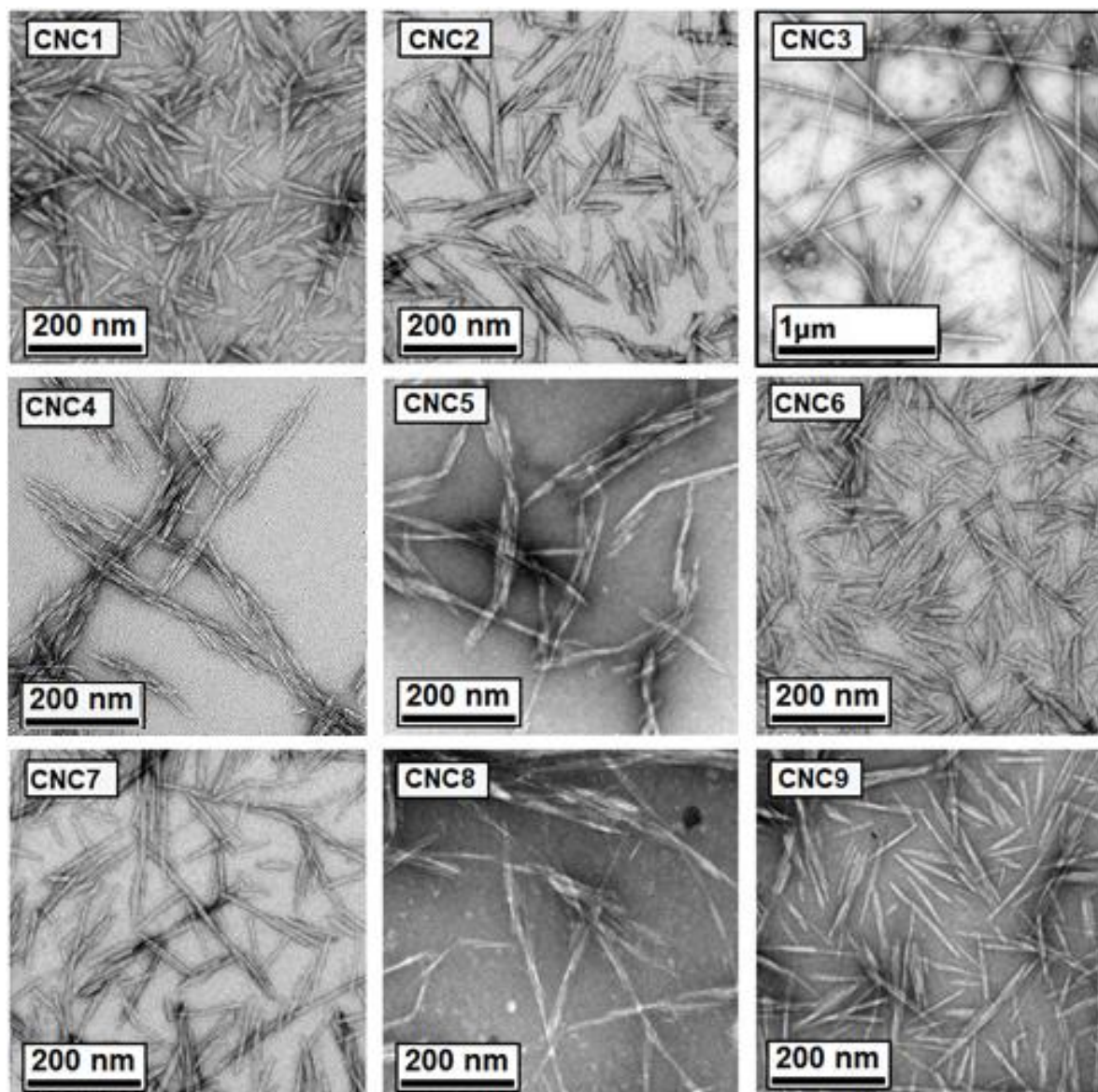


Figure 2-1. Sample of all the TEM micrographs of all nine CNCs used in this study.

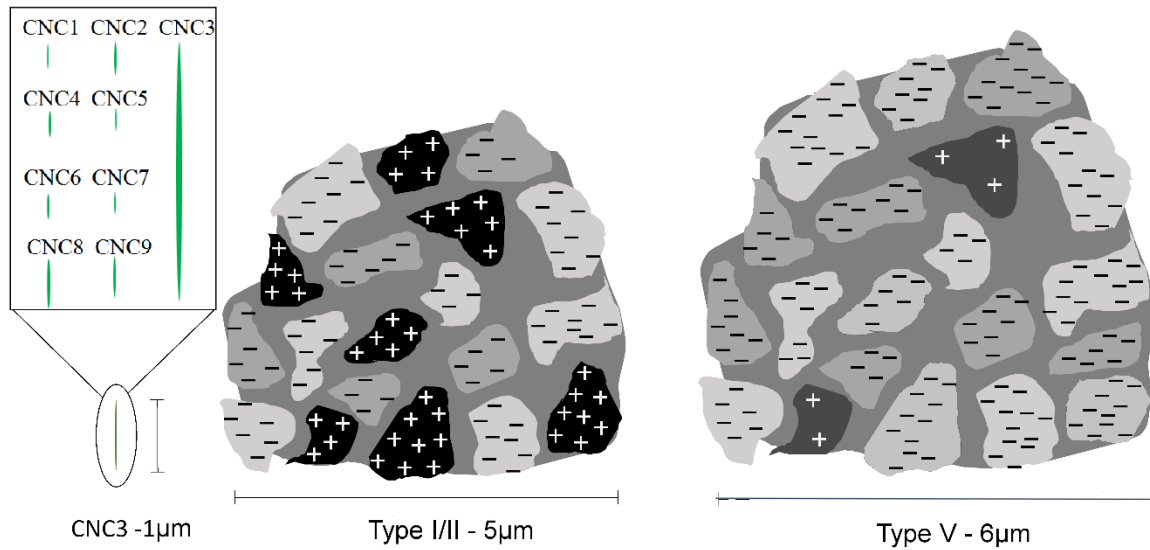


Figure 2-2. Scaled representation of cement particles and CNC.

### 2.2.2 Paste Preparation

The true density of the dry cement powder was  $3.12 \text{ g/cm}^3$ . The dry density of the CNC was  $1.6 \text{ g/cm}^3$  [19]. Aqueous suspensions of different CNC dosages were prepared with reverse osmosis water ( $<20 \text{ ppm}$ ) and mixed using a sonic mixer (Branston Digital Sonifier Model 102C) for 2 min at 25 % intensity and 1 s on/off intervals inside an ice bath. The CNC dosages in water suspensions depended on the selected w/c and the desired % of solid CNC relative to dry cement, *i.e.*, the different CNC slurries were diluted to similar concentrations to be used in similar aliquots and get the dosages listed at the end of Section 2.1. After the desired amount of the prepared CNC suspensions was added to 50 g of cement powder using a syringe, constituents were premixed with a stainless-steel spatula until apparent homogeneity, then the container was closed and taken to a centrifugal planetary mixer (Flack-Tek Speed mixer) at 2000 rpm for 120 s. The resulting paste was used for rheology measurement.

### 2.2.3 Rheometer Setup, Procedure and Analysis

The rheological setup was based on the work of Ferraris *et al.* 2007[51], and NIST Standard Reference Method 2492[52]. The measurements were based on those performed by Cao *et al.*[19]. Serrated parallel plates of 40mm diameter were installed on a Bohlin Gemini HR Nano Rheometer. An ABS vapor-trap cover was designed, and 3D printed to close around the fixed bottom plate without touching the upper rotating plate as shown in Figure 2-3. A wet sponge was placed inside before closing the cover, minimizing moisture loss during the test.

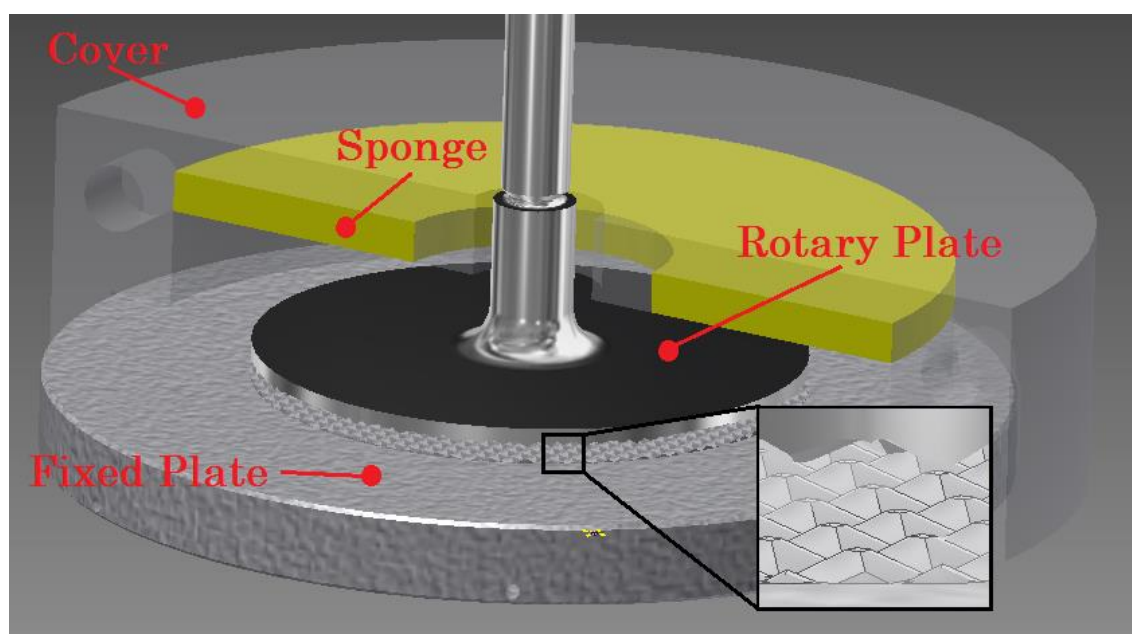


Figure 2-3. 3D Illustration of the rheometer serrated parallel plates, rotary plate 40mm diameter, ABS cover and inner sponge to preserve humidity, 1mm gap.

The rotary plate was homed (zeroed) and a 1mm gap was set just before rising the plate. The top and bottom plates were wiped with a wet paper towel before injecting a 1.5 ml sample of the prepared paste and lowering the top plate to the gap. The ABS cover was closed around the

setup. The experiment was set to run an increasing stress ramp of 50 steps with logarithmic increments, and to return the resulting shear strain rate at every stress.

The initial and final stresses were selected to ensure that the resulting shear strain rate would be within a selected stress range. The initial shear strain rate results should be  $<0.1 \text{ s}^{-1}$  and final shear strain rate at least  $10 \text{ s}^{-1}$ . The test was designed to start  $10 \pm 1$  minutes after water was added to the cement and to last for  $9 \pm 2$  min. Tests were conducted at room temperature ( $23^\circ\text{C} \pm 1^\circ\text{C}$ ).

The Bingham model, as shown in Equation 2-1, was used to analyze the results

$$\tau = \tau_0 + \dot{\gamma}\eta$$

Equation 2-1. Bingham plastic model.

where  $\tau$  and  $\tau_0$  are the shear stress (Pa) and the shear yield stress (Pa) respectively,  $\eta$  is the plastic viscosity (Pa·s), and  $\dot{\gamma}$  the shear strain rate ( $\text{s}^{-1}$ ). Data points from the shear stress vs. shear strain rate plot were used to construct a linear regression to obtain the yield stress ( $\tau_0$ ) value.

An disadvantage of using a Bingham model to describe the behavior of these cement pastes is that viscosity changes are usually observed as particles deflocculated [53], [54]. In addition, CNC solutions display shear thinning behavior by themselves, starting from the dilute regime[55]. It has also been reported interparticle jamming transitions at high dosages of plasticizers[7]. Most of the mixtures, including the plain paste, displayed slope changes at certain shear rates. Some mixtures, as shown in Figure 2-4 (a) and (b), displayed consistent viscosity reduction, some mixtures, as the one shown in Figure 2-4 (d), changed their viscosity more than once, and some of

them, like the sample shown in Figure 2-4 (c), even displayed discontinuity in the slopes of the measured points. As Bingham model considers a constant viscosity for stresses above yield stress, only the points in a shear rate interval, between a selected minimum and a maximum shear rates (blue points in Figure 2-4), were considered to calculate linear regression.

The range used of minimum and maximum shear strain rates was between  $0.1 \text{ s}^{-1}$  and  $100 \text{ s}^{-1}$ . The minimum value was selected 2 orders of magnitude higher than the minimum shear rate that the rheometer would accurately measure, and it was also around the minimum shear rate at which any movement was observed at the naked eye. For the maximum shear rate, based on most measurements, like the ones showed in Figure 2-4, slope changes usually appear after  $100 \text{ s}^{-1}$ , so only the points marked in blue ( $\dot{\gamma} \leq 100 \text{ s}^{-1}$ ) were considered to construct a linear regression.

If all values were considered, linear regression would cross the Y-axis at a stress value where measured strain rate is smaller than the minimum considered. In other cases, a stress value will produce a strain rate greater than the minimum by orders of magnitude, resulting unrealistic yield stress value. These criteria were established for all measurements so the linear regression would cross the Y-axis as close as possible to the mentioned minimum shear rate.

These points were used despite appearing to be a very low number of points to work with. In fact, most of the measurements yielded enough points within the desired range (more than 7), but even in cases where only two or three points are within this range (which usually occurs when measuring pastes with high yield stress, Figure 2-4 (c)), the literature mentions cases where in practice, Newtonian behavior is (wrongly) assumed, and even a single point is used[56]. It is a well-known fact that the Bingham model does not perfectly describe the behavior of all cementitious materials, but this approach is highly used in industry and in literature for its practicality and simplicity[29], [56], [57].

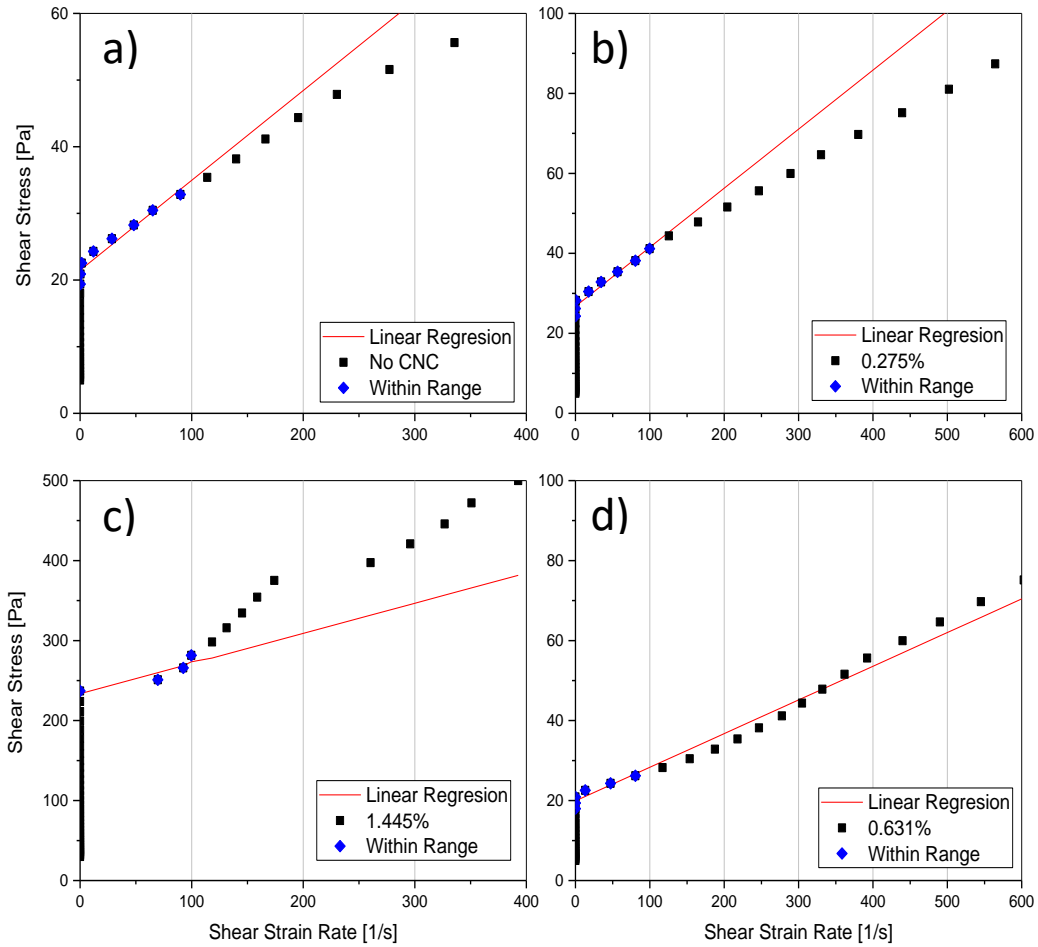


Figure 2-4. Stress strain measurements showing different slope changes at different CNC dosages. Blue markers are within minimum and maximum shear rates (0.1 – 100 s<sup>-1</sup>), range considered for the linear regression (red line) to determine Yield Stress.

## 2.3 Results and Discussion

### 2.3.1 Rheometry of Type V cement at w/c 0.35

Type V cement paste with a w/c of 0.35 was selected to study the impact of different CNCs on paste rheology. Cement paste mixtures were prepared, and the yield stress was measured as described in sections 2.2.2 and 2.2.3 respectively. Figure 2-5 shows the yield stress for all the tested mixtures, normalized to the yield stress value at 0% CNC (control mixture). As both axes are shown in the logarithmic scale, the yield stress of the paste with 0% CNC represented with a horizontal line at the unit value (1.0).

All CNC showed a reduction in the yield stress at initial dosage, except for CNC3 which was used on a different range of dosages than the rest of the CNCs (0.005%, 0.010%, 0.015%, 0.023%, 0.052%, 0.120% and 0.275%). CNC3 showed approximately 5% yield stress reduction at a 0.005% dosage, being the smallest reduction of all CNC, and the increments in yield stress occurred since 0.010% dosage which is lower than the dosage at which the rest of the CNCs increased the yield stress. The maximum dosage of CNC3 that the instrument could measure was 0.275%, pastes with higher CNC3 doses were not sufficiently flowable for accurate measurement with this geometry. Statistical analysis was conducted to compare the yield stress measurements for each CNC. Single tailed, homoscedastic and heteroscedastic, t-student tests were used to compare reduced yield stress values with increased yield stress values of the formulations. Significance was assessed at a 0.05 level.

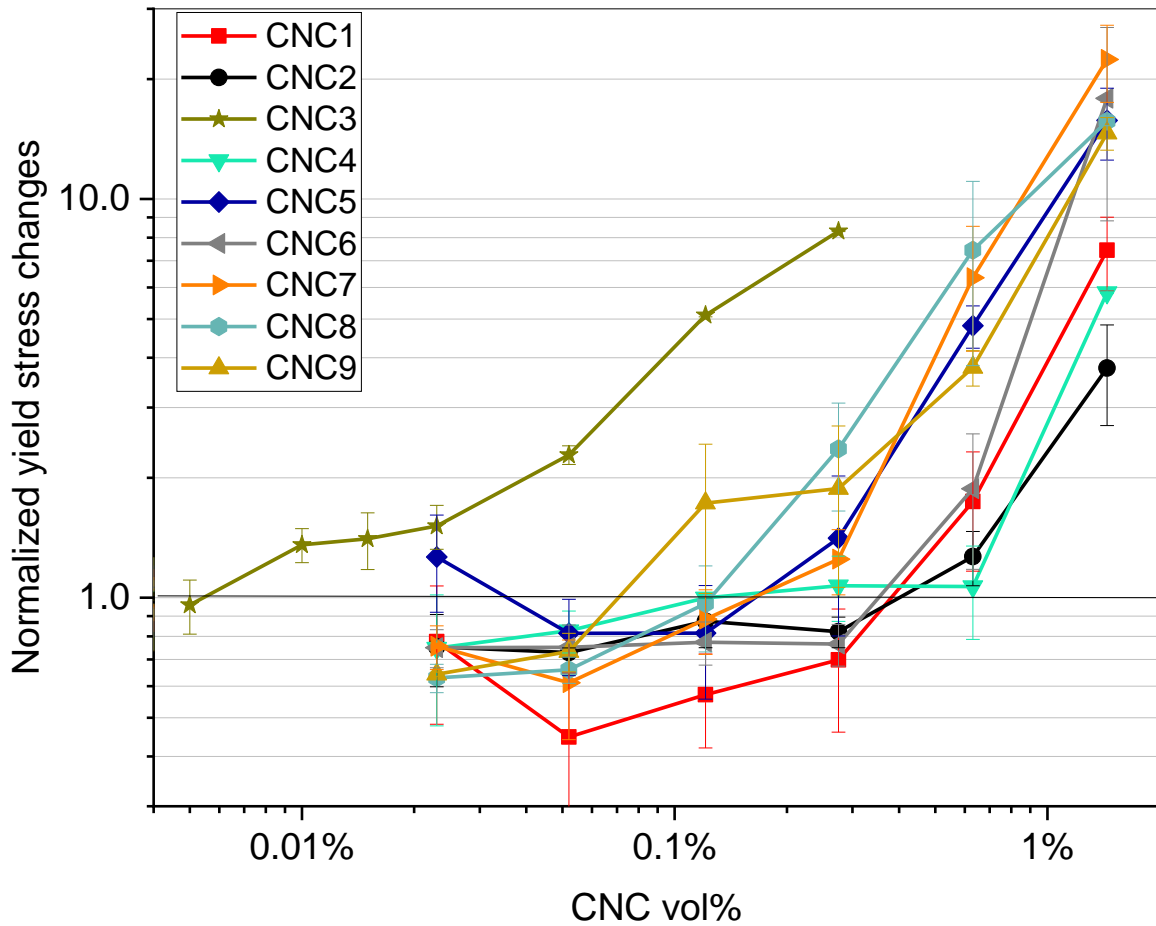


Figure 2-5. Changes in yield stress of Type V paste at a w/c of 0.35 with different CNCs. The values are normalized by the yield stress of plain paste (control, at unit value in vertical axis). Yield stress values of the control mixture had an average of 26 Pa with a standard deviation of 9.4 Pa.

A few aspects of the yield stress of the cement pastes can be highlighted in Figure 2-5. All CNCs were observed to reduce the yield stress of this cement mixture at low dosage, after this dosage, as CNC dosage is increases, also did the yield stress. CNC3, CNC4 and CNC9, have a relatively small dosage range where they reduce the yield stress. CNC1, CNC2 and CNC6 reduce yield stress at dosage ranges of up to 0.275 %. CNC1 reduces the yield stress most significantly,

achieving a yield stress of 46 % when compared to the control mixture yield stress. CNC1 also appears to reduce yield stress over a wider range than any other CNC.

The relationship was analyzed between the yield stress and the measured CNC characteristics (listed in Table 2-2). It was hypothesized that both zeta potential and length play a role in yield stress reduction of cement paste by CNC due to steric or electro-steric stabilization of cement particles[58], [59]. The minimum yield stress achieved by every CNC was compared to the CNC length (Figure 2-6(a)), zeta potential (Figure 2-6(b)), and aspect ratio (Figure 2-6(c)). In addition, the zeta potential to length ratio, which has little, or no physical meaning, was examined in Figure 2-6(d), this comparison was made to look for a second order relationship, *i.e.*, if there was a slight relationship between the yield stress reduction and, the length of the crystals, and with the Zeta potential of the CNC, by combining those factors, the dependence would be more clear, however, as showed in Figure 2-6, no clear relationship was observed. CNC4 and CNC5 are distinguished by squares, as they were made using a different manufacturing process. CNC3 was distinguished as a star as it stands out from the rest because its atypical dimensions and atypical dosages at which yield stress reduction occurs. The dashed line represents the trend of the data points.  $R^2$  values are shown. No strong evidence was found to support the hypothesis that either the CNC dimensions or apparent surface charge are the definitive factor that describes the interaction between cement paste and CNC.

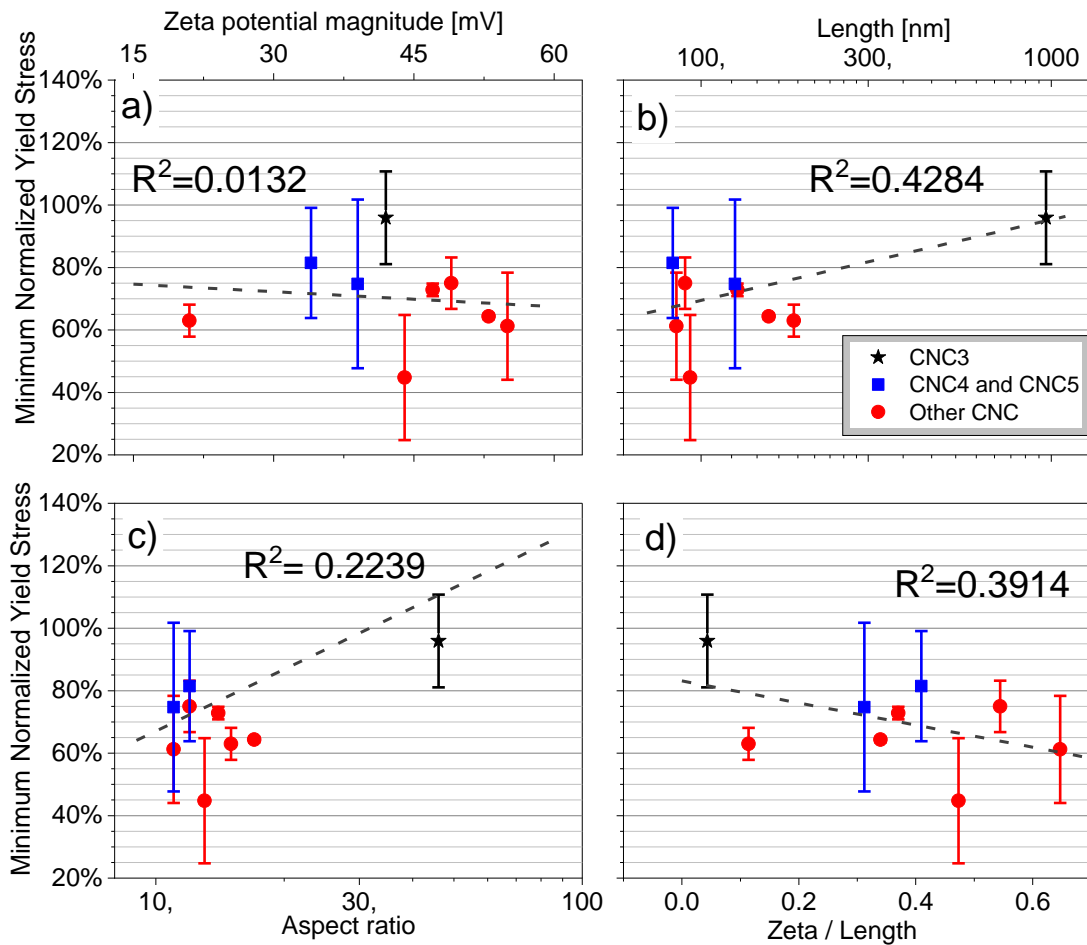


Figure 2-6. The minimum yield stress achieved by each CNC in Type V pastes at a w/c of 0.35 as a function of (a) CNC zeta potential at pH 13, (b) Average CNC length, (c) Average crystal aspect ratio, and (d) Zeta potential divided by CNC length. Linear regressions are shown along with each coefficient of determination ( $R^2$ ).

Pastes prepared with CNC3 had the lowest reduction in yield stress, and considerably greater dimensions (length and aspect ratio) than the rest of the CNCs. Therefore, CNC3 appears as a distant point (shown as a star) from other CNCs in Figure 2-6(b), (c) and (d). The majority of the CNCs tested are approximately 50 times smaller than the average cement particle (as showed in Figure 2-2), therefore the CNCs interact with cement as particles adsorbing to the oppositely charged regions of the cement surface, changing the electrostatic interactions between cement

particles. On the other hand, CNC3 is approximately 10 times larger than the other CNC materials, which makes it approximately 1/5 of the size of a cement particle. Fewer surface portions of the cement have the adequate size and charge conditions to adsorb CNC3. As a result, compared to the rest of the CNCs, fewer CNC3 crystals are adsorbed to the cement surface, resulting in a reduction in the positive-negative interactions of cement particles. Alternatively, CNC3 may be on the brink of bridging behavior between cement particles, which may lead to flocculation or gelation, and an increase in viscosity. Overall, these effects may explain why the CNC3 dosage does not result in yield stress reduction.

Pastes prepared with CNC4 and CNC5 display the two lowest reductions in yield stress. CNC4 and CNC5 were extracted from the raw material by oxidative degradation instead of acid hydrolysis as the rest of the CNCs. The differences in yield stress reductions could be due to the carboxylate functional groups being “softer” acids than sulfate half-esters (despite having similar zeta potential values), even though at this pH both are fully ionized. Regardless, these different functional groups, appear to be a factor in the crystal adsorption to the cement particle surface, affecting the yield stress reduction capabilities.

Finally, cement pastes prepared with CNC1 display the greatest reduction in yield stress. However, CNC1 doesn't stand out in size or zeta potential from the rest of the CNCs, nor that its manufacturing process is any different from CNC2 or CNC3. In summary, within the range offered by most CNCs, no evidence was found to suggest that the length of the crystal (with the exception of CNC3), the aspect ratio of the crystal or the Zeta potential, are a deterministic factor that influences the performance of the rheology.

### 2.3.2 Rheometry of CNC1 with Type I/II and Type V cement

The second set of tests evaluated two cement types (V and I/II) and three different w/c (*i.e.*, 0.30, 0.35, 0.40). These tests were performed using a single CNC material. CNC1 was selected for being the CNC with the greatest yield stress reduction and for having one of the widest range of dosages at which yield stress reduction was observed. Experiments were conducted as described in section 2.2.2 and results were fitted the Bingham model as described in section 2.2.3.

Moreno [34] explains how the yield stress is proportional to the strength of the particle network, and therefore by dispersing cement particles by adding CNC, the network structure would be reduced. Moreno[34] also explains that as the volume fraction of particles is increased from a dilute solution up to the gel volume fraction, particle aggregation exponentially escalates from isolated clusters to particle network arrangements. Similarly, Cao *et al.*[19] showed that at very low dosages, the effect of CNC is similar to that of a plasticizer, by reducing yield stress of cement paste.

Yield stress measurements of pastes prepared using Type I/II cement and CNC1 are shown in Figure 2-7. Although yield stress clearly increases with CNC dosage, at the lower dosages, a slight reduction can be observed from the inset plot. The measurements of pastes prepared using Type V and CNC1 are presented in Figure 2-8. It is proposed that the differences in performance between Type I/II and Type V pastes are due to the tricalcium aluminate[60] (cement chemistry denotes as  $C_3A$ ). The Type I/II cement used in this work has 7 wt%  $C_3A$ , which reacts with water to become positively charged ettringite during the first few minutes after water is added. The ettringite precipitates into the pore solution, filling part of the space originally occupied by water, and promoting positive-negative electrostatic interactions[61]. As the Type V cement used in this

research has zero  $C_3A$ , pastes prepared using Type V cement have much less positive charged hydration products during the first minutes after water is added than paste prepared using Type I/II. In addition, it has been shown that for the same type of cement, higher fineness contributes to higher yield stress. Therefore, it is expected to see higher yield stresses in pastes made using Type I/II cement.

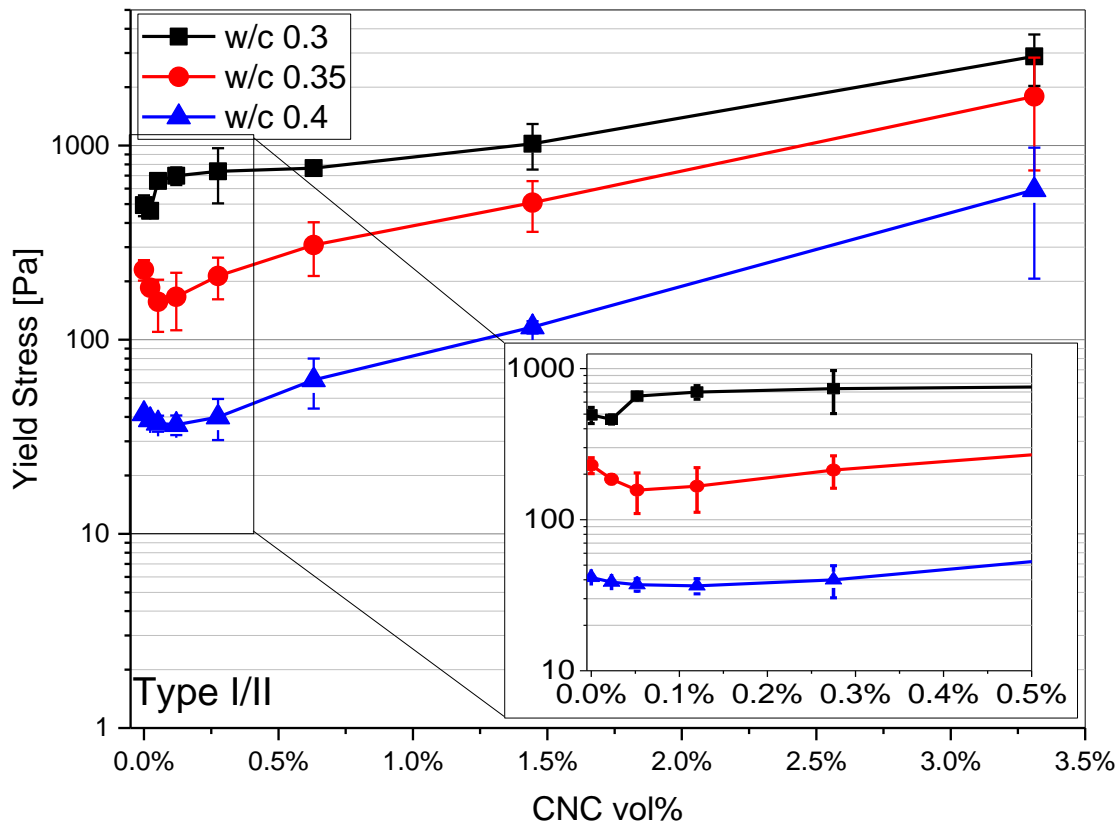


Figure 2-7. Average yield stress of Type I/II cement pastes at different w/c versus CNC dosages.

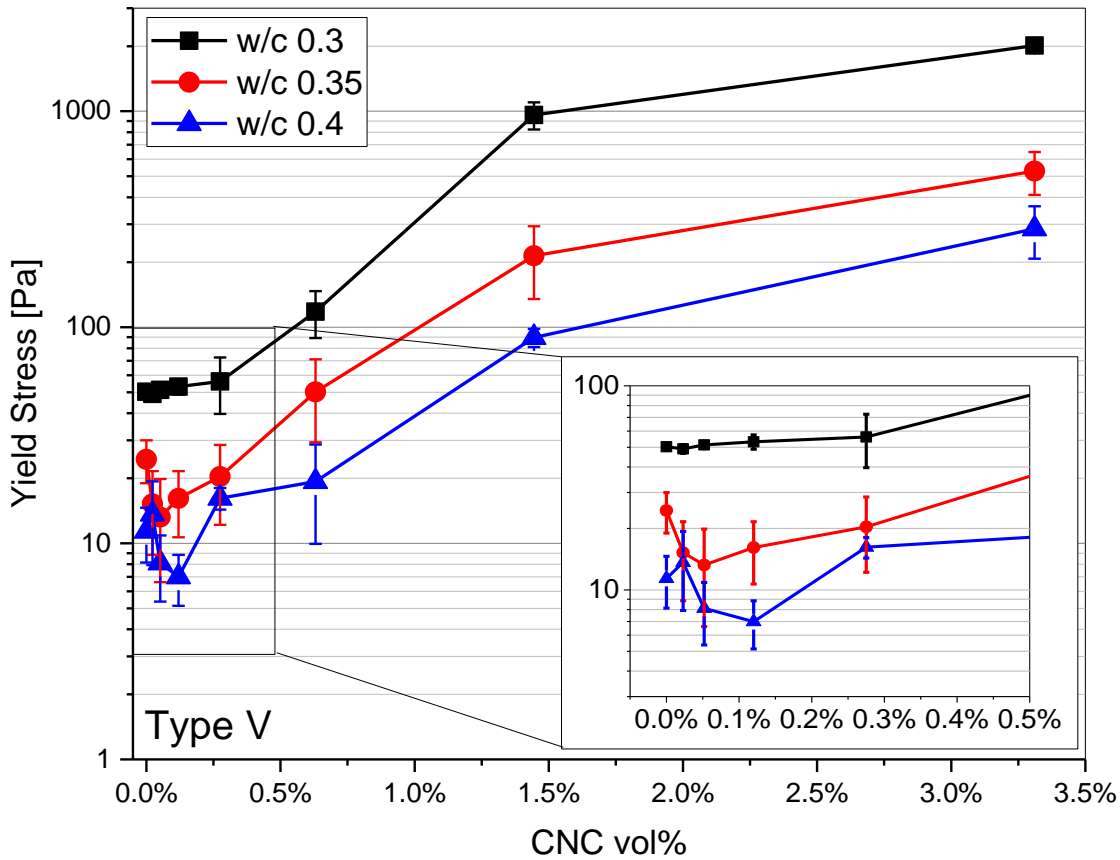


Figure 2-8. Average yield stress of Type V cement pastes at different w/c versus CNC dosages

The overall observable trend of the plots in Figure 2-7 and Figure 2-8, is the non-monotonic change in the yield stress as CNC dosage increases (*i.e.*, at first, yield stress reduces and then it increases). A non-monotonic trend is usually the effect of two competing driving forces. The first competing force appears to be the physical interaction between the negatively charged CNC and the positive portions of the early hydrated cement surface, which are lessened by CNC screening these positive-negative interactions, thus improving the dispersion of the cement particles. The second competing force appears to be the surface area of the cement and the CNC volume fraction[62]. Since the CNC are expected (based on calculation) to cover majority of the adsorption

sites at a dosage at which a minimum yield stress is observed, higher dosages lead to the formation of agglomerates due to interactions between CNC and multivalent cations[35], reducing flowability.

Figure 2-9, Figure 2-10 & Figure 2-11 show the changes in yield stress both in absolute and normalized values (scaled to the value of plain paste) for the same w/c. Figure 2-9 shows the measurements of the w/c 0.30 mixture, where the yield stress reduction is barely noticeable (<10%) and the maximum reduction occurs at 0.023 % for pastes made with both cement types. The plain pastes (*i.e.*, 0% CNC) made using Type I/II initially showed yield stresses almost 10 times higher than pastes made using Type V. This observation is consistent with Bessaies-Bey *et al.*[63], for mixtures under the same conditions, rheological behavior is governed by the nature and intensity of cement particles interactions, which relates to the cement chemical composition and water content. For the pastes with the highest CNC dosages, the yield stress is over 30 times greater than the control value for Type V. For the yield stresses at the highest dosages (3.3 % CNC) are similar, likely due to the rheology being dominated by CNC agglomeration[19].

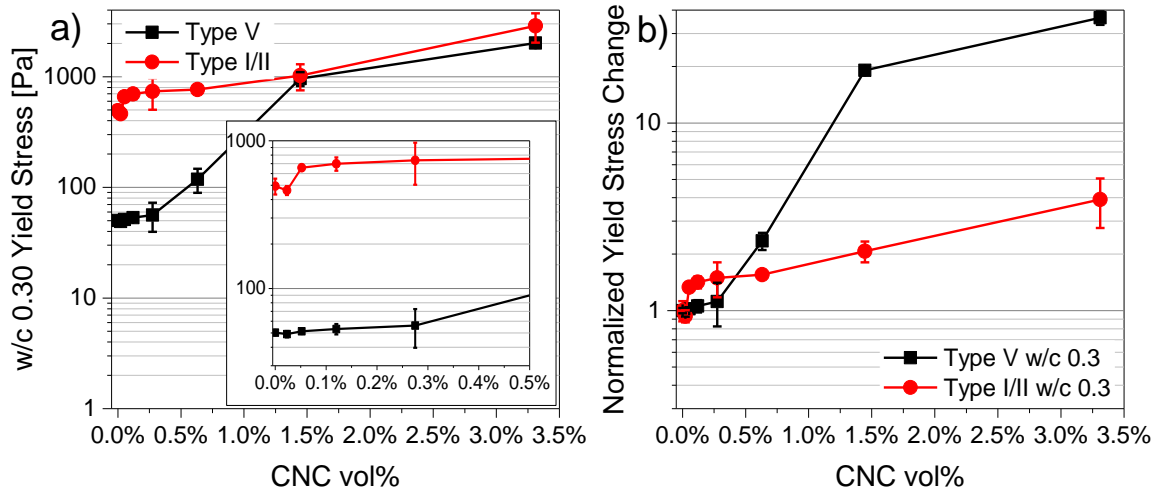


Figure 2-9. Yield stress changes of 0.30 w/c mixtures in a) absolute values and b) changes normalized by the control sample (0 % CNC).

Figure 2-10 shows the yield stress of pastes prepared with a w/c of 0.35. These mixtures have the highest yield stress reduction. The minimum yield stress occurred again at the same dosage for both pastes at 0.052 %. Again, for all dosages, the Type I/II pastes showed higher yield stress than Type V pastes.

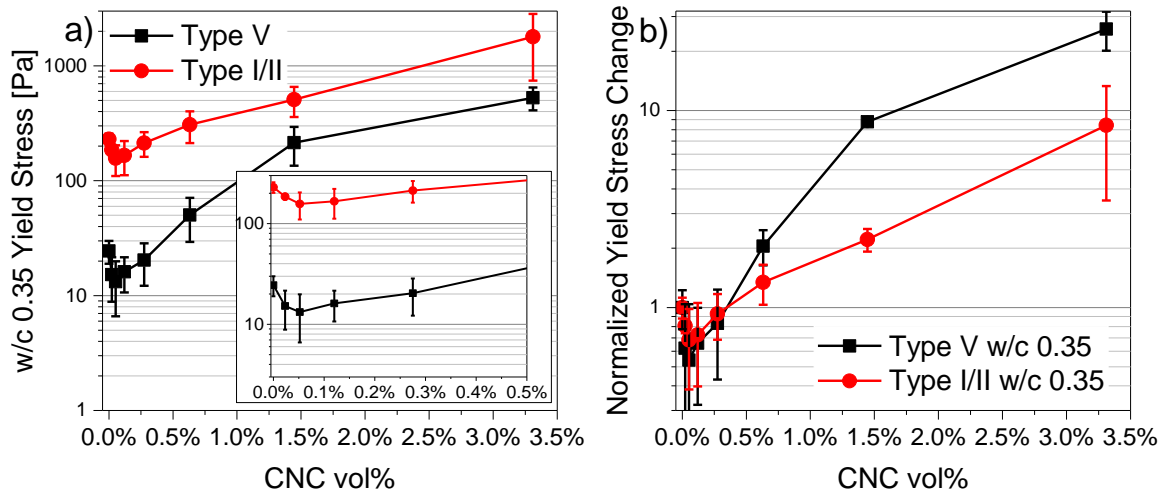


Figure 2-10. Yield stress changes of 0.35 w/c mixtures in a) absolute values and b) changes normalized by the control sample (0 % CNC).

The yield stresses of pastes prepared with a w/c of 0.4 are compared in Figure 2-11. The minimum yield stress was achieved at the same dosage for pastes made with both cement types, at a higher dosage than the previous mixtures (0.120 %). The highest CNC dosage, pastes made using both cement types display similar normalized yield stress increases.

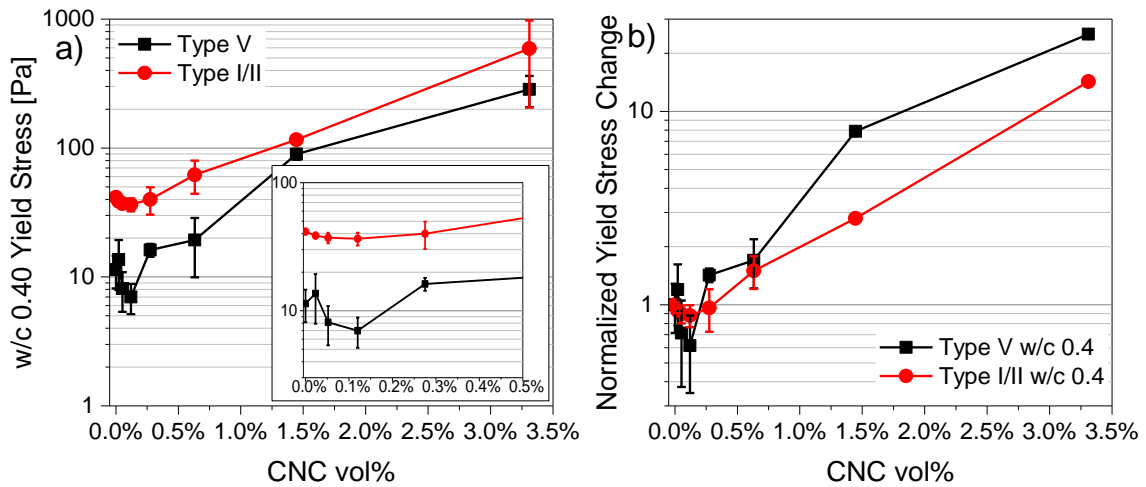


Figure 2-11. Yield stress changes of 0.4 w/c mixtures in a) absolute values and b) changes normalized by the control sample (0 % CNC).

In summary, Figure 2-9, Figure 2-10 and Figure 2-11 show that at lower dosage, CNC addition tends to reduce yield stress and results a more flowable paste. However, as the CNC dosage increases, the yield stress quickly increases, resulting a less flowable paste. A more detailed discussion is given in the following section.

Table 2-3. Cement pastes with CNC1 addition maximum stress reduction dosages and magnitudes.

Yield Stresses change summary	Type I/II			Type V		
	w/c 0.30	w/c 0.35	w/c 0.40	w/c 0.30	w/c 0.35	w/c 0.40
Maximum Yield Stress Reduction Dosage (vol% CNC1)	0.023%	0.052%	0.120%	0.023%	0.052%	0.120%
Yield stresses at 0% CNC1 [Pa] (YS <sub>0</sub> )	493.4	229.5	41.5	50.3	24.5	11.4
Lowest Yield Stresses [Pa] (YS <sub>Low</sub> )	461.6	156.9	36.5	49.1	13.2	7.0
Yield Stresses reduction YS <sub>Low</sub> /YS <sub>0</sub>	0.94	0.68	0.88	0.98	0.54	0.61

\*YS = Yield Stress

### 2.3.2.1 Overall Yield Stress

Pastes prepared using Type V always display lower yield stress than pastes prepared using Type I/II. As previously discussed, Type V pastes are expected to have less positive-negative interactions between particles (thus better dispersion) due its lower C<sub>3</sub>A content. This assumption is consistent with the zeta potential values shown in Figure 2-12. The plain paste (0 % CNC), made with Type I/II cement has a smaller zeta potential magnitude than the paste made with Type V (even though Zeta potential contributes to particle dispersity, it is not a deterministic factor). However, the zeta potential of Type I/II cement at 0.052 % CNC1 has more negative value than Type V cement at the same CNC dosage. This effect is likely due the higher content of positive charged hydration products of paste made using Type I/II cement[60]. It has been shown by Srinivasan et. al.[64] that for hydrated cement phases, the more positive zeta potential, the more negative they become after (negatively charged) plasticizer is added (because of the stronger adsorption).

For same w/c, pastes prepared using Type V cement always showed higher reductions in yield stress than paste prepared using Type I/II. It has been shown by Plank *et al.*[60] that in pore solution, ettringite has the highest positive zeta potential contribution. Pastes made using Type I/II have greater volume of  $C_3A$  and ettringite, making the particle surfaces more electrostatically heterogenic, resulting in regions with high and low concentration of adsorbed CNC. Compared with Type I/II particles, particles of Type V cement would have a more uniform surface adsorption of CNC. For Type I/II paste, surface saturation can improve CNC dispersity, thus yield stress reduction. However, evidence showed that the uniform CNC surface distribution (as in Type V cement paste) is the dominant factor.

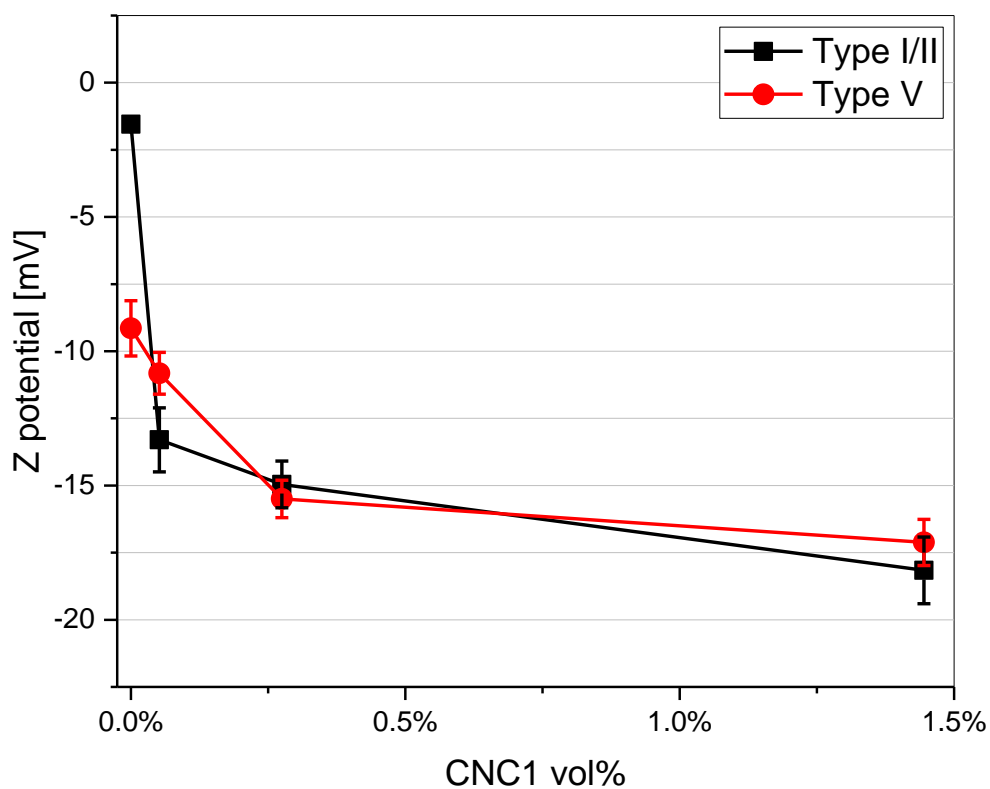


Figure 2-12. Zeta potential measurements of cement pastes diluted in DI water at a dilution factor of 300.

### 2.3.2.2 Maximum yield stress reduction

The CNC dosage at which the maximum yield stress reduction occurs changed with w/c (Table 2-3). The dominant factor is w/c, as the increase in pore solution volume makes it easier for the CNC to flow around cement particles and be adsorbed on the surface. This results in improved particle dispersion. Another reason is that more water is available to form positively charged ettringite, providing more CNC adsorption sites. Many researchers have shown that the positively charged product formed in the early hydration can greatly affect the absorption of negatively charged additives [60], [61], [65], [66].

By comparing Figure 2-9(b), Figure 2-10(b) and Figure 2-11(b), no apparent relationship was found between the magnitude of maximum yield stress reduction and the w/c. This can be better observed in Figure 2-13.

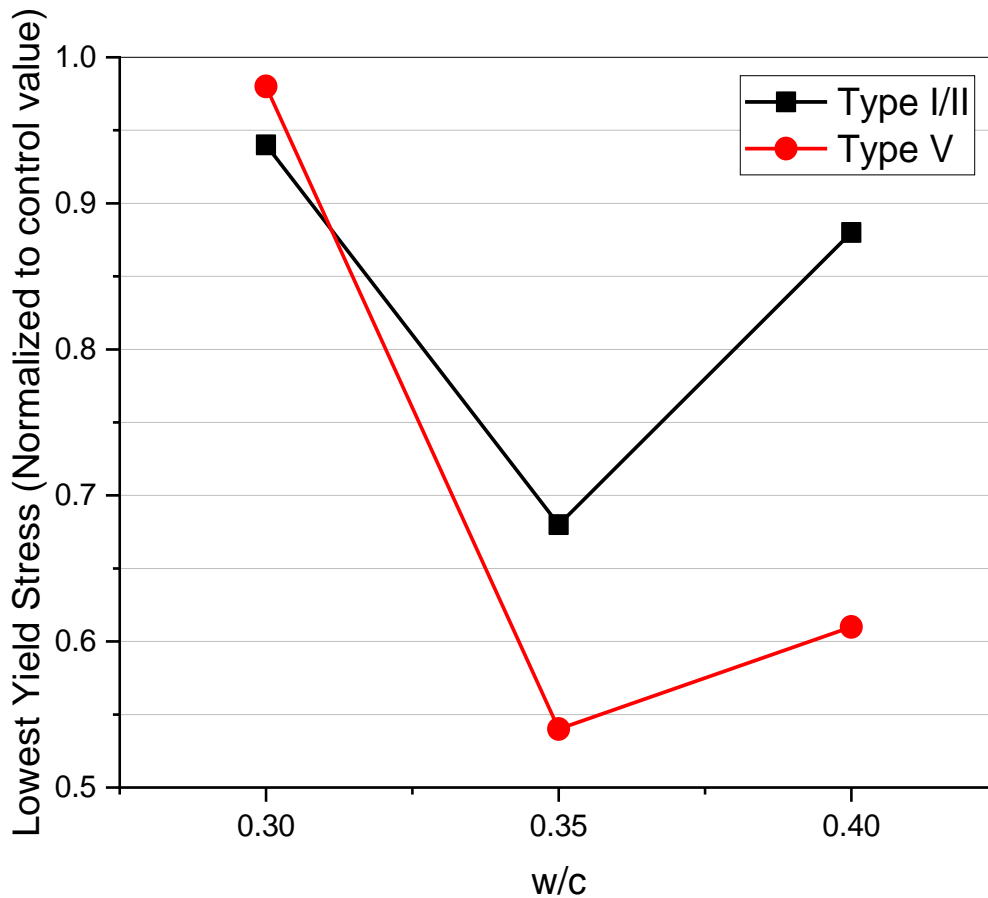


Figure 2-13. Maximum normalized yield stress reduction obtained at each w/c.

### 2.3.2.3 Yield stress increases at high dosages

At some point (assumably just past the dosage at which maximum reduction of yield stress occurs), CNC adsorption sites on the surface of the cement become saturated, so the excess of CNC in the pore solution is responsible for the increase in yield stress, up to 13 times the original value for Type I/II and up to 40 times for Type V at the highest dosage used. Possible reasons for these increments could be that excessive CNCs flocculate by themselves.

In the absence of  $C_3A$ , Type V cement particles have lower density of positive charged surfaces than Type I/II particles, consequently there would be a greater number of free CNCs in the pore solution of pastes prepared using Type V cement[67], thus the higher normalized increase in yield stress. However, as w/c increases, the difference between normalized yield stress increments for pastes prepared with both cement types reduced. This increment similarity may indicate that after a certain CNC dosage, cement particle surfaces (with or without ettringite) reach saturation, and any excessive CNCs will form their own arrangements that result in a higher yield stress. In other words, at high CNC dosages, the excessive CNCs have a more dominant impact on rheology than the differences in the cement composition. This confirms the assumption made in section 3.2 about the second driving force governing the CNC-cement interactions being the solids volume fraction in the mixture.

### **2.3.3 Using CNC as a cement additive.**

The CNC dosage at which the maximum yield stress reduction occurs changed with w/c (Table 2-3). The dominant factor is w/c, as the increase in particle spacing makes it easier for the CNC to flow around cement particles and be adsorbed on the surface or inefficient at colloiddally stabilizing cement particles at low particle distances. This results in improved particle dispersion. Another reason is that more water is available to form positively charged ettringite, providing more CNC adsorption sites. Many researchers have shown that the positively charged product formed in the early hydration can greatly affect the absorption of negatively charged additives[60], [61], [65], [66]. Figure 2-14 also shows that the w/c are the dominant factor in yield stress, as CNC1 at all dosages showed consistent yield stress decrease with increase of w/c.

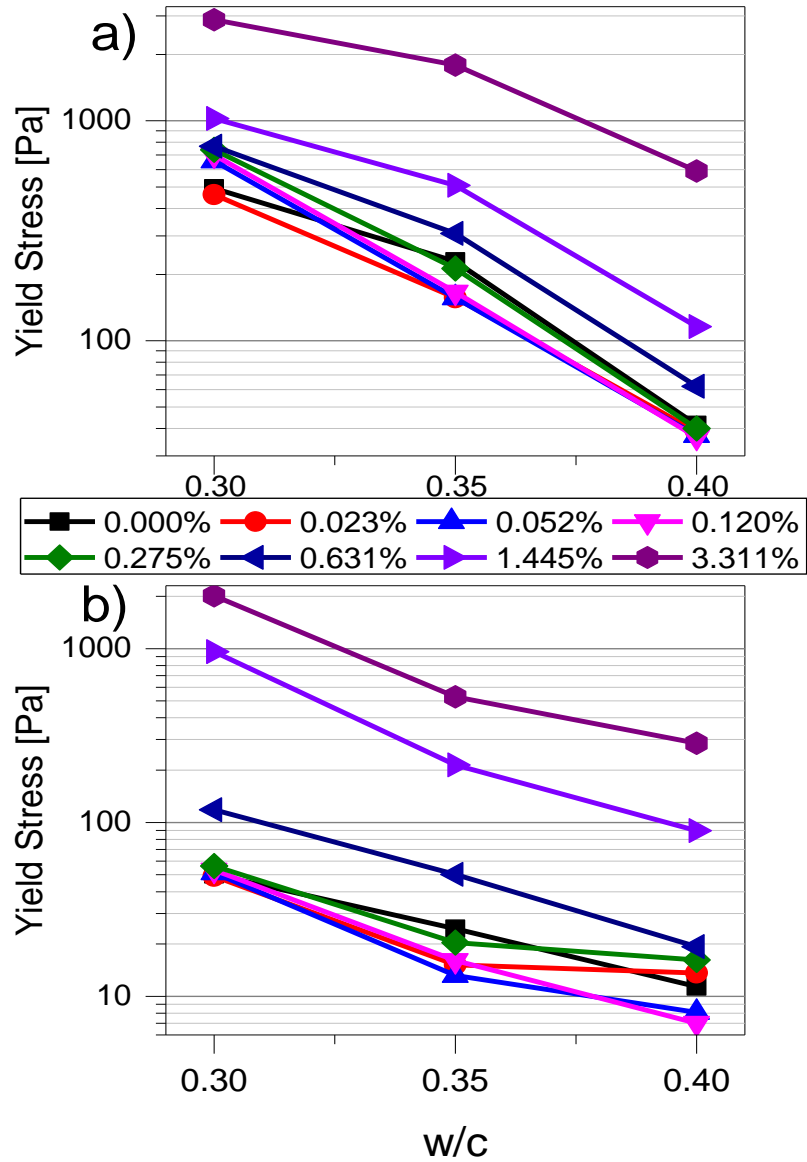


Figure 2-14. Yield stresses of pastes made using Types a) I/II and b) V cement at different CNCI dosages and three w/c.

In terms of CNC dosages, as Figure 2-14 shows, the rheology results indicated that CNC1 behave differently when used with cement at different dosages. At lower dosage (less than 0.2 % in most cases), the addition of CNC would help with the flowability of cement pastes. As discussed previously, this is likely due to the CNC increasing the dispersion of cement particles, resulting in reduction of yield stress by reducing the positive-negative interactions between hydration products. Cao et al.[19] observed similar results when comparing the same CNC (CNC1) with a water reducing admixture with Type V cement. At higher dosages (more than 0.2 %), CNCs increase yield stress, performing similarly to a viscosity modifying admixture (VMA). From the results of Fu *et al.*[33], we know that the improvements in flexural strength and hydration of cement pastes with CNC addition occur at dosages in a range from 0.2 % up to 2 %, and CNC worked most effectively at higher dosage (1.5% for Type V cement and 2.0 % for Type I/II cement). However, it can be observed in Figure 2-14 that CNC1, at dosages above 0.275 %, increased the yield stress of cement paste.

This is also true for all CNC at dosages higher than 0.4 % (Figure 2-5), and at 1 % CNC, yield stresses are between 2 and 10 times higher than the control mixture. Nonetheless, yield stress reduction is not the only desired effect of a cement admixture. Cellulose ethers have been used as VMAs, water retention enhancers[68], and increasing sag resistance of cement mortars[69]. Therefore, considering the effect of CNC on cement rheology and strength, it is suggested that CNC could serve as a double purpose admixture at high dosages (more than 1.5 %) by both significantly increasing the flexural strength and improving consistency of concrete mixtures by reducing segregation[69].

## 2.4 Conclusions

Nine CNCs and two cements (Type I/II and Type V) were used in this study to investigate the rheological behavior of cement paste containing CNCs. Several conclusions can be drawn from the results:

- At low dosages, the CNCs appear to interact with cement particles in a similar way that water reducers behave by adsorbing to the cement surface and improving the particle dispersion to reduce yield stress.
- There was no strong evidence suggesting that either CNC manufacturing process, CNC size or zeta potential are the definitive factors in the cement paste yield stress reduction capabilities.
- As  $C_3A$  and its hydration products are the most positively charged of the cement particles in early hydration products, cement without  $C_3A$  (Type V cement used in this work) showed a more homogeneously charged surface, which appears to be better for dispersion as higher yield stress reductions were observed at low CNC dosages. At higher CNC dosages,  $C_3A$  content became less relevant, likely since the hydrated  $C_3A$  phases would be covered in CNC.
- For every w/c, CNC1 always showed a higher yield stress reduction for pastes made using Type V cement than for pastes made using Type I/II cement. In addition, minimum yield stress appeared at higher CNC dosage for paste with higher w/c, indicating that the paste with higher w/c could accommodate more CNC before the excess CNCs started to increase yield stress. In addition, minimum yield stress appeared at higher CNC dosage for paste

with higher w/c, indicating that the paste with higher w/c could accommodate more CNC before the excess CNCs started to increase yield stress.

- At lower dosages ( $< 0.2\%$ ), CNC can be used in a similar fashion as water reducing admixtures. However, at much higher dosages ( $> 0.5\%$ ), CNC can be better used as viscosity modifying admixtures. This would occur while the hydration and flexural strength are significantly improved with CNCs.

### **3. THE PRESENCE OF OLIGOSACCHARIDES AND DERIVATIVE IMPURITIES IN CELLULOSE NANOCRYSTALS**

This work was made in collaboration with Miran Mavlan, Reaz Choudhury, and Drs. Iman Beheshti Tabar, Alexander Wei, and Jeffrey Youngblood. My contribution consisted in compiling and interpreting most of the raw experimental results made by the other authors (CV, anthrone, BCA, HPLC). I oversaw the MS assays and the CNC washes and analysis. I started writing the first draft and it has been edited collaboratively.

#### **3.1 Introduction**

Various chemical and mechanical methods have been utilized for the extraction of crystalline domains from raw materials. The isolation process is largely divided into three steps. In the first step, pure cellulose is separated from the raw materials, then controlled chemical treatment such as acid hydrolysis or use of a solubilizing catalyst allows for the removal of the amorphous region and finally the separation of CNCs from the reaction media. Different carbohydrate-based impurities like reducing and non-reducing sugars, polysaccharides or sugar alcohol can be formed at the chemical treatment stage. The final step is the most crucial for removal of these impurities, which controls the overall product quality[70].

Even though the use of small dosages of CNC can improve hydration and strength of ordinary Portland cement (OPC) pastes, isothermal calorimetry revealed different delays in hydration of OPC pastes containing CNC. Furthermore, as CNC dosage increased so did the magnitude of the hydration delay[8], [33]. There are also observable differences between pastes

containing similar dosages of different CNC types, some delaying the reaction more than others[19], [33].

Cement hydration can significantly be delayed with carbohydrate additives[41]. In addition, retardation time heavily depends on the type of carbohydrate molecule[41]. Sucrose, raffinose or sorbitol are some of the most effective hydration retarders of OPC pastes[38], [41]. For example, a set delay of 2 days can be induced by 0.40 wt% sorbitol or 0.15 wt% sucrose[41]. Thus, if the CNC aqueous solutions (as acquired) have some sugar derivative impurities like carbohydrates, a precise quantitative analysis of carbohydrate impurities in CNCs should be required for cement applications (and any other processes where impurities are an issue).

Different chemical methods are available for sugar analysis depending on the target such as reducing or non-reducing sugar and/or sugar alcohols. Spectroscopic, chromatographic and electrochemical techniques are the most available methods for carbohydrate analysis. Among the several spectroscopic techniques, 3,5-dinitrosalicylic acid (DNS)[71], anthrone[72], and furfural[73] tests are the most common. The DNS assay is based on the Miller method where only reducing sugar can be detected both qualitatively and quantitatively. In this method, the DNS agent forms 3-amino-5-nitrosalicylic acid by reducing the sugar end at high temperatures and the corresponding absorbance can be observed at 540 nm by UV spectroscopy. However, the DNS assay cannot detect trace amounts of reducing ends and misleading results can arise if a mixture of reducing sugars with different chain lengths are being examined. The bicinchoninic acid assay (BCA) can also be used to detect reducing sugar, but the range is 1-100  $\mu\text{M}$  per glucose equivalent reducing end. Both techniques will be used to narrow down the actual concentration. Finally, anthrone derivative absorption is a promising technique for sugar analysis as it is based on the furfural derivative formation through concentrated sulfuric acid treatment[73]. The acid destroys

any long chain structures and form UV active species based on the reactivity of the hemiacetal. The resultant highly conjugated molecules have a distinct absorption at 630 nm.

Electrochemical techniques[74] are a popular method for carbohydrate detection, but are limited by scope of the target molecules (must be electroactive) and need for a suitable buffer system. Thus, these limitations make the detection of non-reducing sugar not viable. Liquid or gas chromatography methods are also widely used for sugar molecule analysis. Methylation of a polysaccharide is a very successful method for sugar identification and quantitative estimation is possible with aid of mass spectroscopy equipped with gas/liquid chromatography capability[75], [76]. However, for a complex mixture solution, GC/HPLC chromatographic separation is not feasible. Compounds having similar retention times as is the case with complex mixtures makes data interpretation of a chromatography column very difficult.

This study utilizes a variety of tests and assays (anthrone, BCA, DNS, CV, HPLC and MALDI-TOF-MS) to identify and quantify carbohydrate concentration in CNC suspensions. The comparison of these techniques revealed differences between the methods with reducing end sugars, oligosaccharides and unknown compounds measured.

## **3.2 Experiments and materials**

### **3.2.1 CNC Materials**

A total of 9 different CNC was subjected to tests. The differences lie both in the method of fabrication and in the raw material. As far as raw materials are concerned, CNC1 through CNC5 were extracted from wood pulp (different batches). CNC6 was extracted from cotton fibers, CNC

7 from algae (*Cladophora*), and CNC8 and 9 from acetate grade dissolving pulp (Western Hemlock).

CNC1 through 7 were extracted through sulfuric acid hydrolysis (64% by weight) at 40°C for two hours. CNC1 and CNC2 are from different batches (1 year apart) of the same material. CNC3, CNC4 and CNC55 are all from another batch (a year newer than CNC1) but purified by 3 different methods. CNC8 and 9 were both extracted by transition metal catalyzed oxidation, using iron and hydrogen peroxide for CNC8, and copper and sodium hypochlorite for CNC9.

After hydrolysis or oxidative degradation, all CNC materials were purified using similar steps:

1. CNC were allowed to sediment, then supernatant was removed and replenished with RO water. This method was repeated until CNC no longer sedimented (below conductivity of 2 mS/cm).
2. The suspension, in their acid conditions, were diafiltrated using a 200 kDa NMWL membrane to a conductivity target of about 500  $\mu$ S/cm to remove acid soluble contaminants such as metal salts.
3. Sodium hydroxide was added to the suspensions to a pH of 10. Diafiltration continued until conductivity reached a steady state, usually around 60  $\mu$ S/cm.

It is believed by the authors that CNC3, CNC4 and CNC5, which were respectively labeled as UF, HS and SD, were CNC samples provided after conducting up to the second purification step for CNC3, all three steps for CNC4 and only the first step for CNC5.

## **3.2.2 Experiments**

### **3.2.2.1 Ultrafiltration**

To separate the CNC from the continuous media and detect the free impurities in the slurry, Ultrafiltration was carried out utilizing an Amicon Stirred Cell Model 8200 equipped with a stirrer, air pressure line and a Millipore<sup>TM</sup> membrane (NMWL: 300,000, Diameter 63.5 mm). All samples were passed through the filter at room temperature and the filtrates were collected in vials.

### **3.2.2.2 Cyclic Voltammetry**

Cyclic voltammetry (CV) was carried out using a CH Instruments 650 Potentiostat. A 1.5 mm diameter Pt working electrode was used, with an Au auxiliary electrode and Ag/AgCl reference in the voltammetric cell. NaCl was used as supporting electrolyte, phosphate buffer with pH 7 and Nano pure water as a solvent.

### **3.2.2.3 Anthrone Assay**

Anthrone solution was prepared by adding 200 mg of anthrone to 100 mL of concentrated sulfuric acid. Working glucose solution was prepared by dissolving 100 mg of glucose (Dextrose) in 100 mL of DI water and from this solution a 10 mL aliquot was dissolved in 100 mL of DI water to obtain the final solution. The standard curve was made according to the Figure 3-2 in the results section. Here, sample assays were diluted in a range of glucose concentrations (20, 40, 60, 80 and 100 mg/L) and 4 mL of anthrone reagent was added to 1 mL of each sample. Absorbance at 630 nm was read by UV-Vis spectroscopy using a Varian Cary 50 Bio UV-Vis, Baseline Zero with Water, 2 mL in disposable cuvettes.

#### 3.2.2.4 Bicinchoninic Acid Assay

There are various assays for quantification of reducing ends with different concentration ranges with this technique. The two assays utilized in this report were Bicinchoninic Acid (BCA)[77] and the 3,5-dinitrosalicylic acid (DNS) based on the Miller method[78]. The BCA method determines the molar concentration of the reducing ends. A temperature dependent reaction occurs and the reducing ends in the carbohydrate sample reduce the  $\text{Cu}^{2+}$  ion from the copper sulfate to  $\text{Cu}^+$ . The range for the BCA assay is 1 – 100  $\mu\text{M}$  glucose equivalent reducing ends. A 100  $\mu\text{M}$  glucose concentration was used as standard. BCA working solution was freshly made according to the method described by Zhang and Lynd[77]. The DNS reagent reacts with the reducing sugars at elevated temperatures to form 3-Amino-5-Nitrosalicylic acid resulting in a change in absorbance. The DNS assay can measure glucose equivalent of up to 1 g/L in the solution (approximately 5 mM). While these methods are efficient in measuring the reducing ends, they cannot differentiate between a monomer and polysaccharide as they both have a single reducing end. Moreover, since these assays do not involve severe acidic treatment or high enough temperatures to breakdown the polysaccharides the quantified amount is expected to be lower.

#### 3.2.2.5 HPLC Analysis

To corroborate the presence of known saccharides in the filtrates, samples were analyzed in the HPLC before and after concentrating by oven drying at 55 °C. The samples were analyzed using an ion exchange Bio-Rad Aminex HPX-87H column (Bio-Rad Laboratories Inc., Hercules, CA) with 5mM  $\text{H}_2\text{SO}_4$  as eluent and flow rate of 0.4 ml/min.

### 3.2.2.6 MALDI-MS and TOF

Matrix-assisted laser desorption/ionization (MALDI) is a Mass spectroscopy technique used to detect molecules over a wide range of molecular weights, especially when coupled with time of flight instrumentation (TOF) the range becomes unlimited. These techniques were used to identify the molecular weights of the molecules detected by the techniques mentioned in the previous sections[79], [80]. Analysis of the filtrates was performed on a Voyager-DE PRO (Applied Biosystems). The matrix used was 2,5-Dihydroxybenzoic acid (DHB). Spectra were obtained in the positive ion mode with an accelerating voltage of 22kV. From the MALDI results, four recurrent ions were selected for MS/MS. Data from these ions was obtained on a 4800 Plus MALDI TOF/TOF Analyzer (Applied Biosystems/MDS SCIEX). The matrix used was 2,5-Dihydroxybenzoic acid.

## 3.3 Results and Discussion

### 3.3.1 Reducing ends

Using cyclic voltammetry, a sample of the filtrate from CNC1 was investigated of reducing species. It should be noted that only electroactive molecules can be responsive for this analysis[81]. A reduction peak is observed at -0.85V position where oxidation was at -1.00V for 20 mV/s scan rate (Figure 3-1). Increasing scan rate separates the peak position between oxidation and reduction state and so electroactive molecules must be present in CNC slurries. It should be noted that the slurry might contained non-reducing end impurities which are not detectable in this technique. Moreover, information of chain length impurities cannot be determined from a complex mixture of impurities until individual voltammogram is known for each impurity.

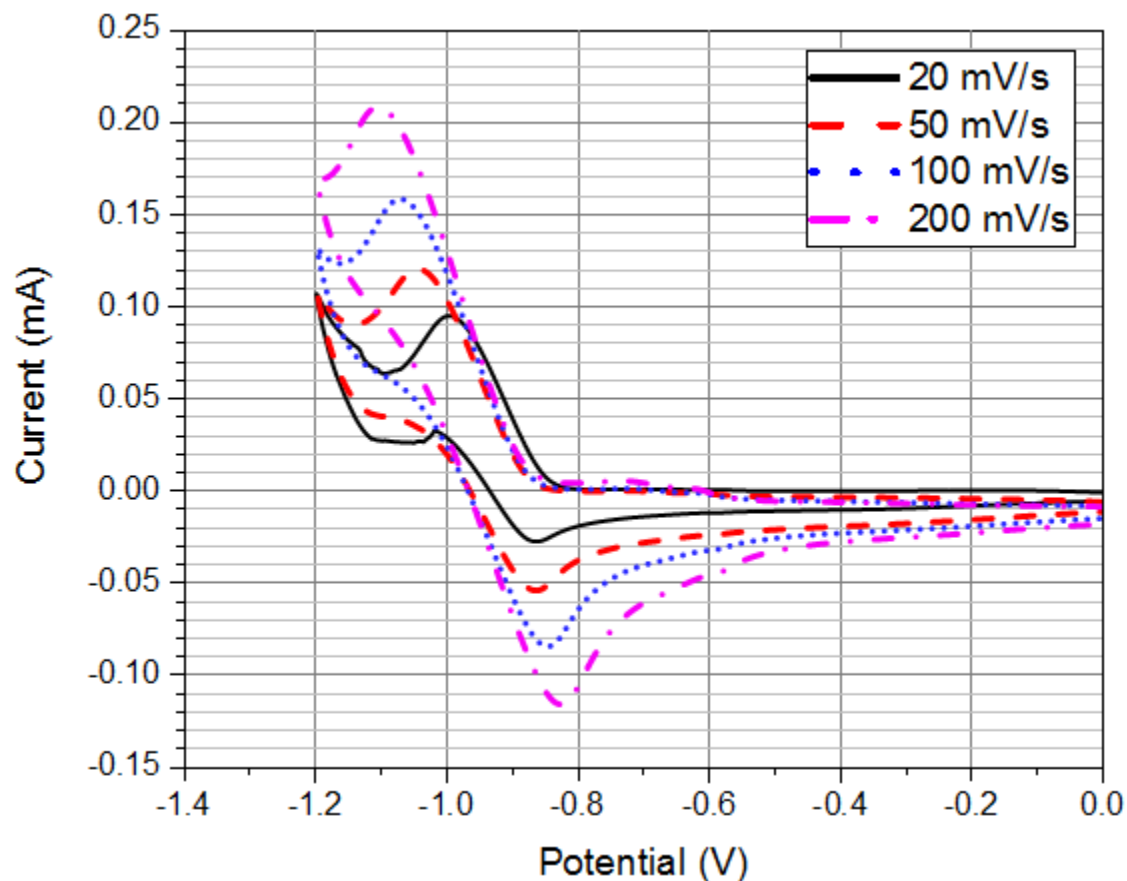


Figure 3-1. Four different scan rates to determine the Cyclic Voltammetry response of CNC1 filtrate.

### 3.3.2 Total amount of foreign sugar- like species in CNC samples

After qualitative detection of impurities, the total amount of sugar-like impurities was measured using anthrone analysis. The determination of free sugars present using anthrone reagent provided an easy and rapid method to assess the sugar-like concentration from various CNC stock solutions. The Anthrone reagent reacts with carbohydrates in the presence of sulfuric acid to furnish a furfuryladenine complex indicative via a greenish color that is responsive at 630nm. Finally, a standard calibration curve is prepared with different known glucose concentrations (Figure 3-2). Due to the anthrone reagent containing concentrated sulfuric acid, CNC crystalline

domains are destroyed, forming furfural derivative. Hence, cellulose nanocrystals must be removed from the aqueous solution before anthrone reagent is added for the analysis.

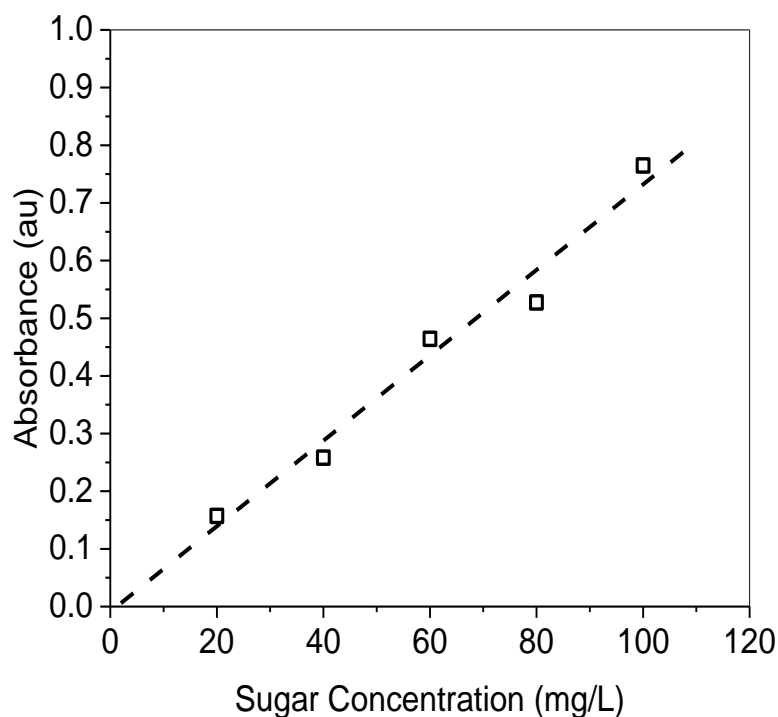


Figure 3-2. Standard calibration for anthrone analysis.

After successful separation of the crystalline domains from the continuous media, by the method described in Section 3.2.2.3, the filtrates from different stock solutions were diluted in a 1:10 ratio and subjected to anthrone analysis. After each analysis, the absorbance at 630 nm (Figure 3-3) was measured and compared with the standard curve. Absorption measurements and the resulting concentrations are shown in Figure 3-3.

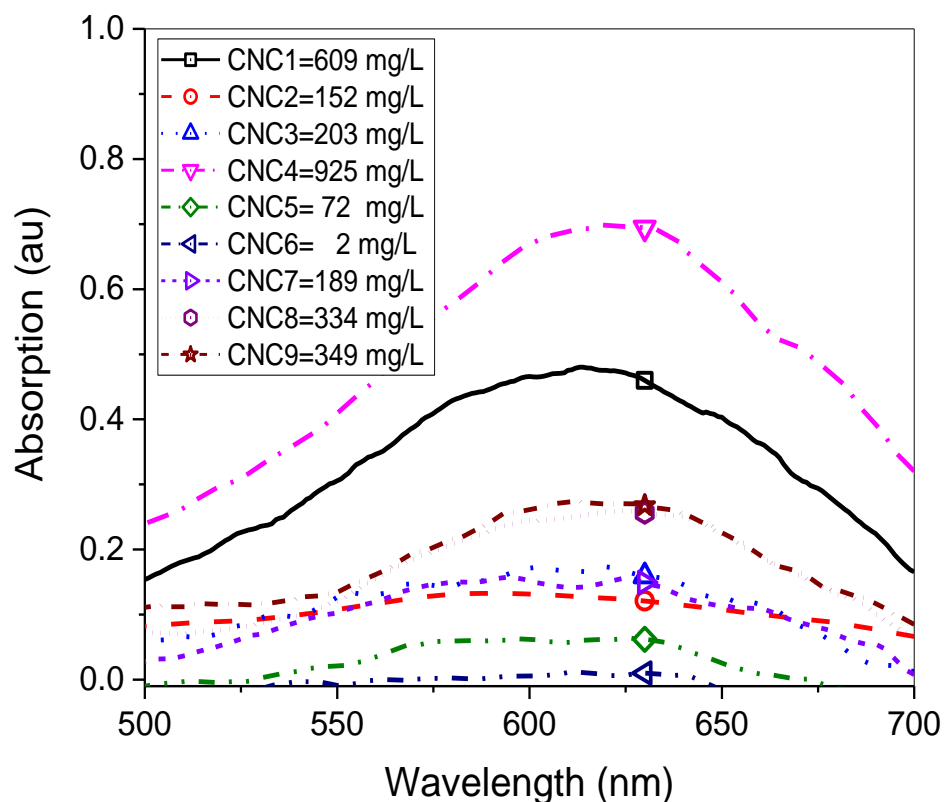


Figure 3-3. Anthrone assay response of filtrates diluted at a dilution factor of 10. Sugar concentration are calculated using the base line form Figure 3-2.

Based on above analysis, we find that CNC4 had the highest concentration with an absorbance reading of 0.69, and at the low end was CNC6 with 0.0091 absorbance. The intermediate concentrations are as follows (from high to low concentrations): CNC1, CNC9, CNC8, CNC3, CNC7, CNC2 and CNC5. It should be noted that, anthrone analysis is responsive to both reducing and non-reducing sugars. Moreover, concentrated sulfuric acid destroys molecular chains of any length and forms single ring furfural derivative. Hence, this analysis

method can be used only to determine the mass concentration, not the types of sugar molecules or chain length.

Remembering what was stated at the end of Section 3.2.1, by comparing the three CNC of the same batch with different filtration method, CNC4 filtrate presented the most sugar-like impurities of them, and CNC5 was the one with the least impurities. If the correlation made from the labels of these materials and de purification processes is true, it would mean that each purification process releases (or detaches) more sugar-like impurities from the CNC.

When comparing CNC1 and CNC2, the differences in the detected impurities could be due to the aging of the material, over time, the impurities and the CNC could have been reattached. This assumption is also consistent with the fact that the CNC4, CNC1 and CNC2 were fabricated by the same methods and using the same raw materials, with a year difference in their manufacture, and the older they are the less impurities were detected in the filtrates.

CNC6 filtrate resulted to be the one with less detected impurities, CNC7 filtrate had a similar response to CNC3. Differences between the response of CNC6 and CNC7 filtrates, and the rest of the CNC, are most likely due the origin of these materials and the CNC affinity to bind with these impurities. Although the fabrication of CNC8 and CNC9 was also a year apart, the response of these filtrates was similar. They are also made from a different raw material and fabricated by different processes than the rest of the CNC.

### **3.3.3 The amount of reducing sugars in CNC samples**

In addition to quantifying the sugars, the presence of the types of sugar molecules in the filtrate was investigated through DNS assay. Initial reducing end assay results were distorted due to the presence of CNC particles in the filtrate. After centrifuging the nanoparticles out, the filtrate

was analyzed by the DNS assay but the amount of reducing end in the sample was lower than the detection range of DNS assay. BCA analysis confirmed the presence of reducing ends. It has to be noted that the BCA assay is not efficient in quantification of polysaccharides as only the reducing ends are measured. Hence, a reducing end in a long chain and in a single glucose monomer would have the same response. Table 3-1 shows the quantification of reducing ends based on the BCA glucose standard and converted into glucose equivalent mg/L with the assumption that the detected reducing ends belong to a Glucose molecule. The samples were diluted at different factors to bring them within the range of the standard curve readings.

Table 3-1. Results of the BCA reducing end analysis. Values in the last columns were calculated under the assumption that every reducing end detected, is from a monosaccharide.

<b>Sample ID</b>	<b>Original Sample Weight</b>	<b>Sample Weight after drying</b>	<b>Concentration Factor</b>	<b>Average AU</b>	<b>Glucose equivalent (<math>\mu\text{mol/ml}</math>)</b>	<b>Equivalent Glucose (mg/L)</b>
<b>CNC1</b>	3.6	3.6	1	2.246	124.3	22.4
<b>CNC3</b>	5	5	1	0.778	43.2	7.8
<b>CNC5</b>	8.3	2.9	0.35	0.24	13.5	2.4
<b>CNC6</b>	26.36	15.64	0.59	0.896	49.7	8.9
<b>CNC7</b>	10.83	4.76	0.44	1.124	62.3	11.2
<b>CNC8</b>	8.72	2.28	0.26	1.964	108.7	19.6
<b>CNC9</b>	14.75	6.88	0.47	2.05	113.5	20.4

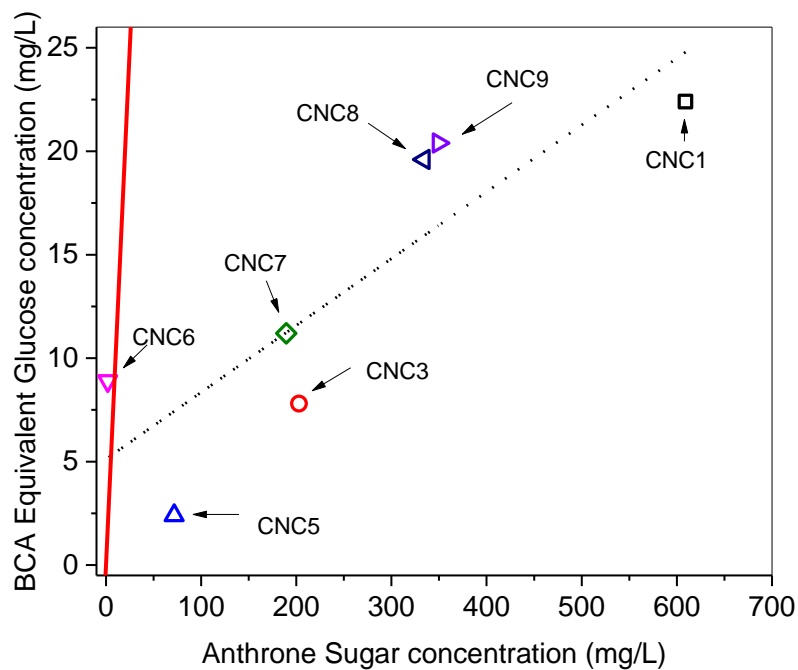


Figure 3-4. Sugar concentration measured by anthrone assay are compared with the Glucose concentration assumed by the BCA results. Dashed line fits the proportion of the total sugar rings detected and the sugar rings with a reducing end. Solid red line represents the 1:1 proportion of sugar rings and reducing ends.

Figure 3-4 shows the relationship between Anthrone and BCA results. As Anthrone measures the number of sugar rings and BCA measures the number of reducing ends, it is clearly shown that in most of the materials, there are 17-40 times more sugar rings than reducing ends. Figure 3-4 also evidences that not all detected sugar rings have necessarily a reducing end, as it was assumed in Table 3-1.

There is however one anomaly, CNC6 displays more reducing ends than sugar rings and an average molecular weight under 180 Da. One explanation for this observation is that BCA could be detecting other materials that are not detected by Anthrone, a molecule that could reduce the copper in the copper sulfate pentahydrate which BCA detects, such as vegetable proteins[82], [83].

We could assume that every polysaccharide chain has a reducing end and calculate an average Molecular Weight of the carbohydrates detected, or we could assume that there are 40 times more non-reducing sugars than reducing sugars. However, Anthrone and BCA essays don't provide any evidence that supports any of these assumptions.

### **3.3.4 Identification of different types of sugar molecules**

In order to have a better idea of the nature of the detected molecules, HPLC measurements were conducted. The results showed some known peaks in a couple of the materials tested (glucose, cellobiose), but mostly peaks with retention times characteristic of large molecules, larger than any of the standards from the suspected oligosaccharides (Cellobiose, Glucose, Xylose, Arabinose, Acetic Acid).

Another explanation of the longer peak retention times in most samples (as compared to monomeric 5 and 6 carbon sugars) showed in Figure 3-5, is that in addition to the detected polysaccharides there were various oxidized carbohydrate components. The ionic interactions between oxidized carbohydrates and the stationary phase can explain the longer retention in the H column used in the HPLC.

The unavailability of such charged components in the HPLC standard meant that they were not quantified but served a qualitative proof of presence of impurities only, with a rough estimate of the low amount based on the y-axis coordinate. The oxidized carbohydrates could be a consequence of the chemical method used to produce CNC[10].

The HPLC runs were able to measure 77 mg/L Glucose in CNC7 and 234 mg/L Cellobiose in CNC8 (Figure 3-5). Note that although the chromatograms confirm the presence of other impurities with differing molecular weights (just as in CNC4 from Figure 3-5) it is impossible to quantify them without knowledge of their structure. Small peaks with longer retention times than

a disaccharide (cellobiose) are observed in the chromatograms of the rest of the samples (All HPLC results are presented in section 0). While the peak areas are not necessarily representative of the amount of material measured, they may be attributed to oligosaccharides which are oxidized during the CNC production process. Oxidation of oligosaccharides can lead to charged groups on the surface leading to interaction with the stationary phase in the HPLC column and an increased retention time. Without means of identifying these compounds for a standard solution, HPLC is not capable of quantifying them.

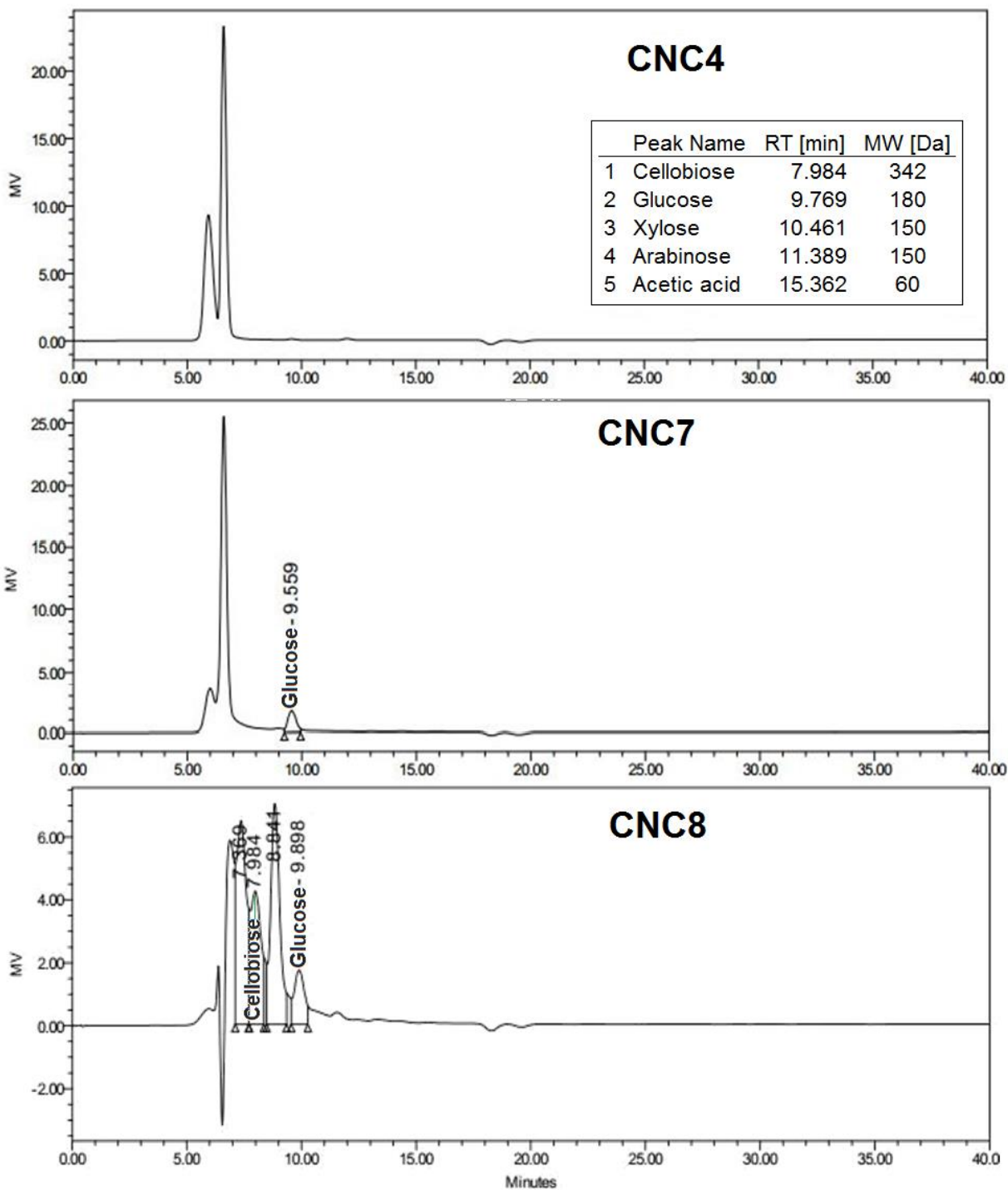


Figure 3-5. Selected HPLC Results of CNC filtrates. Peaks with retention times similar to known molecules are indicated. Standard molecules and retention times are shown at the bottom right corner.



Given the original assumption that the molecules we are seeing are polysaccharides, the NIST Chemistry WebBook[84] was used to narrow the obtained molecular weights to documented carbohydrates. However, the combinations would be endless, as there are hundreds of documented carbohydrates with each of the obtained molecular weights. Despite the complication, there are a couple interesting observations within the 273-274 ions: While there was no C-H-O molecule that matched the 273 or 274 molecular weights, if nitrogen was added to the formula, several matches (aminoacids, nitrates, and nitrate esters) appeared. Although the origin of aminoacids or even the mere presence of Nitrogen in these materials is not clear, these are two more examples of the possibilities mentioned at the end of section 3.3.3, where a molecule could be detected by BCA but not by Anthrone assay.

Sample Name	CNC4	CNC1	CNC3	CNC2
Selected Molecular Weight [amu]	<b>273</b>	<b>372</b>	<b>413</b>	<b>551</b>
MS/MS detected Fragments [amu]	136	10	112	154
	137	173	140	159
	161			
	Dextrose MW 180 amu			
	198		238	

Figure 3-7 MS/MS. Result from selected MALDI Ions. Dextrose is pointed out to show the proximity of the detected fragments to a single ring saccharide.

Once again, the results obtained by MS/MS did not match the expected single ring molecular weight, but yielded unexpected values around it. Taking into account the different measured characteristics of the detected impurities, finding an exact match for the molecules detected by MALDI that could also break into the fragments detected by MS/MS, with the same retention times as the molecules detected by HPLC, would be not only be time consuming but improbable. On the other hand, if the CNC are going to be used in an application concerned by the presence of specific molecules, with MALDI responses similar to the detected ions, and links of the size of the fragments detected by MS/MS, the combination of these two methods could be useful to confirm its presence.

### **3.3.5 How washable are the impurities.**

To get an idea of how much of the impurities can be washed out, four materials (CNC2, CNC6, CNC4 and CNC9) were selected to be separated from the continuous media through the process described in section 3.2.2.1.

To make the slurries more fluid, 40-45ml samples were dispersed using a sonic mixer (Branston Digital Sonifier Model 102C) for 2 minutes at 30 % intensity and 1 s on/off intervals inside an ice bath, next samples were mixed using a vortex mixer (BV1000 BenchMixer). Then, after approximately 12 hours of filtration, filtrates were collected and weighed, so the same mass of water could be replenished using nanopure water ( $>18\text{M } \Omega/\text{cm}$ ). The remaining slurries inside the filter were of a higher concentration than the initial samples, after replenishing the water, these had to be redispersed using the previous method of ultrasonication and vortex mixing up to five times until a fluid and homogeneous slurry was obtained. Samples were washed 5 times by this process and filtrates were saved to perform Anthrone assays to measure the washability of the impurities.

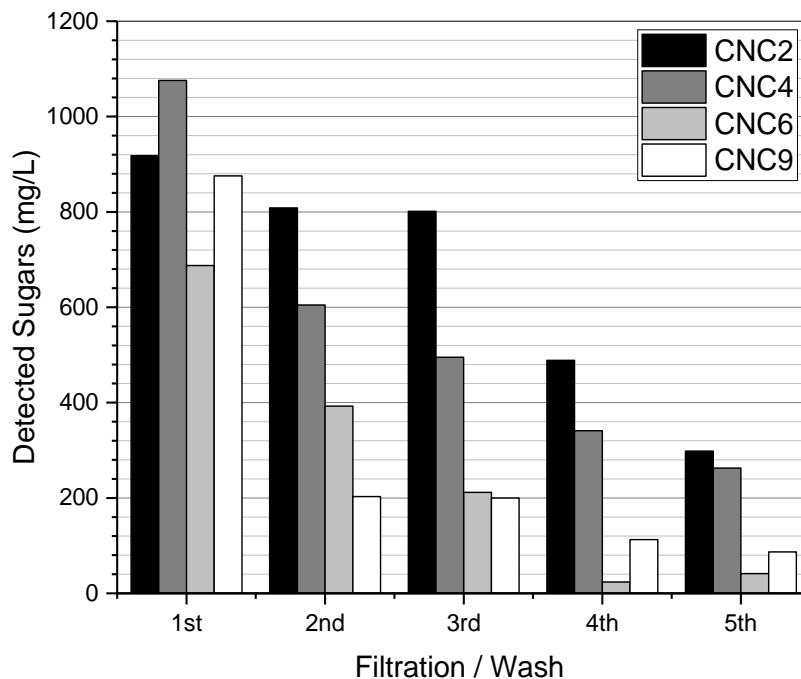


Figure 3-8. Sugars detected by anthrone assay in CNCs washed 5 times with ultrasonication before every filtration.

The results in Figure 3-8 show that the impurities can be washed away from the slurries. Another aspect is that the amount of detected impurities in these samples (first wash) do not keep the same proportion between CNC samples, nor the values are the same as the ones obtained in section 3.3.2. An explanation for these differences is the high amount of energy exerted, since the first wash, by the sonication to redispersing the remaining slurry, This is also consistent with the similar amounts of impurities detected in some of the CNC's 2nd and 3rd washes, as sugars continue coming out of the CNC domains as the ultrasonication energy keeps being exerted. This experiment confirms that the sugars in the CNC slurries can be washed away. However, it is observed that the amount of impurities can be decreased with every successful washing, but complete removal is almost impossible. It is assumed that ultrasonication may introduce additional impurities by the cleavage of the amorphous region of the crystalline domains. The adsorption behavior of CNC domains can be effected from this proposed phenomenon as the disassociated

impurities (the free amorphous regions) can reassociate via hydrogen bonding of its surface OHs back to the CNC scaffold. Thus, although additional washes may reduce some impurities from the slurry, the strong H bonding prevents full deattachment of the impurities.

### **3.3.6 What can we know about the impurities in CNC slurries.**

After the results of all the experiments in this work, several questions about the nature of the impurities in CNC slurries can be addressed by the thought process listed in Table 3-2.

Table 3-2. Information obtained in this work.

Question	Method and Answer
Are there reducing sugars?	CV detected the presence of reducing ends.
How many Reducing ends?	BCA detected different concentration of reducing ends for each sample, however, no information about the rest of the molecule is provided by these results. A concentration can be inferred if Glucose molecules are assumed.
How much sugar is there?	Anthrone assay proved being an easy and reliable method to measure the free sugars in the filtrate. The impurities content could be related to aging, production and purification method.
Are there any Known sugars?	HPLC detected very few of the suspected saccharides, most of the molecules detected had a retention time characteristic of molecules larger than a disaccharide.
Exactly how big are they?	MALDI detected several ions in the range of one to four sugar rings molecules. No exact match of a traditional oligosaccharide was found. However, four ions were detected in almost all the samples tested.
Can single rings be obtained through fragmentation?	MS/MS showed how the previously detected ions fragmented into two or three smaller molecules. No fragment was an exact match for a single glucose ring.
Can the impurities be washed away?	Ultrasonication and Ultrafiltration can be used several times to reduce the amount of impurities in the CNC slurries. It is possible that Impurities keep appearing after several washes due to amorphous regions being cleaved from the crystalline domains.

### 3.4 Conclusions

This work originated from the suspicion of the existence of impurities in the form of free sugars in the CNC slurries. After the CNC were separated from the continuous media by ultrafiltration through a 300 kDa membrane, several chemical assays were conducted to confirm the existence of carbohydrate contaminants in the CNC slurries. Chemical methods also helped to characterize the impurities and provided valuable information about their nature.

It was found that there were free reducing sugars in the slurries, but also other oligosaccharides were detected, so a more comprehensive technique than a simple sugar test or a conductivity measurement is needed to detect and quantify these contaminants. Anthrone assay proved to be useful tool for determining the content of carbohydrate contaminants.

The exact determination of the nature of the impurities is highly unlikely. Although, the amount of detected impurities by anthrone assay were small (under 0.1 wt%), if the desired application demands a high purity, or if it requires the absence of a particular component with a known response to the methods presented in this work, impurities can be washed away following the methodology described in Section 3.3.5. The impurities appeared to be bound to the CNC, thus it should not be assumed or expected that these impurities would come out as easy as glucose or salts. Therefore, ultrasonication in between washes is advised to facilitate this process.

## 4. RETARDATION EFFECTS OF CELLULOSE NANOCRYSTALS (CNC) IN PORTLAND CEMENT PASTES

This section is the application of the results from previous chapter to cement. It is all my doing except for the experiment that resulted in Figure 4-7, performed by Yvette Valadez at Oregon State University.

### 4.1 Introduction

Cellulose Nanocrystals have been studied as a cement additives, resulting beneficial to characteristics like workability[19], strength and hydration[8], [33], microstructure[85], and (earlier in this document) paste stability. In a previous work, Fu *et al.*[33] found that by using 0.2% addition by volume, the cement flexural strength can be enhanced up to 19% after 7 days of hydration, and from 2% to 50% after 28 days of hydration. It was also found that every CNC added delayed the cement hydration in its own way, and that as the dosage increased so did this delay effect.

The CNC that worked the better for Type V cement, did not necessarily work as well for Type I/II, and the CNC that at 0.2% increased the flexural strength of Type V cement the most, delayed the cement hydration for over a week used at a 1% dosage (the paste did not set)[33]. This effect became of a concern as the same material that was used at low dosage as a strengthening additive, when used in higher dosages, delayed the hydration of cement in a similar fashion as known cement retarders[38], [41]. Because of these concerns, the presence of contaminants in the form of free sugars was suspected in the CNC slurries, and the previous chapter provides an extensive description of the efforts made to remove and understand the nature of these impurities.

Isothermal calorimetry is a useful tool to measure the heat release rate and the total heat of cement hydration, and it is commonly used to investigate the effects of additives on the hydration of cementitious materials[86], [87].

In this chapter, we combined the previous ultrafiltration and anthrone essays techniques with isothermal calorimetry to assess the effects of the presence, and absence, of the detected impurities.

## **4.2 Experimental and Materials**

### **4.2.1 CNC and Cement**

In this chapter, 4 different CNC materials were used. CNC1 and CNC2 were provided from the USFS Forest Products Laboratory, and CNC3 and CNC4 were provided from Blue Goose Biorefineries Inc. The methods used to degrade the amorphous regions of the cellulose used to produce these materials were 64% sulfuric acid hydrolysis for CNC1 and CNC2, and transition metal catalyzed hypochlorite oxidative degradation for CNC3 and CNC4. The raw materials used, to extract these CNC from, were wood pulp for CNC1, cotton for CNC2, acetate grade dissolving pulp for CNC3, and raw wood for CNC4.

After degradation was carried out, the CNC had to be isolated from the dissolved cellulose. The steps are described in Section 3.2.1 from the previous chapter. CNC3 is the same material used by Fu *et al.*[33] that delayed the hydration of Type V cement the most, and CNC4 is a similar production method as CNC3 but as it used wood instead of cellulose pulp as a starter material, the degradation required more hypochlorite, more raw material and more time than CNC3.

The cement used in this work, is a Type V cement, particularly a Class H cement, used for oil well casing because it has a better performance at high temperatures and pressure[88], [89]. This cement is the same used before in Chapter 2, and its composition is listed in Table 2-1.

## **4.2.2 Experiments**

### **4.2.2.1 Ultra-filtration and sugar detection.**

The CNC samples were vigorously dispersed using a Branston digital sonifier (Model 102C) for 1 minute at 30% intensity in an ice bath, then samples were mixed using a vortex mixer (BV1000 Bench Mixer). This process was repeated until the slurry looked with similar viscosity as water.

For this work, slurries were filtered using a different device and a different membrane than in the previous chapter. The filter used was a Sterlitech HP 4750 stirred cell under compressed air pressure. The membrane used was PS35 Sterlitech Corp. with a 20kDa NMWL. This membrane is of a smaller pore size (and NMWL) than the one used in the previous chapter (Millipore™, 300 kDa NMWL).

Water was replenished, and the slurry was dispersed again by ultrasonication and vortex until a dispersed slurry was obtained. Each slurry was washed 5 times. Filtrates were collected and saved for anthrone analysis as described in Section 4.2.2.3. A small sample of the re-dispersed slurries after the first and 5<sup>th</sup> wash was also saved to be used with cement.

#### **4.2.2.2 Paste Preparation.**

The CNC concentration of the collected slurries from the first and fifth washes was determined by thermogravimetric analysis (TGA, TA Instruments, Newcastle, DE). Using a Nitrogen purged-furnace, a small drop of the slurry (approximately 30mg) was placed in a platinum crucible and heated at 10 °C/min up to 110 °C, this temperature was held for 15 minutes. TGA was run 3 times per slurry to get an accurate weight percentage.

The selected dosage of CNC was added to 50 grams of dry cement powder, then the rest of the water was added to have a 0.36 water to cement ratio (w/c). Paste was manually mixed with a stainless-steel spatula before being mixed in a centrifugal planetary mixer (Flack-Tek Speed mixer) at 2000 rpm for 120 s.

#### **4.2.2.3 Isothermal Calorimetry**

The prepared pastes were then poured in 20ml glass ampules and closed using an aluminum cap seal disc. Ampules were weighed before and after pouring the paste to get the sample mass (approximately 14 g). Samples were tested in a TAM Air system (IC, TA Instruments, New Castle, DE, USA). The testing chamber was set at  $23 \pm 0.03$  °C and had a stable base line. Heat of hydration was measured over 3 days (72 hrs.). Heat values were then normalized by the weight of dry cement in the sample.

## **4.3 Results and Discussion**

### **4.3.1 Anthrone Assays**

The collected filtrates were tested by anthrone assay. The results shown in Figure 4-1 are different and smaller than the results from the previous chapter (Figure 3-8). A smaller pore size membrane, than the one used in the previous chapter, was purposely selected because of the suspicion of some small crystals passing through it. It was previously stated that a complete removal of the detected impurities will be difficult as the energy exerted on the CNC could cleave off the amorphous regions as no CNC is 100% crystalline[50]. By using a smaller pore size, the sugars in the filtrate are expected to be more oligosaccharides than actual crystals.

Overall, these results show that the sugars in the slurry can be reduced by ultrafiltration and ultrasonication. It is expected to see some differences in the next section as, the more times the slurry is washed, the less sugars will be added to the cement paste.

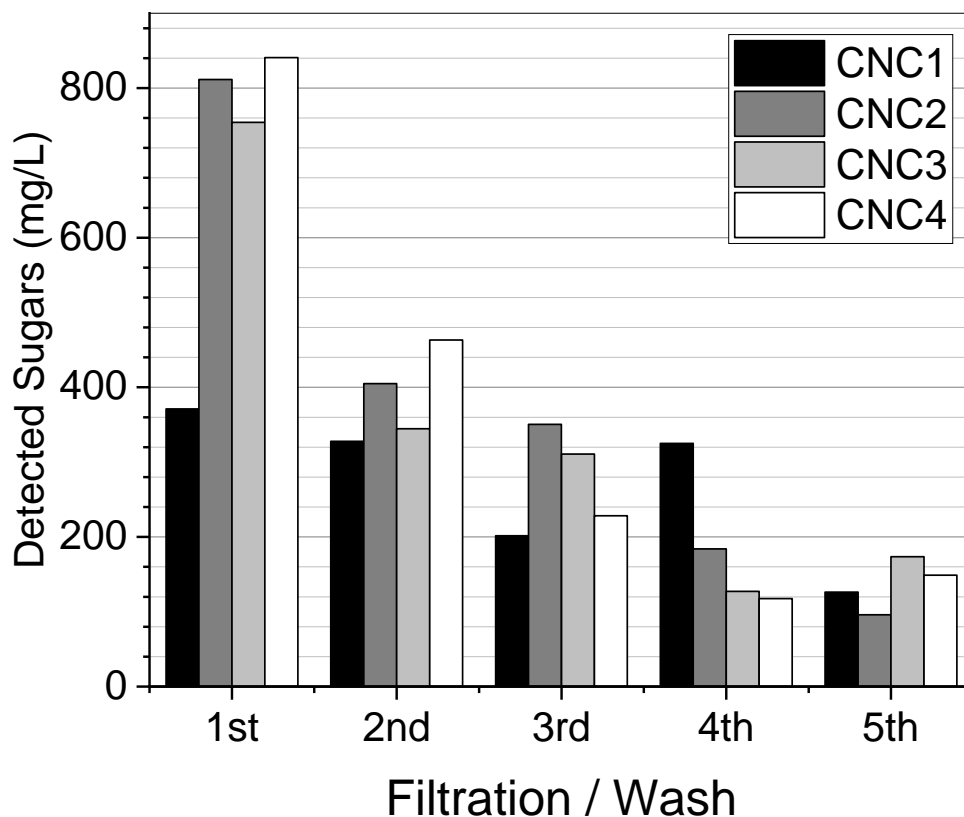


Figure 4-1. Sugars detected by anthrone assay of 5 consecutive washes of CNC slurries. Samples were ultrasonicated and vortexed before every filtration.

#### 4.3.2 Isothermal Calorimetry

Cement pastes were analyzed by isothermal calorimetry to observe the effect of washing away free sugars from the CNC slurries. Figure 4-2 and Figure 4-3 show the heat release rate of pastes made using Type V cement with 0.36 w/c and 1% CNC1 and CNC2 addition respectively. These two CNCs have sulfate half esters functional groups as consequence of their fabrication method[10] (sulfuric acid hydrolysis). As it is expected, pastes with CNC show a delay in the hydration peak. When these CNC are washed the delay increased, a small amount for CNC1 (Figure 4-2), who initially delayed hydration peak for over 5 hours, and after being washed, one

and five times, the delay increased for 10 and 12 minutes respectively. CNC2 (Figure 4-3) initially delayed hydration for only 3 hours, but after being washed one and five times, the delay respectively increased 13 minutes and 1 hour. Although it was expected to observe a decrease in the delay time, the opposite effect was observed.

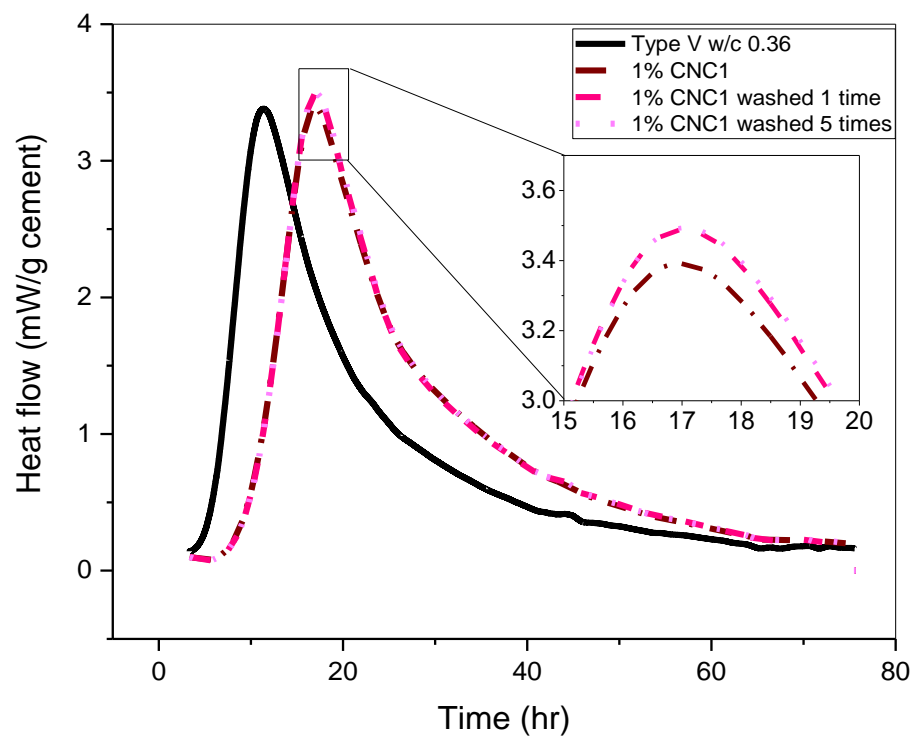


Figure 4-2. Heat release rate of Type V cement pastes with CNC1 addition. Pastes made using 0.36 w/c and 1% by volume CNC as acquired, washed 1 time and washed 5 times.

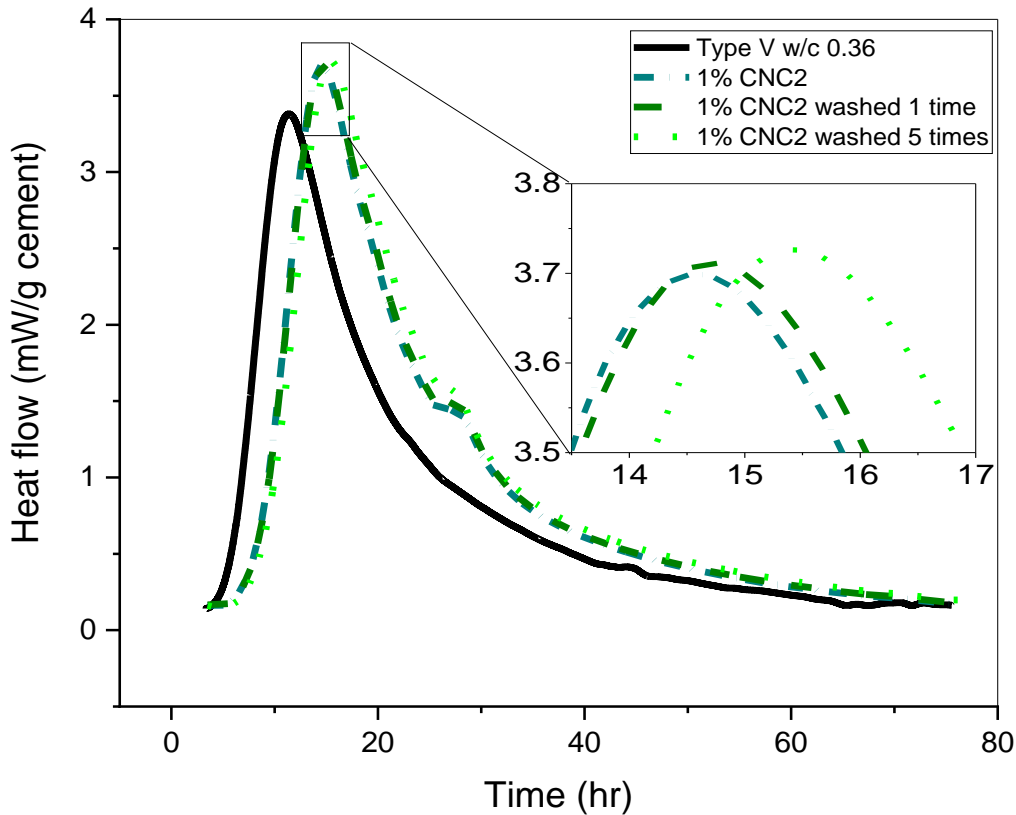


Figure 4-3. Heat release rate of Type V cement pastes with CNC2 addition. Pastes made using 0.36 w/c and 1% by volume CNC as acquired, washed 1 time and washed 5 times.

The delay observed in pastes containing dosages of CNC1 and CNC2 were not of a concern[33]. As the result show, the nature of the detected impurities didn't appear to contribute to the observed delay. The increase delay is to be expected from these materials if we consider that the higher the CNC dosage, the more delay is observed, and if we remove the free sugars (impurities), the more CNC will be in a gram of slurry, and the more impurities we remove, the bigger the difference will be.

If it is assumed that all carbohydrates detected in the washes from Figure 4-1 are impurities, a new (higher) CNC concentration can be calculated for the remaining slurries. If the original concentration of CNC1, CNC2, CNC3 and CNC4 were 11.9%, 11.4%, 8% and 5% respectively, the concentration after washes are presented in Table 4-1, and the new dosages can also be calculated, and are shown in Table 4-2.

Table 4-1. New CNC wt% of the washed slurries.

Wash	CNC1	CNC2	CNC3	CNC4
1st	11.94%	11.48%	8.08%	5.08%
2nd	12.01%	11.60%	8.19%	5.21%
3rd	12.10%	11.76%	8.33%	5.37%
4th	12.22%	11.93%	8.48%	5.53%
5th	12.35%	12.12%	8.65%	5.71%

Table 4-2. Resulting dosages from purified slurries (when used as the original wt% to get a 1% by volume of cement).

Wash	CNC1	CNC2	CNC3	CNC4
1st	1.00%	1.01%	1.01%	1.02%
2nd	1.01%	1.02%	1.02%	1.04%
3rd	1.02%	1.03%	1.04%	1.07%
4th	1.03%	1.05%	1.06%	1.11%
5th	1.04%	1.06%	1.08%	1.14%

By using the results from Fu *et al.*[33] for the hydration peak delay observed in pastes made using Type V cement and containing different dosages of CNC1(Figure 4-4), and the information from Table 4-2, the expected differences in hydration peak delay of pastes with CNC1 dosages can be calculated. The difference in peak hydration delay are 23s for CNC1 washed 1 time, and 5min for CNC1 washed 5 times. These results are shown also in Table 4-3.

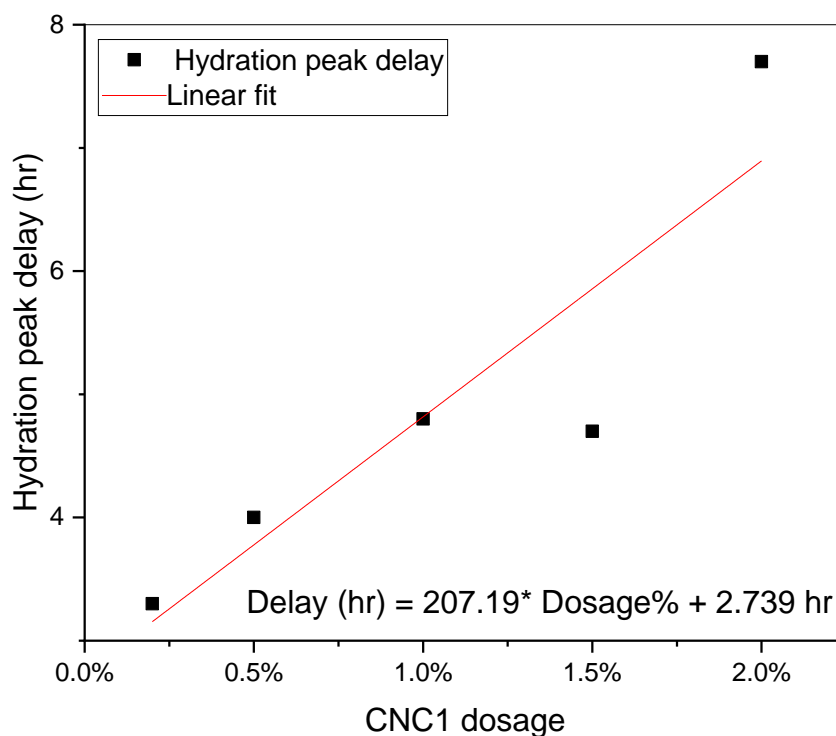


Figure 4-4. Relationship between CNC1 dosage and hydration peak delay, from the work of Fu et al.[33]

As expected from the observations made by Fu *et al.*[33], the pastes prepared with 1% CNC3 addition didn't set like the previous pastes, Figure 4-5 shows how no significant heat release was observed during the 75 hours that the experiment was done (<5 J/g over 3 days). The filtrate from the 5<sup>th</sup> wash of CNC3 had 173 ppm sugar rings, and the dosage used in the paste was 1% CNC by volume, which is around 0.5% by weight, so considering only the sugars detected in the 5<sup>th</sup> filtrate, the paste containing 1% CNC3 by volume had less than 1 ppm sugars in cement. These calculations suggest that the free sugars in the CNC3 slurry (if at all) are not entirely responsible for the observed delay.

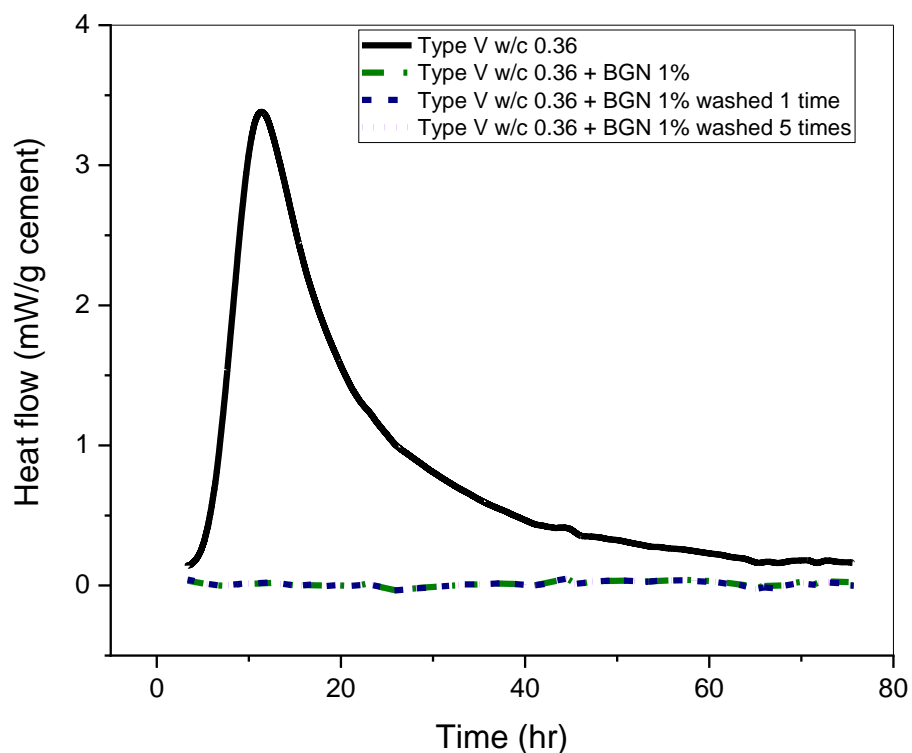


Figure 4-5. Heat release rate of Type V cement pastes with CNC3 addition. Pastes made using 0.36 w/c and 1% by volume CNC as acquired, washed 1 time and washed 5 times.

To observe a traditional heat rate release within a 3-day window, similar cement pastes were prepared with a 0.2% CNC3 dosage and measured by IC. The heat released was now observed in a similar magnitude as the previous CNC at a higher dosage.

The results in Figure 4-6 show that even at a low dosage (0.2% CNC), the hydration delay was of more than 10 hours. The pastes containing washed CNC3 show a decrease in the hydration delay time of 49 minutes when washed 1 time, and more than 2 hours difference when washed 5 times. These differences suggest that the sugars removed from CNC3 slurry by ultrafiltration,

played a more evident role in the observed retardation effect than the sugars removed from the CNC made through acid hydrolysis.

During the production of CNC3, hypochlorite could have caused the oxidation of glucose molecules (from cellulose), breaking them up into carboxylic acids (which are a known cementitious material retarder[44]–[46]), these acids could be strongly attached to the CNC surface as functional groups[10], and removing them from the CNC appears to be a harder task than the efforts made.

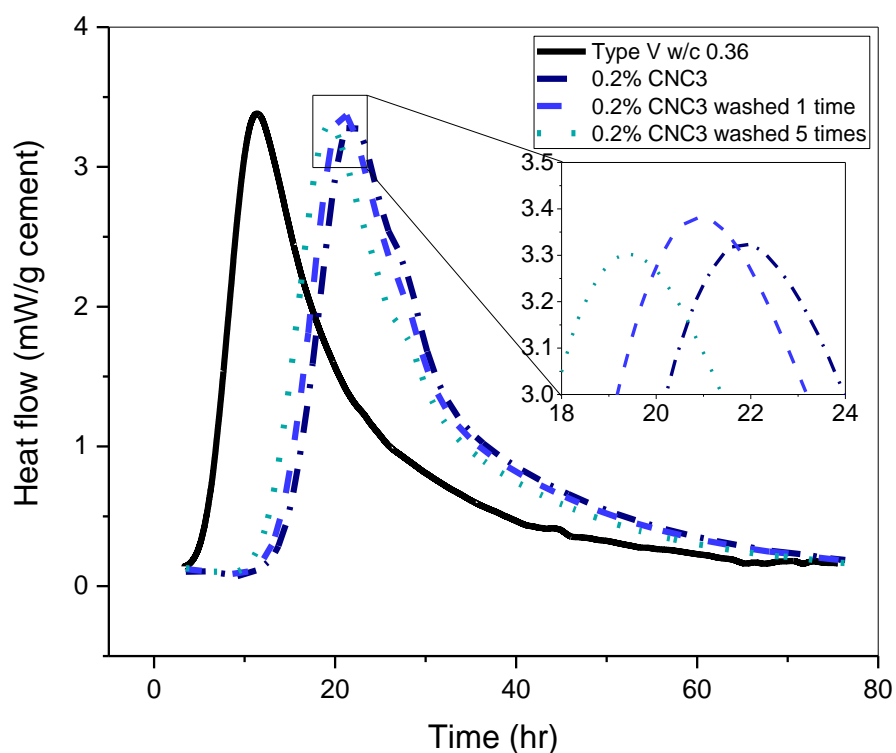


Figure 4-6. Heat release rate of Type V cement pastes with CNC3 addition. Pastes made using 0.36 w/c and 0.2% by volume CNC as acquired, washed 1 time and washed 5 times.

The other CNC made by oxidative degradation (CNC4) was acquired as a part of another project where various producers used their nanocellulose production methods on recycled sources of cellulose to find the best suited material to use in the concrete of a bridge deck. The most evident difference between CNC3 and CNC4 is that CNC3 is of a clear color and CNC4 has a slight brown color, which suggest that is not completely delignified.

To confirm that the chemical nature of the CNC made using oxidative degradation played a role in the retardation of cement hydration, cement pastes with a 0.35 w/c, containing 0.2% by volume CNC4 were prepared and analyzed by isothermal calorimetry. Heat of hydration was measured over 6 days.

Table 4-3. Heat release peak retardation of pastes made with 0.36 w/c and CNC. Values in Delayed column are from neat paste for Unwashed materials and from the Unwashed CNC for the washed ones. Bold blue numbers are the calculated delay increments using the values from Table 4-2 and the trend calculated in Figure 4-4.

Heat release peak of paste made using Type V 0.36 w/c, 11:23 hrs after water addition						
	Unwashed		Times washed			
	Peak	Delayed	Peak	Delayed	Peak	Delayed
CNC1	16:48	+5:25	16:57	+0:09 <b>(23s)</b>	16:59	+0:11 <b>(5min)</b>
CNC2	14:40	+3:17	14:53	+0:13	15:47	+1:07
CNC3	21:35	+10:12	20:46	<b>-0:49</b>	19:23	<b>-2:12</b>

The heat flow measurements from Figure 4-7 only show the hydration of cement pastes containing CNC, the reference used this time was a paste containing 0.2% CNC3. The addition of CNC4 retarded the cement hydration for more than 10 hours over the hydration peak of the paste containing CNC3 washed 5 times. After washing CNC4 1 time, retardation was reduced for more

than 4 hours, and after being washed 5 times, peak of hydration occurred more than 8 hours before the peak from the unwashed slurry.

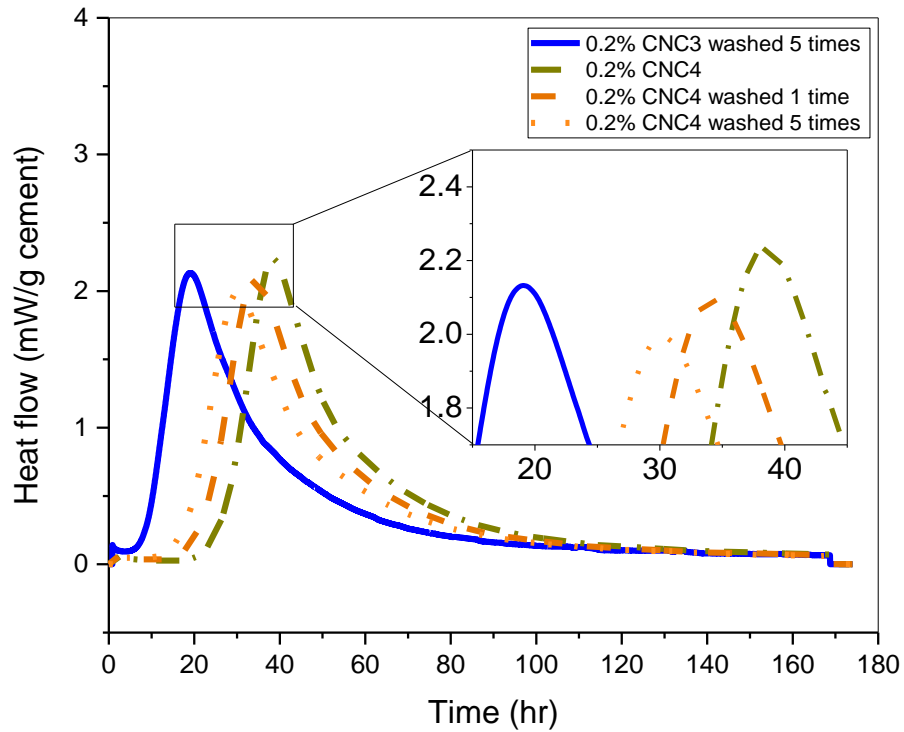


Figure 4-7. Heat release rate of Type V cement pastes with CNC3 and CNC4 addition. Pastes made using 0.35 w/c and 0.2% by volume CNC4 as acquired, washed 1 time and washed 5 times.

From the results of Fu *et al.*[33], we know that Type V cement pastes with a 0.35 w/c, and 0.2% CNC3 show a hydration peak at 24 hours after water is added (12.6 hours more than paste without CNC), if this CNC is washed 5 times, hydration peak occurs more than 4 hours earlier (Figure 4-7). The pasted containing 0.2% CNC4 presented both the highest delay in hydration and the highest differences between pastes containing washed and unwashed CNC, 26.8 hours when unwashed, 22.6 hours when washed 1 time, and 18.5 hours when washed 5 times (Table 4-4). The

suspected origin of this abrupt difference is the presence of lignin (as it was mentioned before because of the brown color). Lignin derivatives had been studied as plasticizers[47] and it has been found that some of these lignin based additives (as most carbohydrates) delay cement and mortar setting times [31].

Table 4-4. Heat release peak retardation of pastes made with 0.35 w/c and CNC. Values in Delayed column are from neat paste for Unwashed materials and from the Unwashed CNC for the washed ones.

Heat release peak of paste made using Type V 0.36 w/c, 11:42* hrs after water addition						
Times washed						
Unwashed		1 time		5 times		
	Peak	Delayed	Peak	Delayed	Peak	Delayed
CNC3	24:25*		N/A	-	19:20	-5:05
CNC4	38:32	+26:50	34:18	-4:14	30:10	-8:22

\*Results from Fu *et al.*

#### 4.4 Conclusions

Four different CNCs were, ultrasonicated and washed by ultrafiltration, 5 times. Samples after the first and fifth wash were saved to be used in cement pastes. The filtrates obtained from each wash were analyzed by anthrone essay to measure the amount of free sugars removed from the CNC slurries. The sugars detected after the fifth wash were in the order of 20 mg/L. The heat released from the cement pastes with: not washed, washed once, and washed five times CNCs, was compared to determine if the removed free sugars were responsible for the retardation effects observed in previous work.

Results suggested that free sugars in CNCs made through sulfuric acid hydrolysis are not responsible for the observed delay, but slightly prevents it by replacing CNCs, which do delay cement setting.

The pastes containing CNCs made from oxidative degradation showed a reduction in the retardation effect when washed 1 and 5 times, as carboxylic acids could be present in the slurries because of the degradation mechanism. Residual lignin from one of these CNC was also suspected to cause an even longer delay, as the differences between not washed and washed 5 times was 60% more than the apparently delignified CNC.

## **5. CELLULOSE NANOCRYSTALS CHARACTERIZATION**

This section compiles experiments carried out as part or because of the previous studies, however they were not finished in order to form another chapter, or they were not part of the previous chapters in a fundamental way. It is expected that the results shown here may be useful in the future, whether for work in progress or future work.

All the work presented in this document follows the intent to learn about the CNC properties, select the best CNC for cement related applications, and identify what makes this CNC better than others. Previous chapters suggested that the CNC manufactured by USFS Forest Products Laboratory, and Blue Goose Biorefineries Inc. had the best performance as cement additives, however the one property that made them stand out from the rest was not fully understood.

Several attempts were made to identify the CNC properties that worked the best for plasticization, viscosity modification, strengthening and hydration enhancement. This section presents different measurements made to the CNC materials used during the previous years. The results in this section may be useful for future work.

### **5.1.1 Size Distributions**

TEM (as described in Section 2.2.1) images and ImageJ were used to measure the crystal dimensions.

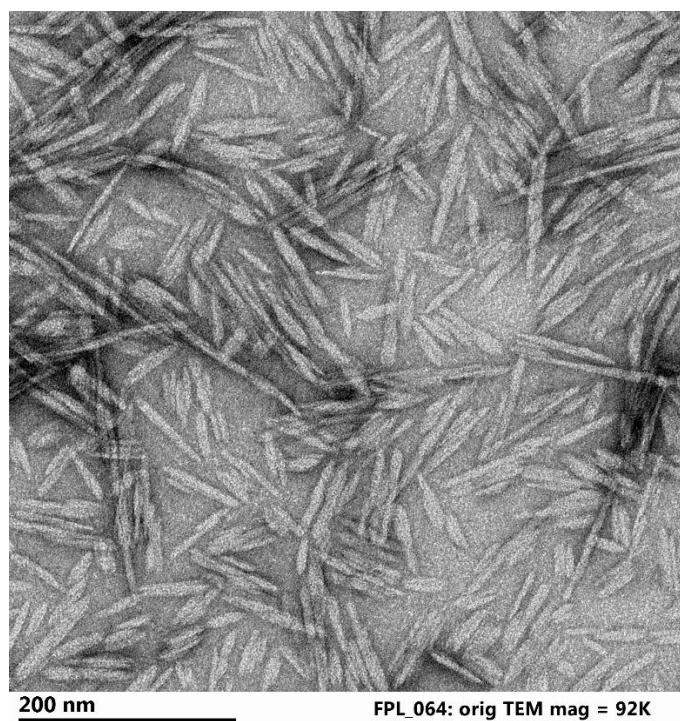


Figure 5-1. TEM image of CNC1.

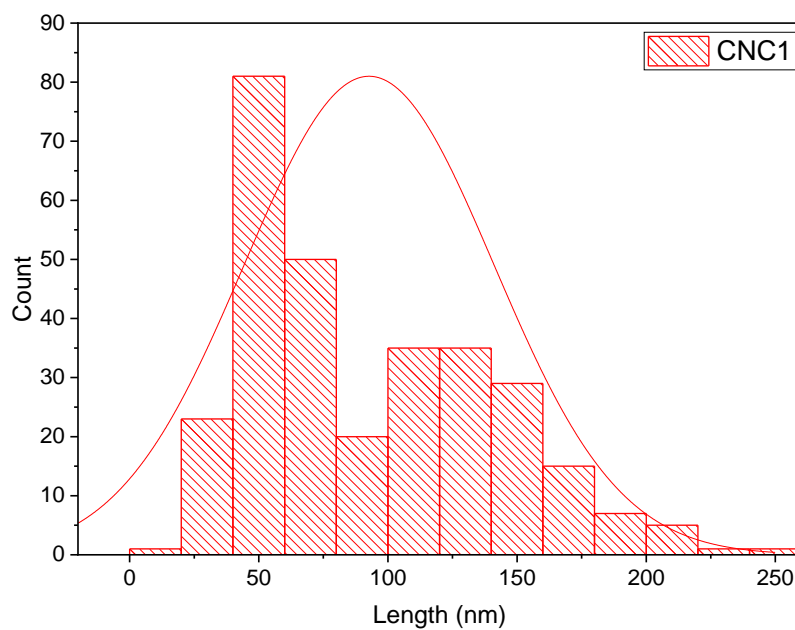


Figure 5-2. Length distribution of CNC1. Average Length of  $92.7 \pm 48.3$  nm, average width of  $7.1 \pm 4$  nm, for an aspect ratio of  $13 \pm 5.9$ .

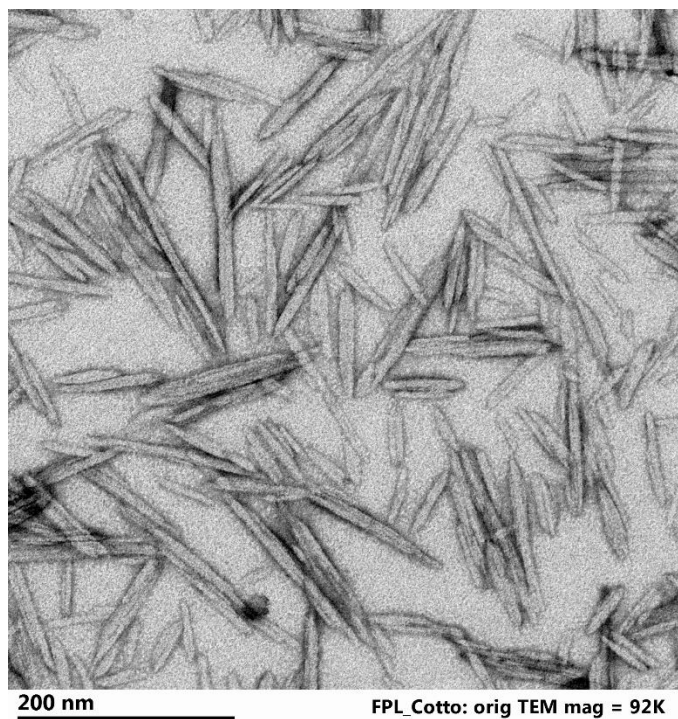


Figure 5-3. TEM image of CNC2.

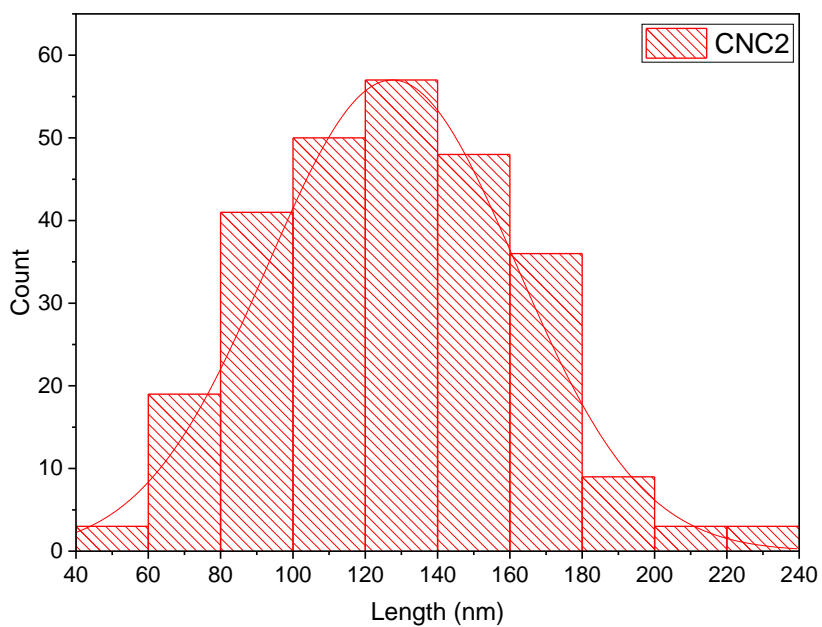


Figure 5-4. Length distribution of CNC2. Average Length of  $127.4 \pm 34.4$  nm, average width of  $9.5 \pm 2.6$  nm, for an aspect ratio of  $14.5 \pm 6$ .

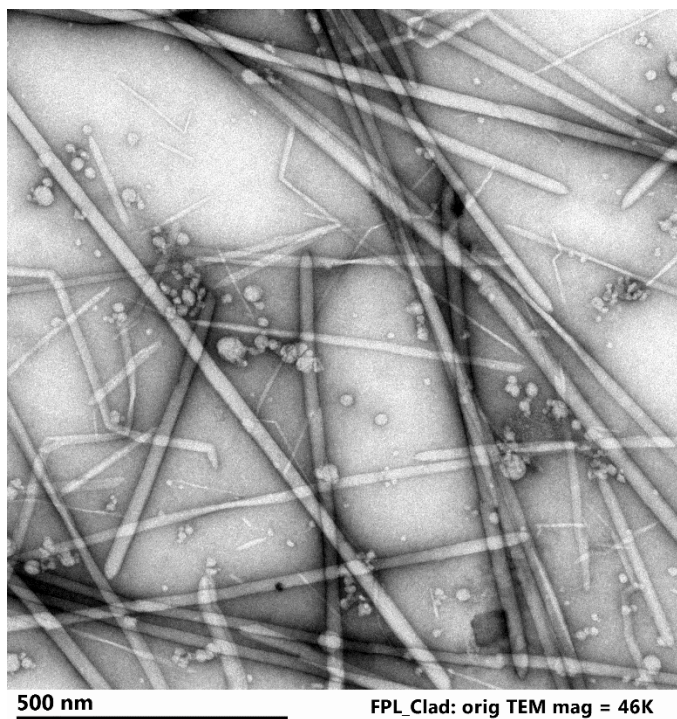


Figure 5-5. TEM image of CNC3.

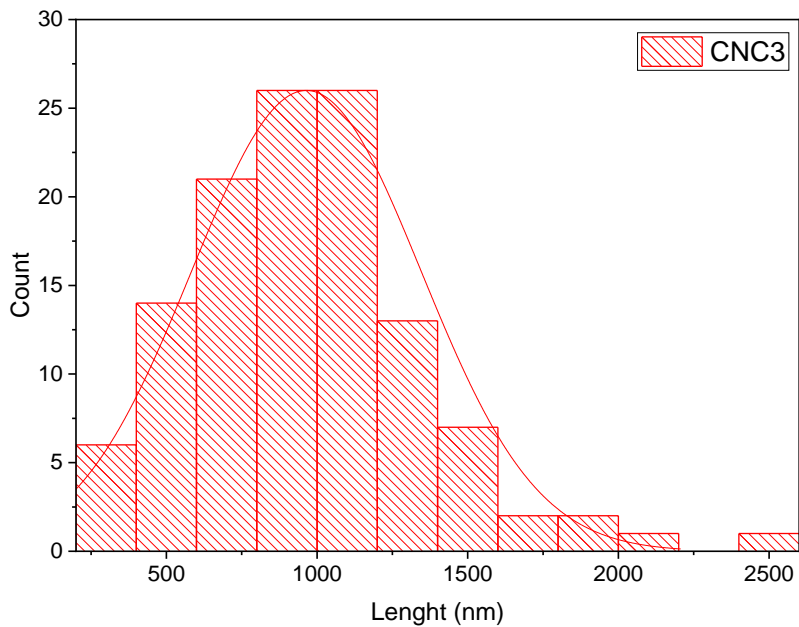


Figure 5-6. . Length distribution of CNC3. Average Length of  $964.5 \pm 381.8$  nm, average width of  $28.5 \pm 9.5$  nm, for an aspect ratio of  $46 \pm 48.2$ .

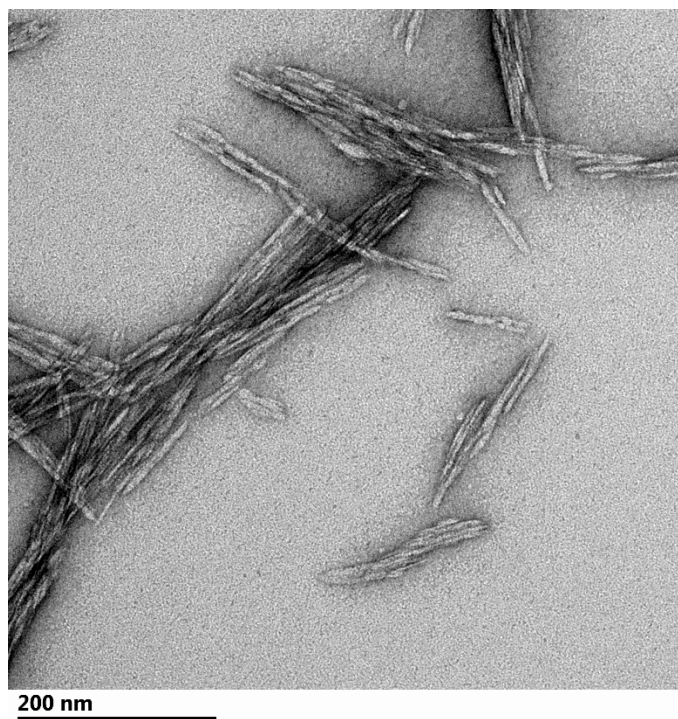


Figure 5-7. TEM image of CNC4

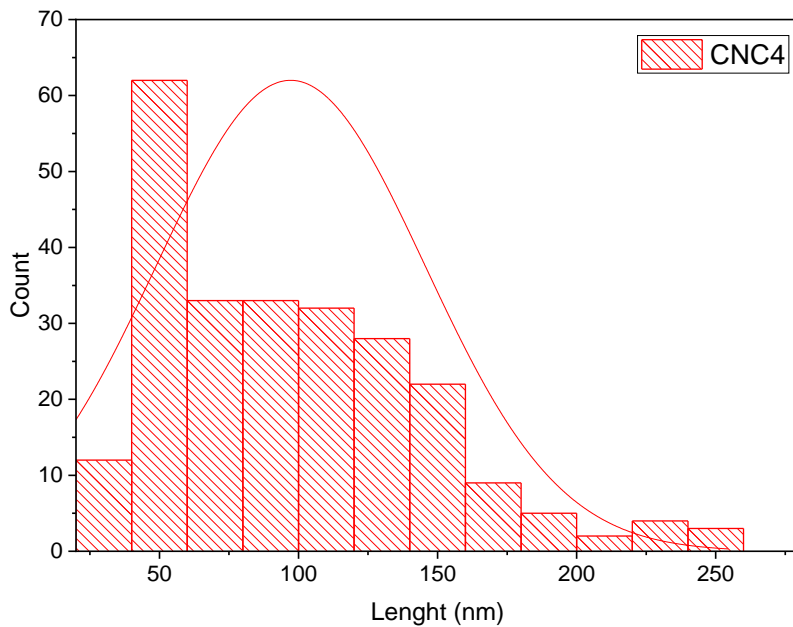


Figure 5-8 . Length distribution of CNC4. Average Length of  $97.2 \pm 48.3$  nm, average width of  $6.7 \pm 3.2$  nm, for an aspect ratio of  $15 \pm 4.7$ .

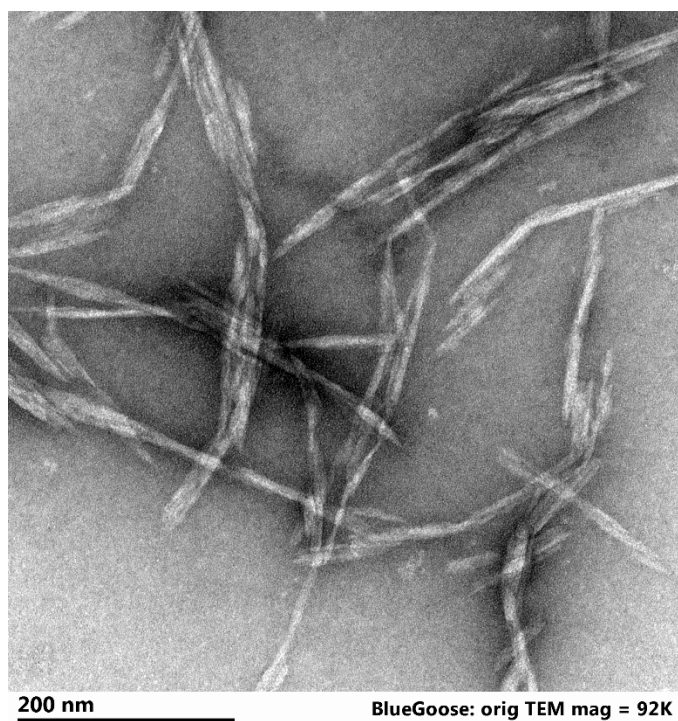


Figure 5-9. TEM image of CNC5.

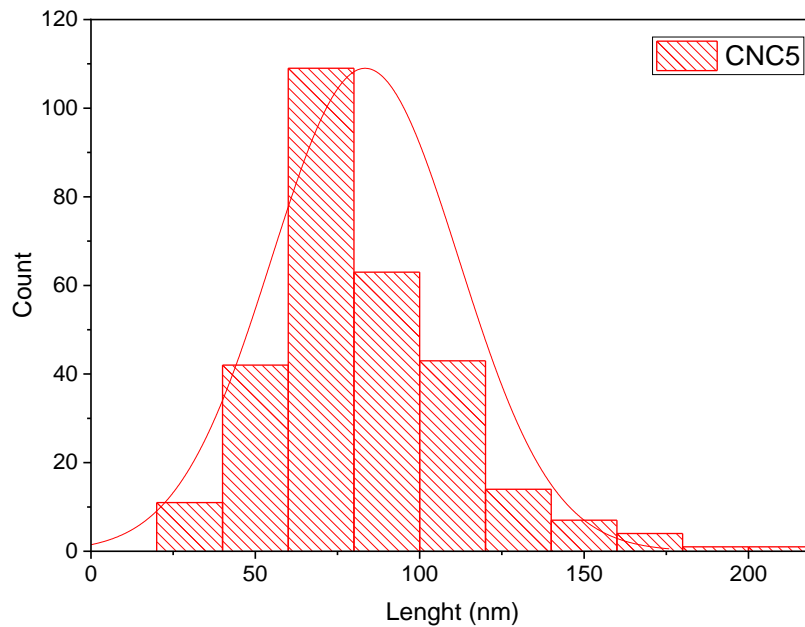


Figure 5-10 . Length distribution of CNC5. Average Length of  $83.4 \pm 28.4$  nm, average width of  $7.6 \pm 2.4$  nm, for an aspect ratio of  $12.3 \pm 6.1$ .

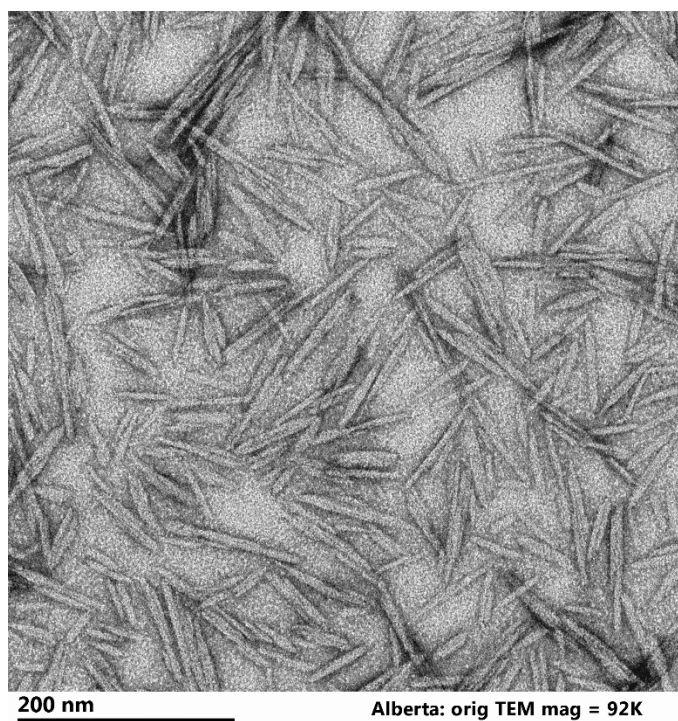


Figure 5-11. TEM image of CNC6.

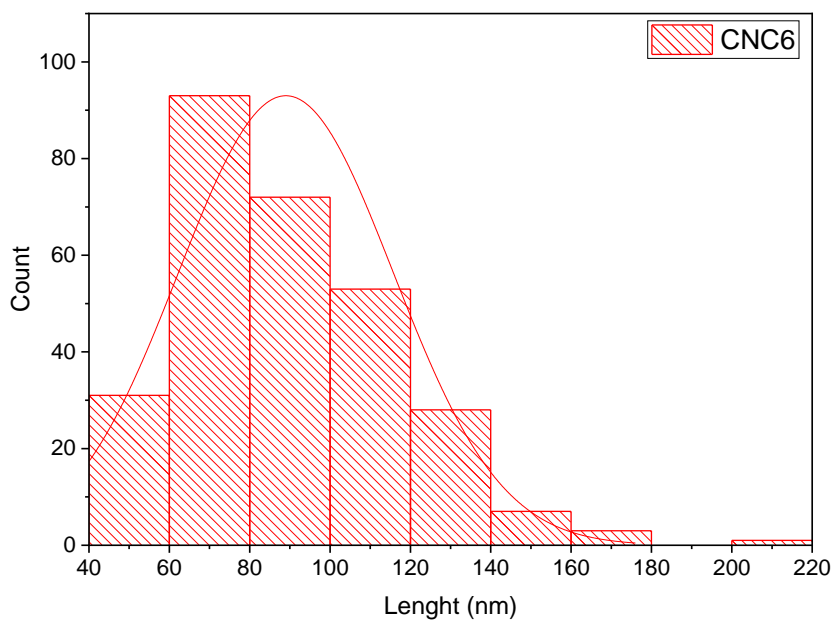


Figure 5-12 . Length distribution of CNC6. Average Length of  $89 \pm 26.7$  nm, average width of  $8.2 \pm 2.7$  nm, for an aspect ratio of  $11.8 \pm 6.8$ .

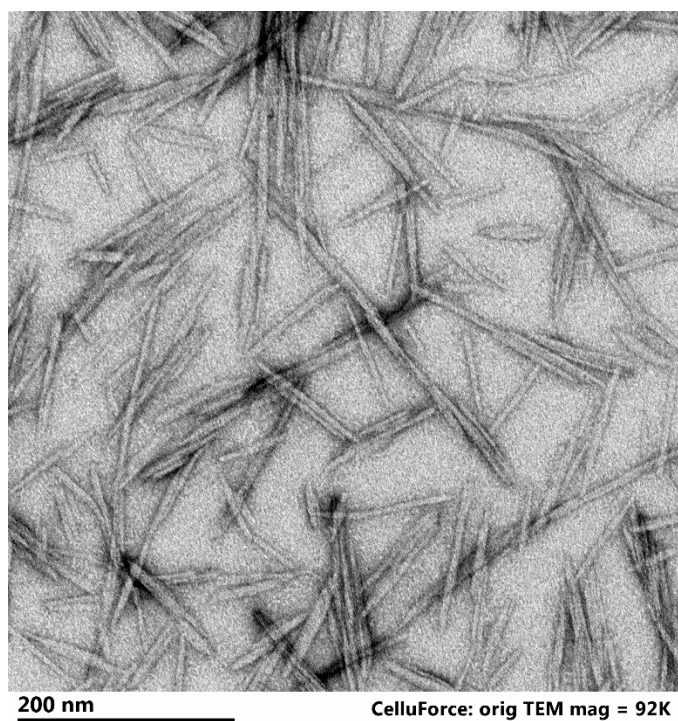


Figure 5-13. TEM image of CNC7.

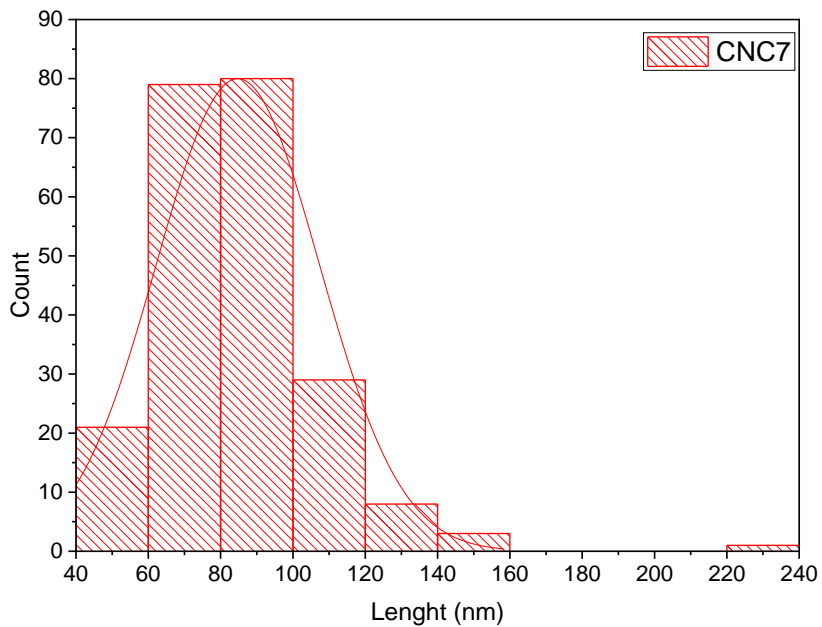


Figure 5-14 . Length distribution of CNC7. Average Length of  $84.8 \pm 22.6$  nm, average width of  $8.5 \pm 2.3$  nm, for an aspect ratio of  $10.7 \pm 4.5$ .



Figure 5-15. TEM image of CNC8.

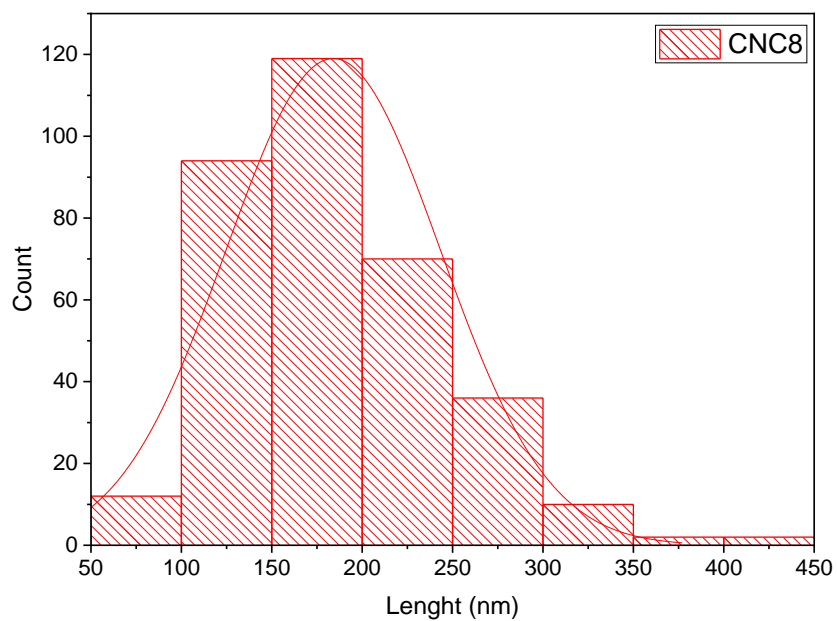


Figure 5-16 . Length distribution of CNC8. Average Length of  $184 \pm 51.7$  nm, average width of  $13.8 \pm 4.6$  nm, for an aspect ratio of  $15 \pm 6.7$ .

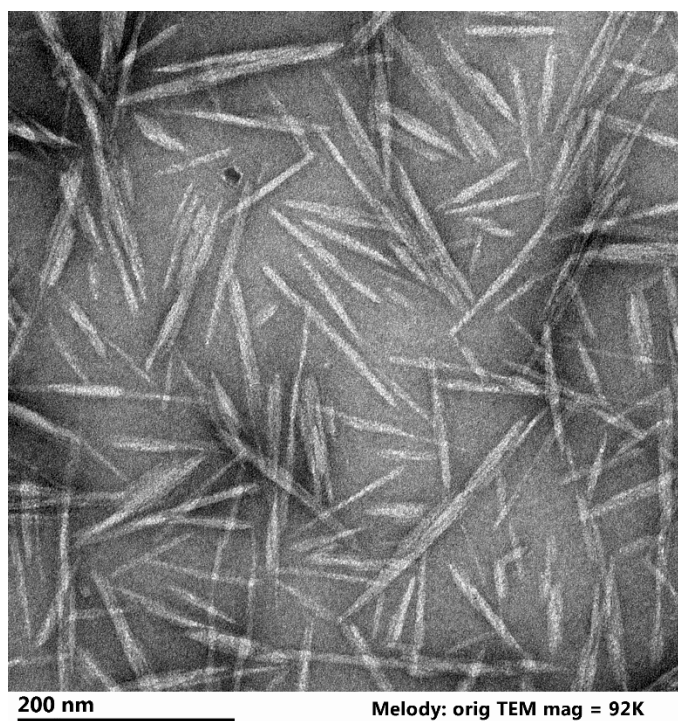


Figure 5-17. TEM image of CNC9.

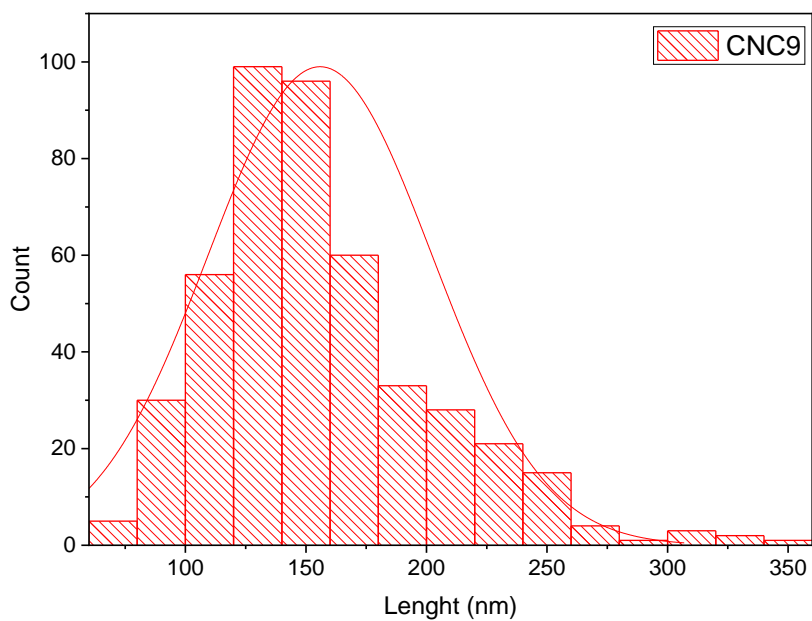


Figure 5-18 . Length distribution of CNC9. Average Length of  $155.9 \pm 39.9$  nm, average width of  $10.1 \pm 1.7$  nm, for an aspect ratio of  $16.4 \pm 5.5$ .

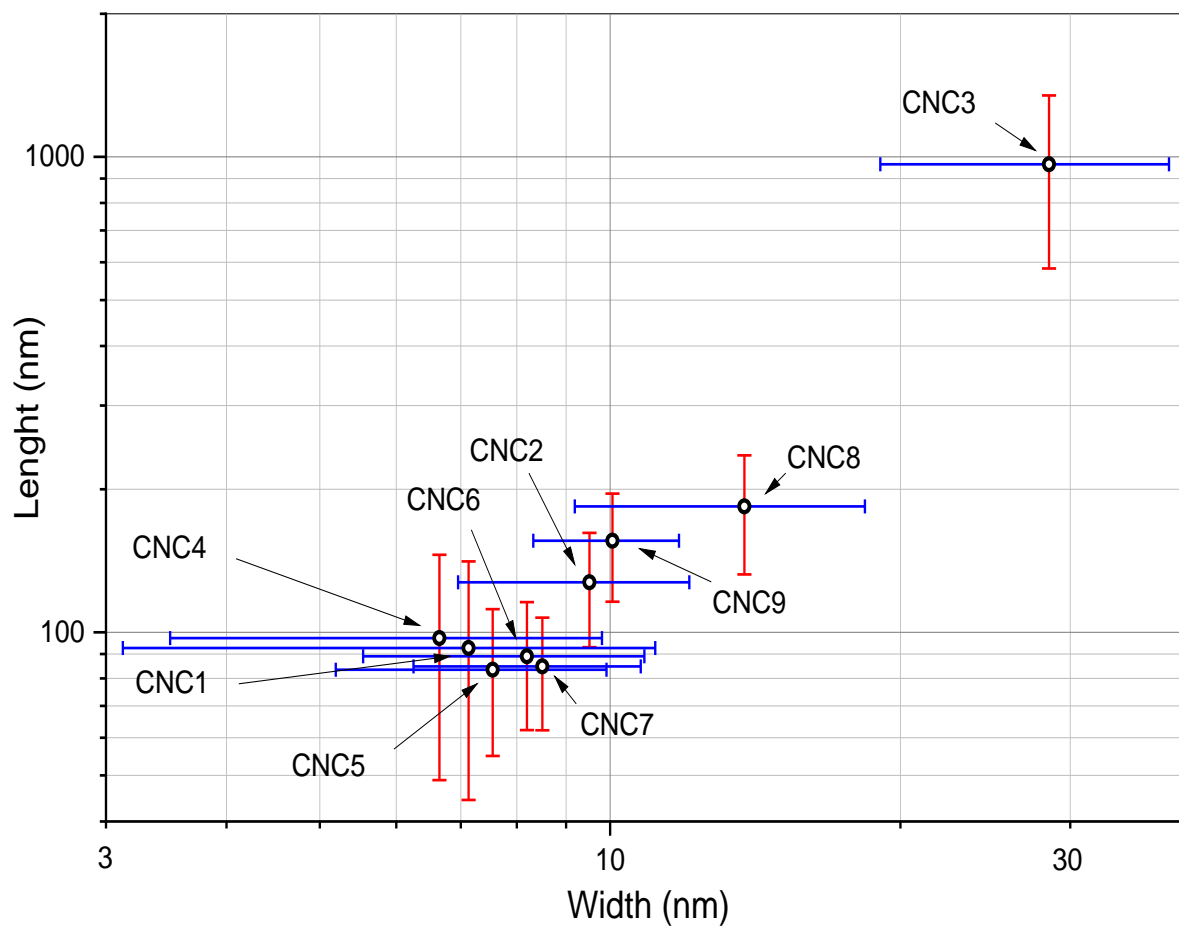


Figure 5-19. CNC lengths and widths with error bars.

### 5.1.2 Turbidity

Turbidity of CNC aqueous suspensions were measured using a Varian Cary 50 Bio UV-Vis, Baseline Zero with pure water, and Zero by blocking the beam with a 3D printed piece of ABS. Samples were measured using 2 mL in a disposable cuvette. Transmittance percentage of wavelengths from 300 to 1000 nm was measured.

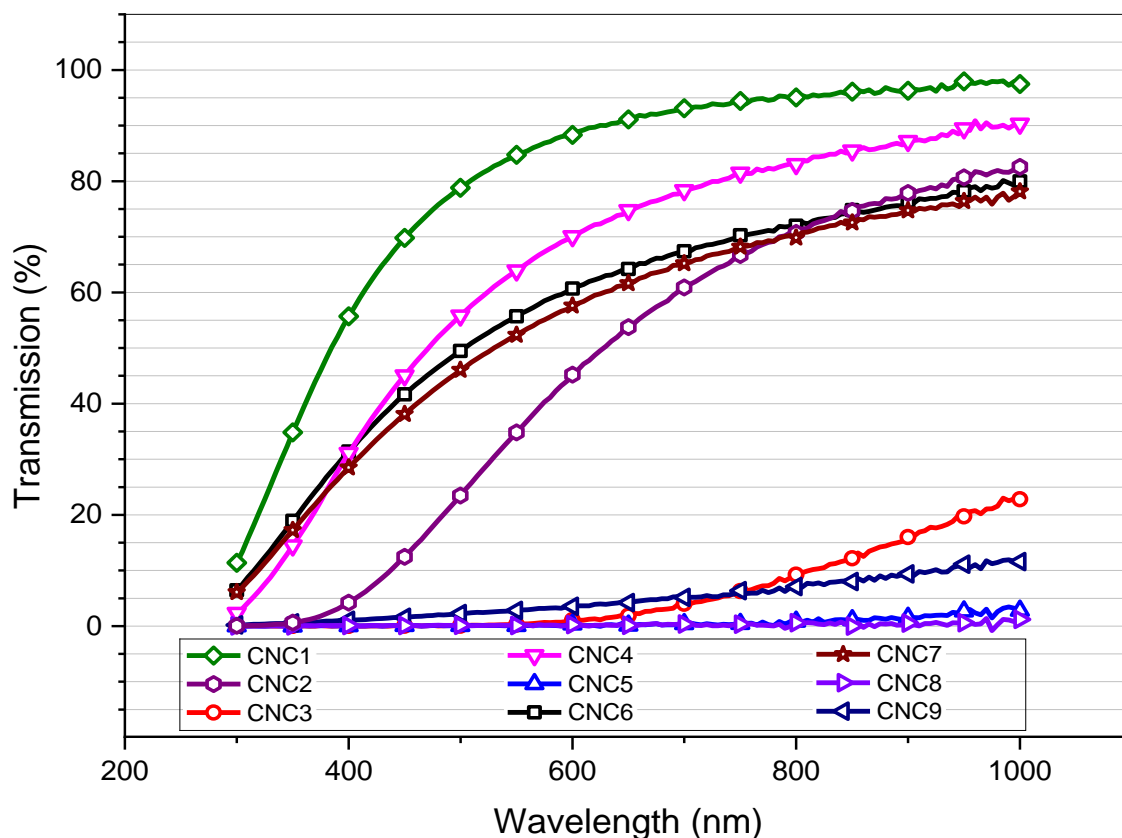


Figure 5-20. Turbidity of CNC 2wt% aqueous suspensions measured by transmittance %.

### 5.1.3 Crystallinity

CNCs from Chapter 2 were diluted into a 2wt% aqueous suspension. Suspensions were mixed using the ultrasonic mixer, at 30% intensity, in an ice bath for approximately 2 minutes. Suspensions were poured into 50mm polystyrene petri dishes and were left to dry in a fume hood. After 72 hours, resulting films were analyzed using a PANalytical Empyrean Powder X-ray Diffractometer, with Cu radiation ( $1.540598 \text{ \AA}$ ) at 45 kV and 40 mA. The angular interval was set from 5 to 40 on a Si single crystal wafer in rotational mode with a period of 2s. No background correction was made.

Results were first plotted, and peaks were identified using a datasheet. Not all detected peaks were absolute maximums, so it was necessary to also look at the first and second derivatives for maximums and minimums. The peaks from Cellulose I $\beta$  and II were identified based on the work from Nam *et al.*[90].

Refraction signals were then deconvoluted using the multiple peak analysis from OriginPro 2016. Peak positions were fixed at the previously selected angles and several iterations were made until the software reached convergence. The values from the deconvoluted peaks were used to calculate the crystallinity index of the dominating refraction's plane. Segal crystallinity indexes from the I $\beta$  (200) plane was calculated by the following equation.

$$CI\% = \frac{(I_{I\beta(200)} - I_{I\beta Amorphous})}{I_{I\beta(200)}}$$

Equation 5-1. Segal crystallinity index.

Where each  $I$  is the deconvoluted peak intensity of the plane indicated by the sub index. CI% values are listed in Table 5-1.

Table 5-1. Crystallinity index of CNC films.

CNC	Plane	Position ( $2\theta$ )	CI%
CNC1	I $\beta$ (200)	22.4°	89.6%
CNC2	I $\beta$ (200)	22.9°	92.9%
CNC3	II (1-10)	14.7°	98.6%
CNC4	I $\beta$ (200)	22.9°	85.2%
CNC5	I $\beta$ (200)	23.1°	91.8%
CNC6	I $\beta$ (200)	23°	85.7%
CNC7	I $\beta$ (200)	22.7°	83.3%
CNC8	I $\beta$ (200)	22.8°	86.7%
CNC9	I $\beta$ (200)	22.9°	80.2%

Most of CNCs had predominant Cellulose I $\beta$  diffraction, CNC1 showed several peaks from both cellulose I $\beta$  and II, which is attributed to the raw material being mercerized cellulose[90]. CNC3 was cellulose II dominant, which is common for algae and bacterial CNC[10].

Full refraction spectra and deconvoluted peaks are shown in the following Figures.

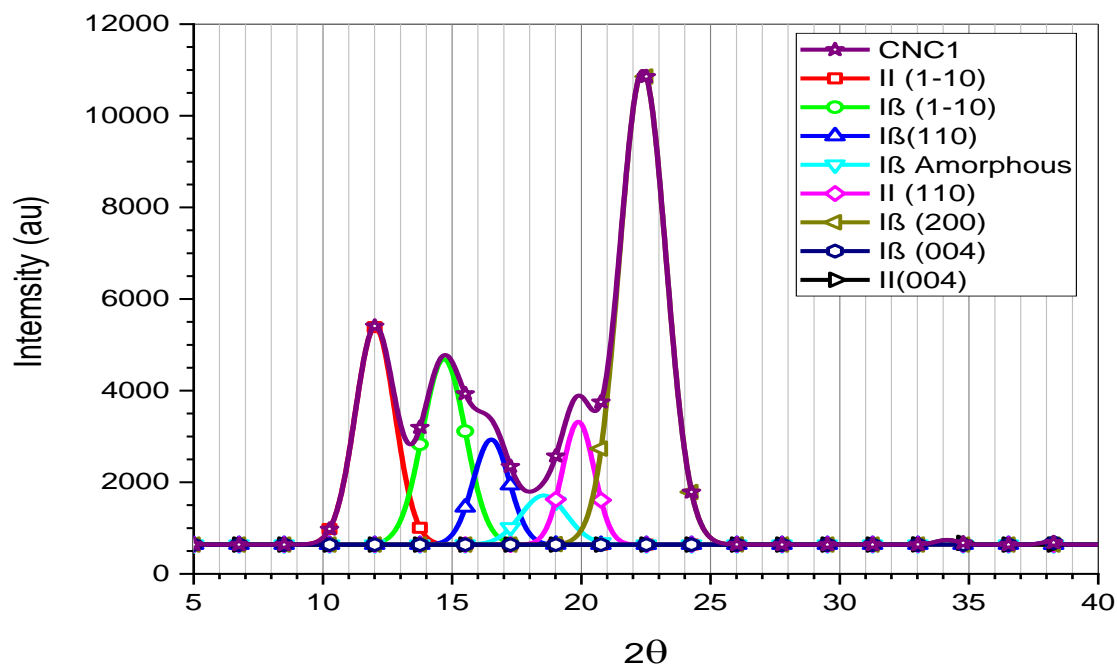


Figure 5-21. X-ray diffraction of CNC1 film.

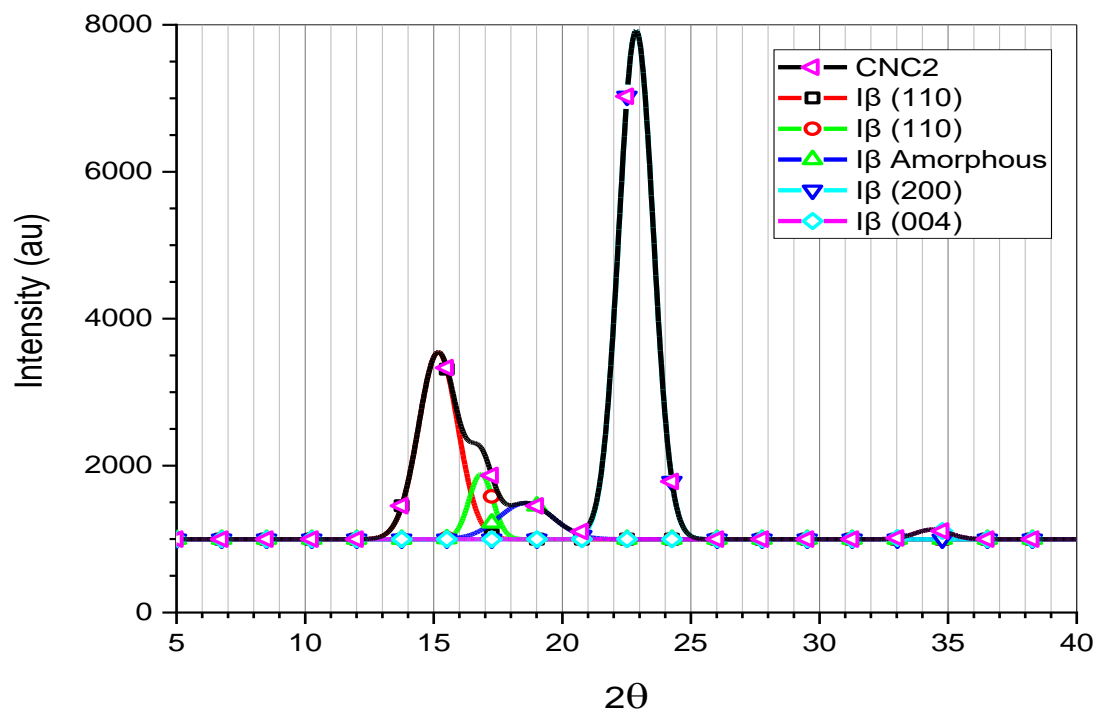


Figure 5-22. X-ray diffraction of CNC2 film.

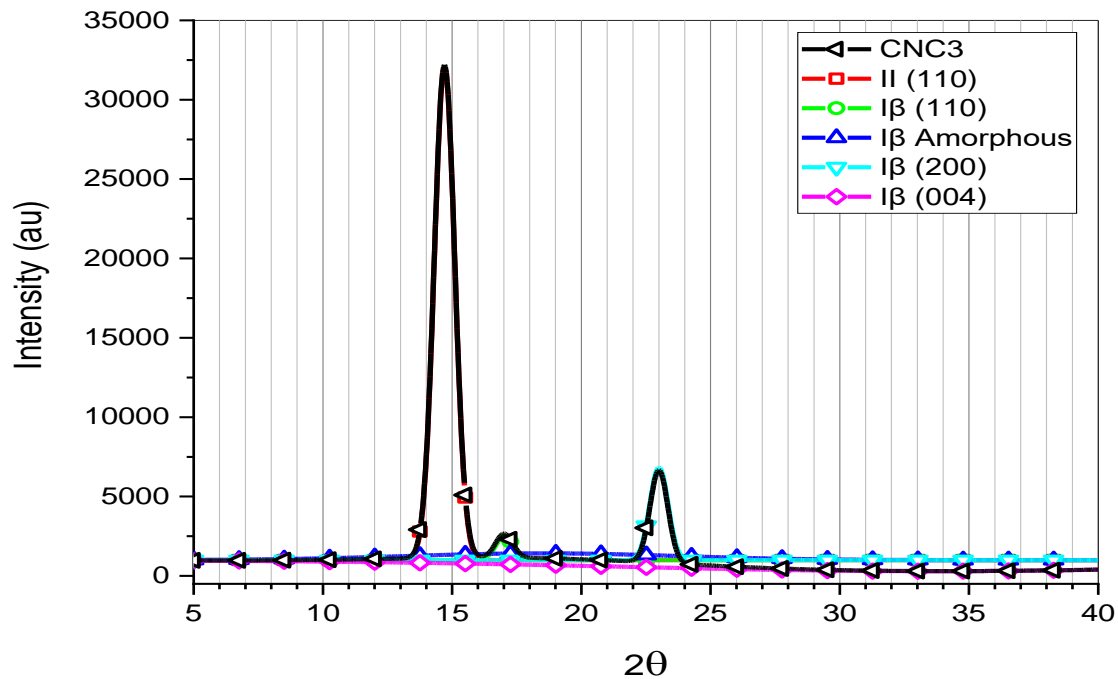


Figure 5-23. X-ray diffraction of CNC3 film.

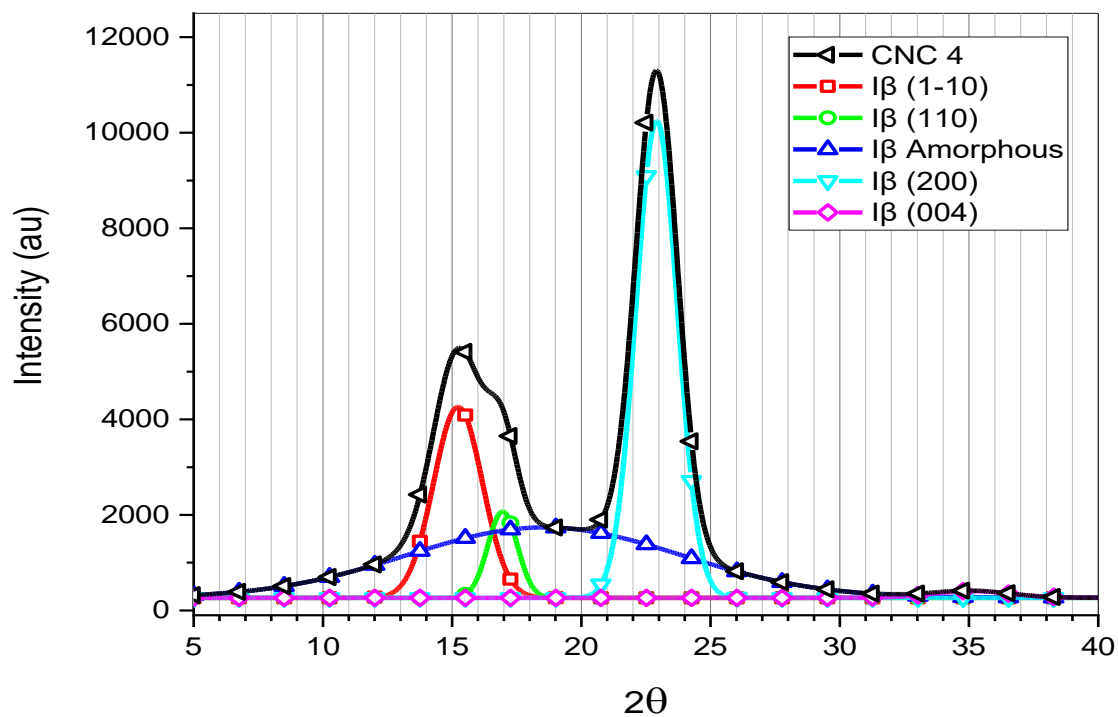


Figure 5-24. X-ray diffraction of CNC4 film.

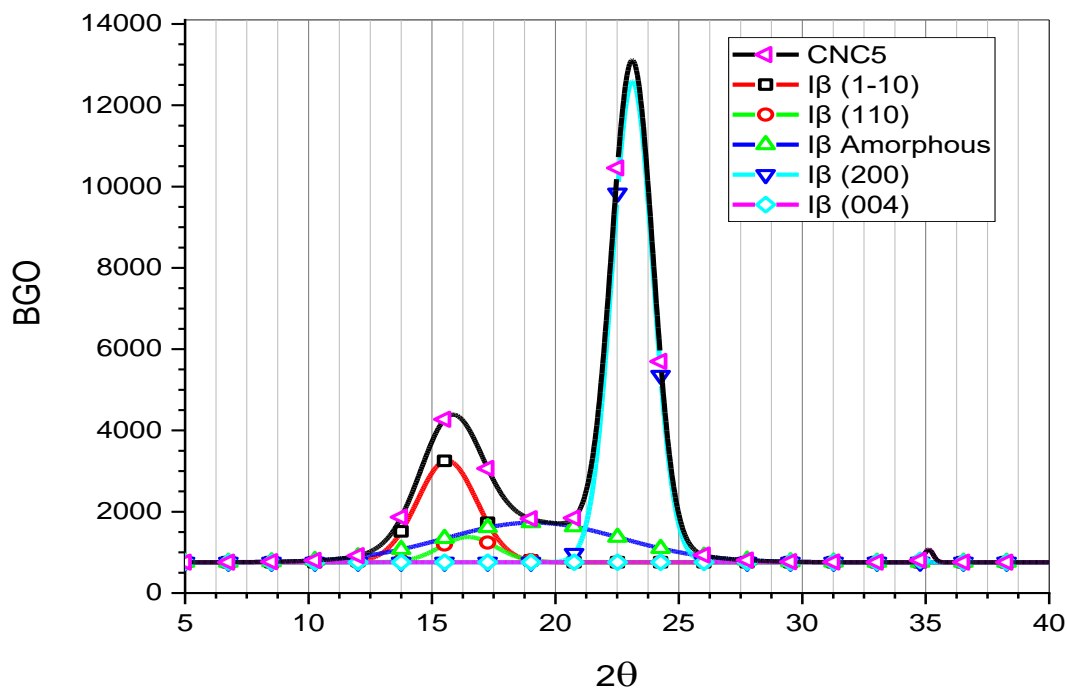


Figure 5-25. X-ray diffraction of CNC5 film.

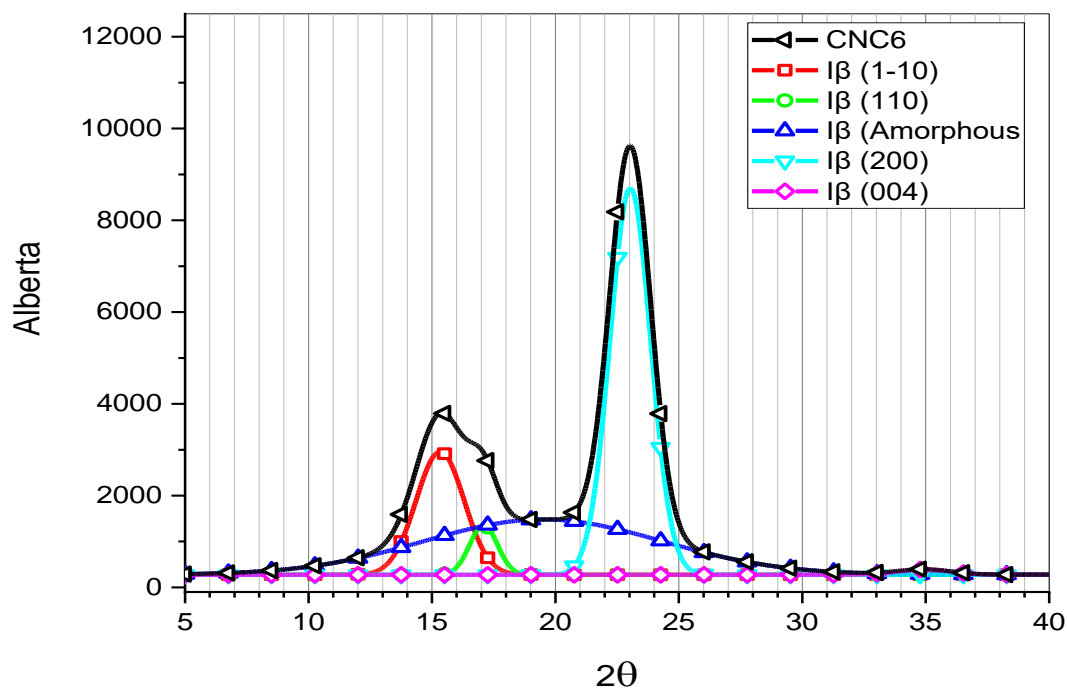


Figure 5-26. X-ray diffraction of CNC6 film.

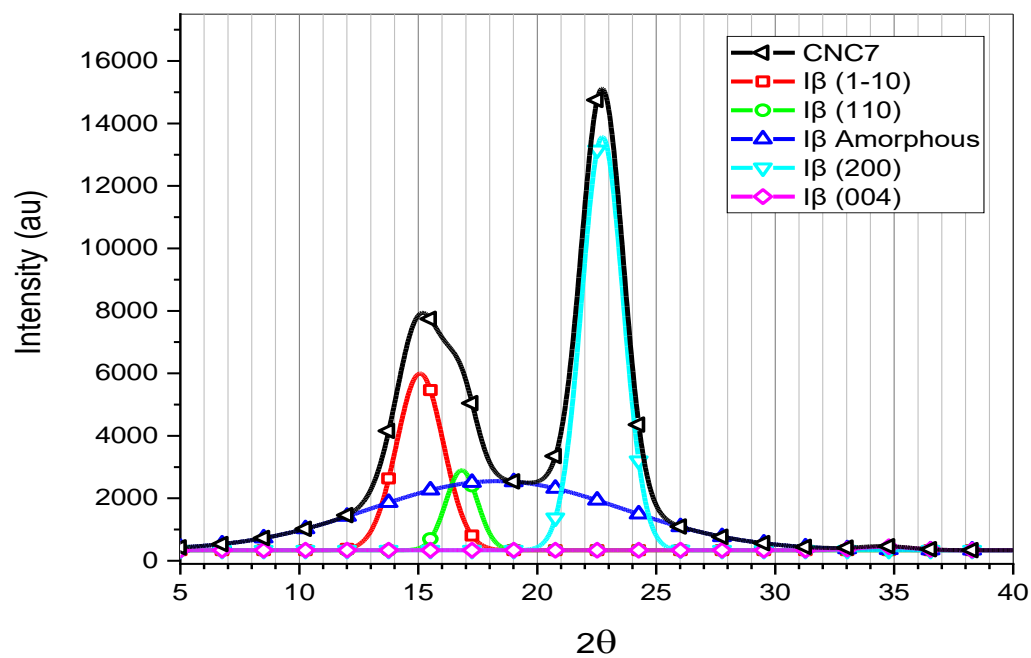


Figure 5-27. X-ray diffraction of CNC7 film.

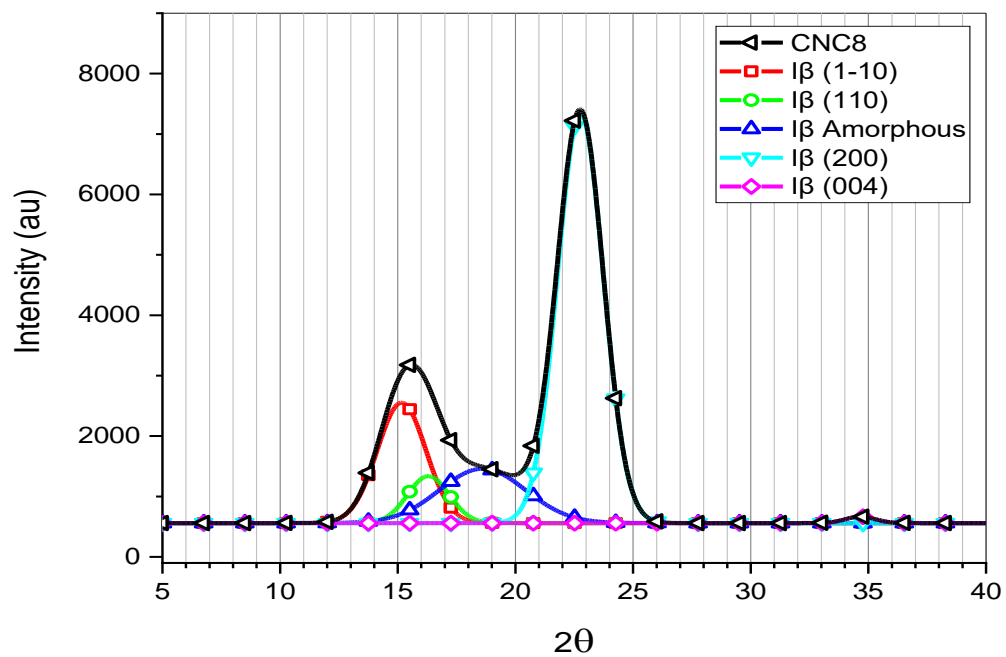


Figure 5-28. X-ray diffraction of CNC8 film.

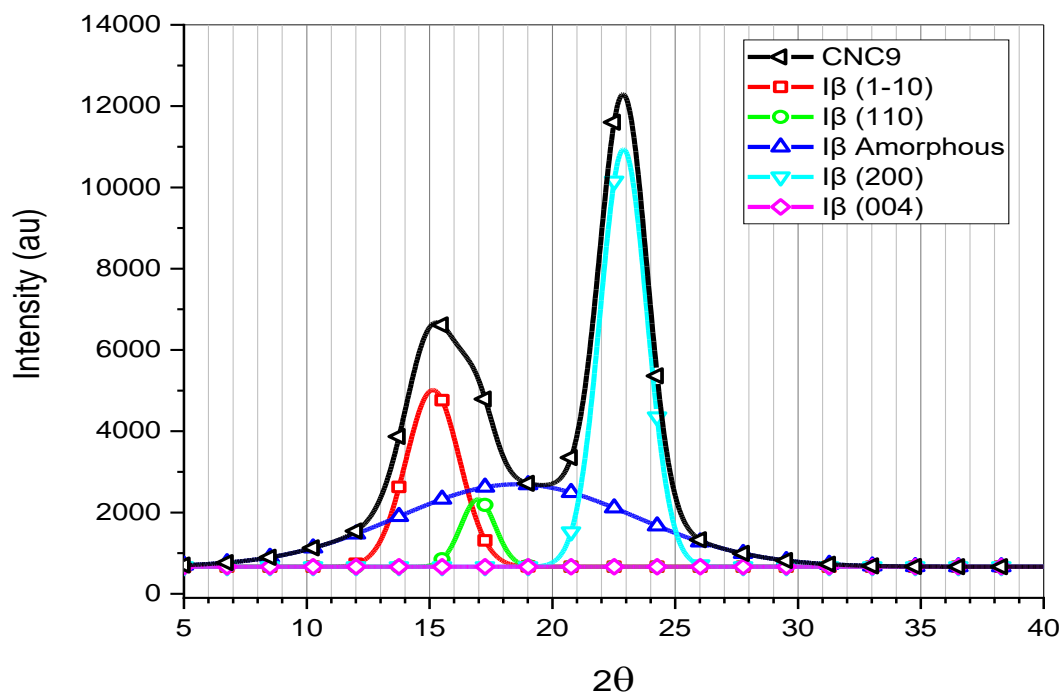


Figure 5-29. X-ray diffraction of CNC9 film.

## APPENDIX

### **Rheology of Cement Pastes with CNC and Plasticizers.**

After concluding that CNC could be used as both cement strengthener and as a viscosity modifier, the need for flowability was still unsatisfied. We then resorted to commercial plasticizers. The rheological effects of adding plasticizer to cement pastes containing CNC was investigated. For some cement pastes with certain CNC dosages, the addition of plasticizer resulted in a higher yield stress reduction than the plasticizer alone. The observed effects are yet to be further investigated.

### **Experiments and Materials**

The first step was to select a Plasticizer. The two admixtures that were at hand were a PAA backbone with PEO grafted chains[4] MasterGlenium7700[91] and a *naphthalene sulfonate* polymer Rheobuild® 1000[91] (BASF, Ludwigshafen, Germany).

Three CNC were of interest for this study, CNC-065 from the USDA Forest Products laboratory, (CNC1 from Chapter 4), BGB-CNC-Ultra from Blue Goose Biorefineries Inc. (CNC4 from Chapter 4), and a CNC from American Process Inc. (CNC8 from Chapter 2).

For these experiments, Type III cement was also used, which is known for having a higher specific surface area[92] than the Type I/II and Type V cements previously used (Table 2-1 ), so the yield stress measurement protocol used in Chapter 2 (not the geometry), had to be modified to circumvent the thixotropy differences of these powders.

Pastes were mixed using the same protocol used in section 2.2.2, and the Rheometer set-up was the same as in section 2.2.3. The experiment protocol changed. Dynamic yield stress was now measured and compared between the different pastes, the measurement protocol was based on the method described by Qian *et al.*[93].

After paste was placed between the rheometer plates, a pre-shearing condition was applied, by shearing the sample at  $50\text{s}^{-1}$  for 60s and 10s resting time. A Shear rate-controlled ramp was then applied, 30 steps from 1 to  $50\text{ s}^{-1}$  in logarithmic increments. Experiment returned the measured stress at each shear rate. Results were fit to a Bingham model and Yield stress was recorded for each tested paste.

### **Choosing a Plasticizer.**

The recommended dosages for the used plasticizers are 650-1,600 mL/100 kg of Rheobuild and 130-780 mL/100 kg for Glenium. Both were tested in Type V cement paste. As Type V cement is the most flowable of the tested cements, a low w/c (0.24) was used so the Plasticizer effect could be clearly observed with the Rheometer's available geometry.

The yield stress of Type V pastes was measured as Plasticizer dosage was increased. Although, Rheobuild requires almost twice as much as Glenium to perform as designed, the results in Figure A-1 show that Glenium addition was more consistent with what was expected, as it consistently decreased the pastes yield stress as dosages was increased. For this reason, and for collaborators' experience, Glenium was chosen as the plasticizer to be used in this study.

First, pastes made using Type V cement at a 0.24 w/c were measured at different MG dosages. Then pastes containing CNC addition dosages were tested at the same plasticizer dosages.

Next step was to measure the yield stresses of pastes with Type I/II. A higher w/c was used (0.36), as Type I/II cement at 0.24 didn't mixed well with CNC. Lastly, pastes made using Type III cement were tested following the same procedure as Type I/II pastes.

### **Cement Paste Rheology**

The CNC dosages used were 0.65% and 1.00%, which are typical dosages at which strengthening was observed by Fu *et al.*[33]. From the results from Chapter 2, yield stress reduction is not expected at these high dosages. For type V cement, the only mixture displaying a reduction in yield stress was the paste with 1.00% BGU. Plasticizer was then added in increasing dosages, but at no plasticizer dosage, the combination of CNC and plasticizer resulted in a lower yield stress than pastes containing no CNC and the same plasticizer dosages.

Type I/II and Type III cement were tested at the same CNC dosages and 144 mL/100kg plasticizers. The results showed that for almost all the pastes made using Type I/II, the addition of CNC before adding plasticizer reduced the yield stress of the paste more than using the plasticizer alone. For the pastes made using Type III cement, the only CNC working better with plasticizer than the plasticizer alone was BGU at 0.65% dosage.

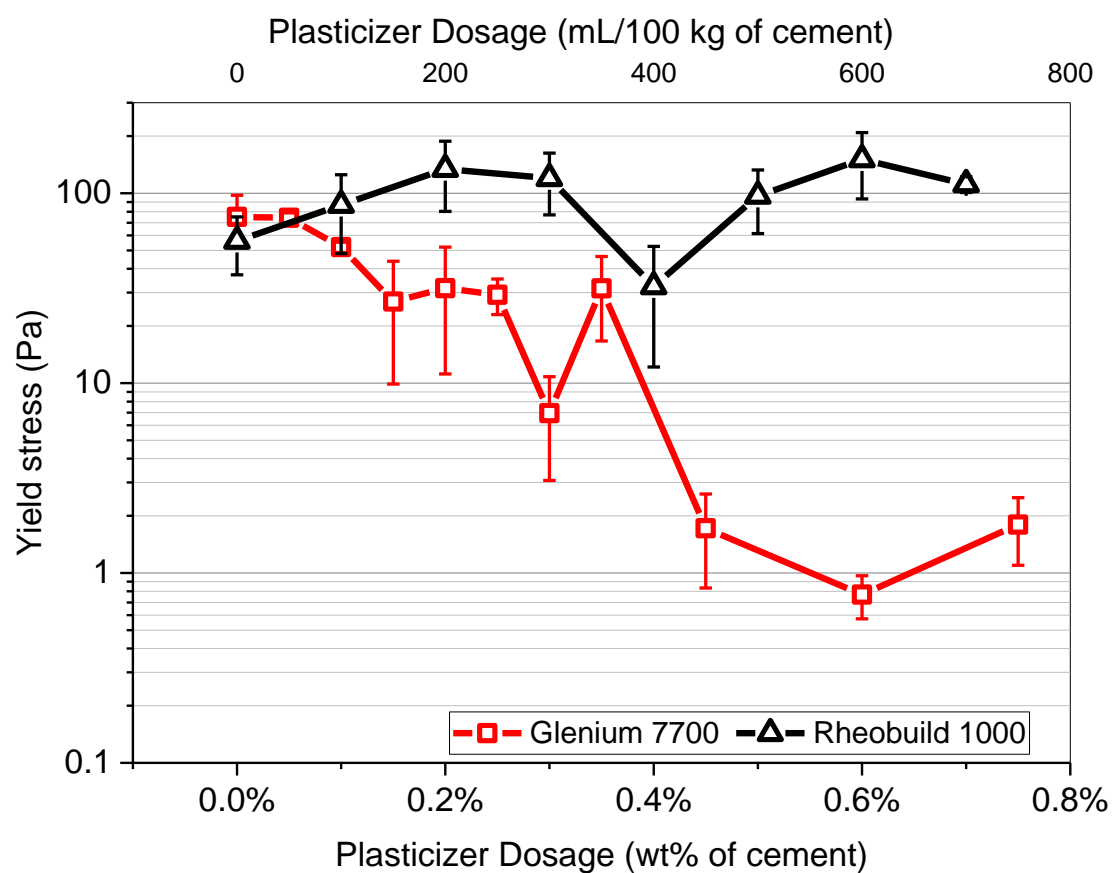


Figure A-1. Yield stresses of cement pastes made using Type V cement at a 0.24 w/c at different additions of Plasticizers.

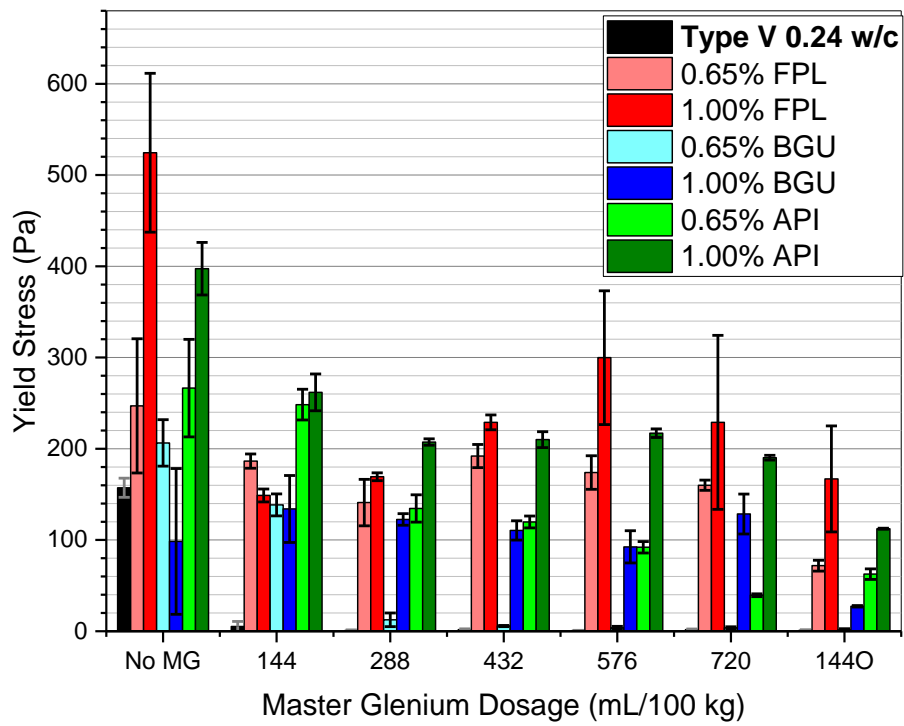


Figure A-2. Yield Stresses of Pastes made using Type V cement at a 0.24 w/c, CNC addition and Plasticizer.

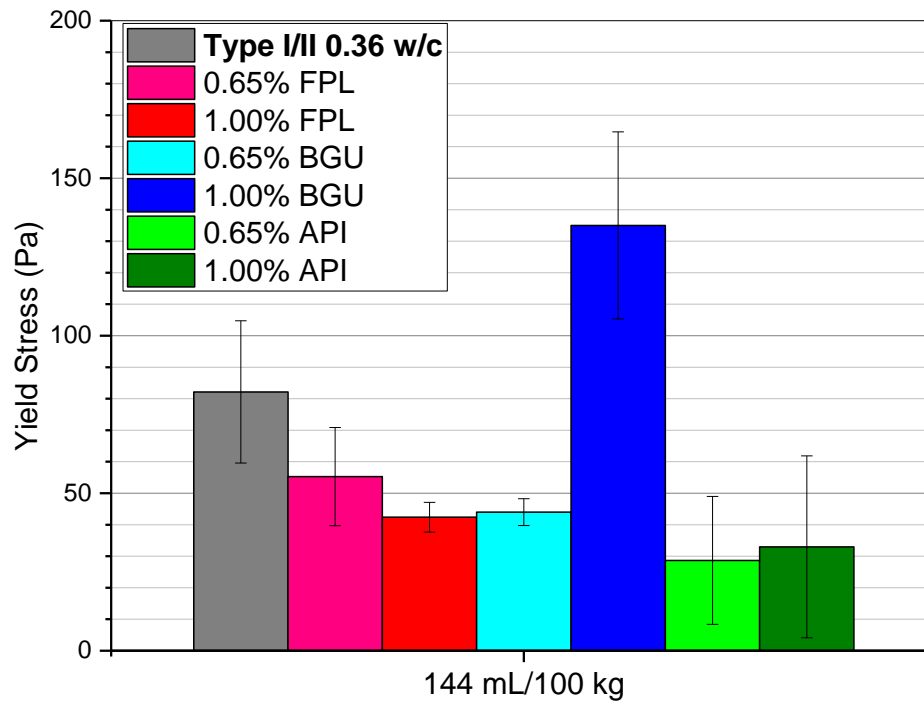


Figure A-3. Yield Stresses of Pastes made using Type I/II cement at a 0.36 w/c, CNC addition and 144 mL/100 kg of Plasticizer.

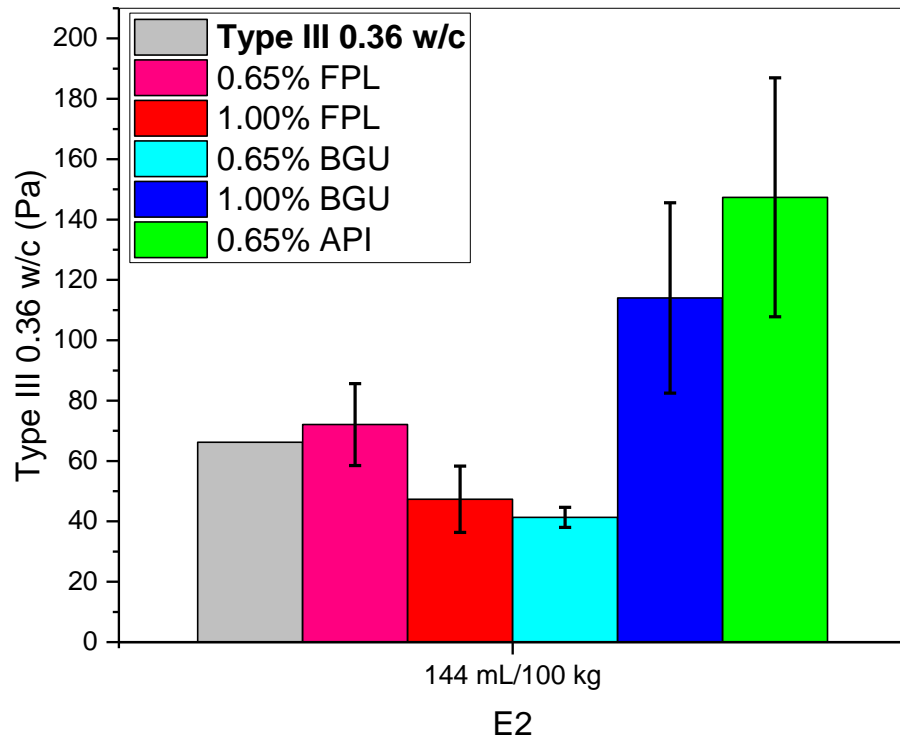


Figure A-4. Yield Stresses of Pastes made using Type III cement at a 0.36 w/c, CNC addition and 144 mL/100 kg plasticizer.

## Chapter 3 HPLC Results

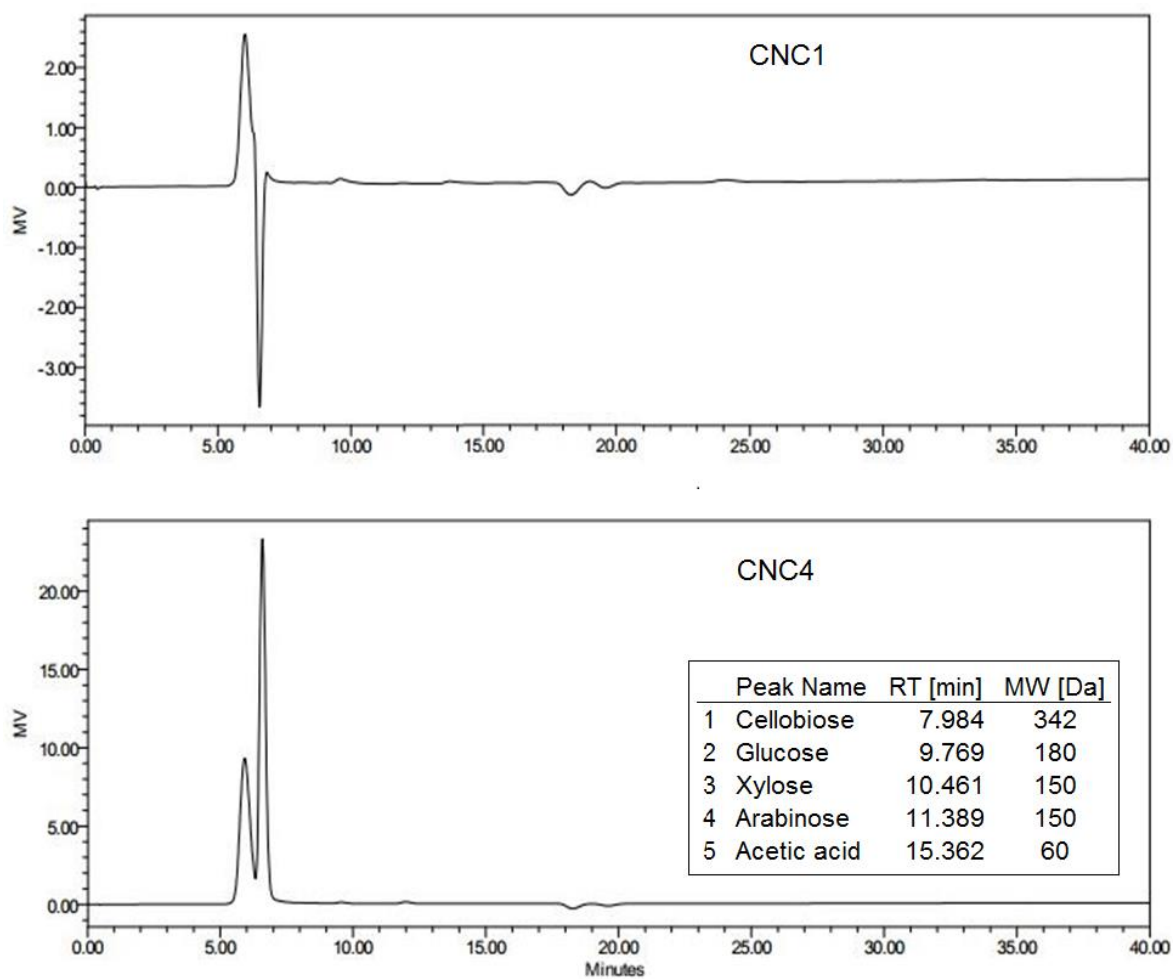


Figure A-5. HPLC results from CNC1 and CNC4 filtrates

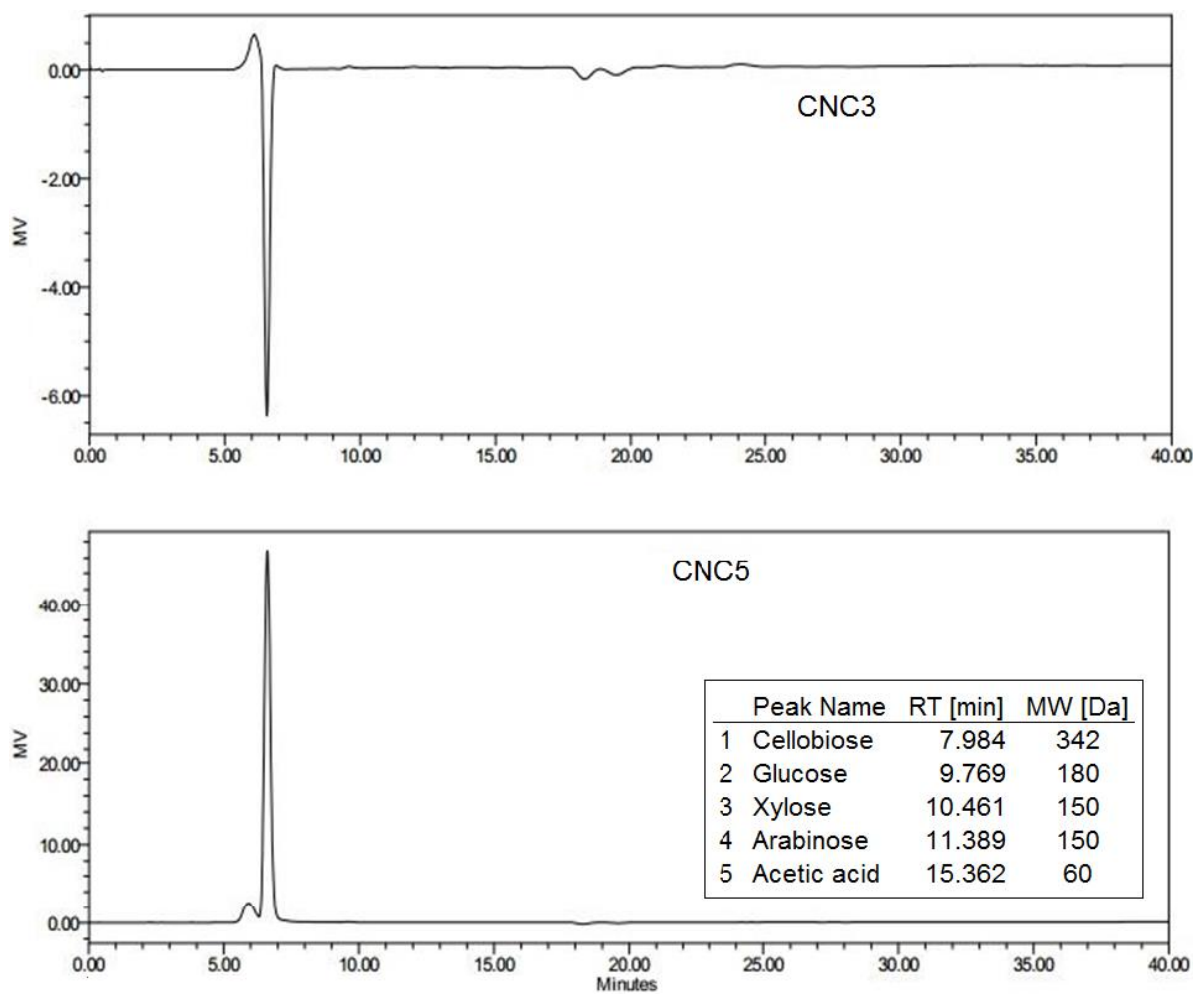


Figure A-6. HPLC results from CNC3 and CNC5 filtrates

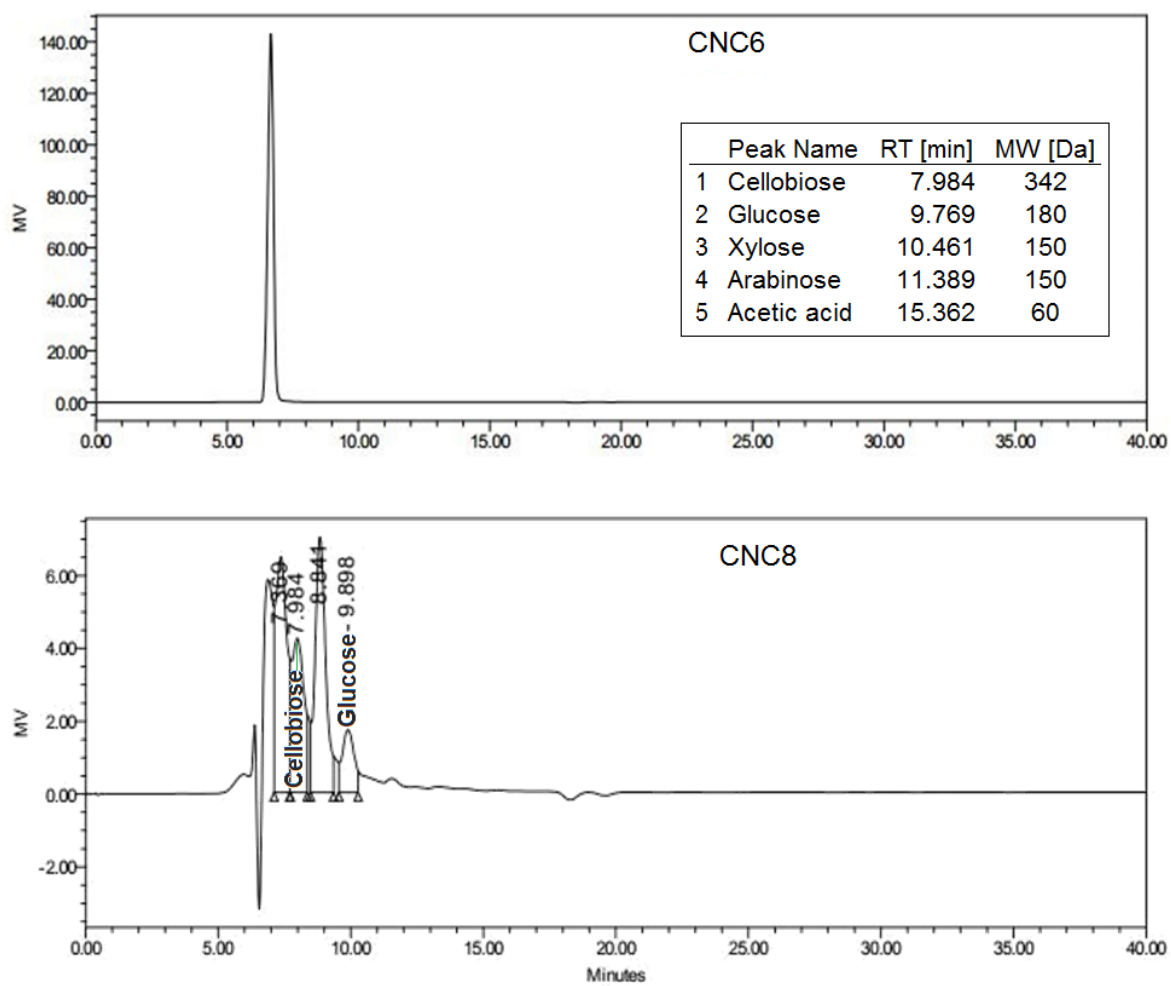


Figure A-7. HPLC results from CNC6 and CNC8 filtrates

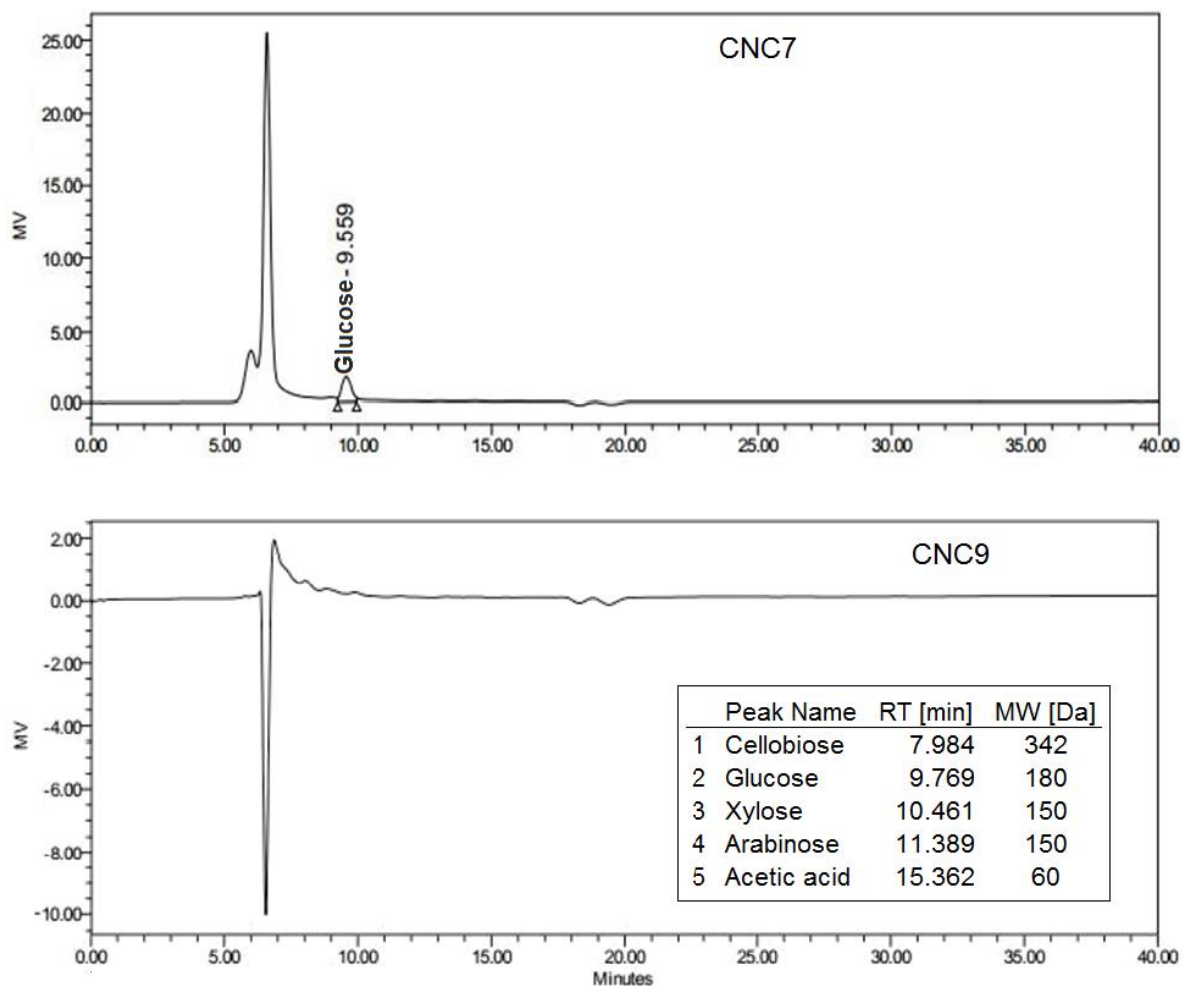


Figure A-8. HPLC results from CNC7 and CNC9 filtrates

## Chapter 4 Total Heat of Hydration

The goal of Chapter 4 was not to assess the total hydration of pastes; it was aimed to the concern about the retardation effects of the sugars detected in Chapter 3. However, as it is still potentially valuable information, the total heat of hydration is listed in Table 6-1.

Table A-1. Total heat of hydration by the end of the isothermal calorimetry measurements.

Type V 0.36 w/c + 1% CNC1	5 washes	1 wash	Unwashed
Heat Released at 75 hrs hydration [J/g]	246.1	244.5	216.7
Type V 0.36 w/c + 1% CNC2	5 washes	1 wash	Unwashed
Heat Released at 75 hrs hydration [J/g]	255.6	248.9	245.3
Type V 0.36 w/c + 0.2% CNC3	5 washes	1 wash	Unwashed
Heat Released at 75 hrs hydration [J/g]	226.2	230.8	229.7
Type V 0.35 w/c + 0.2% CNC4	5 washes	1 wash	Unwashed
Heat Released at 148 hrs hydration [J/g]	233.9	242.0	250.0

## REFERENCES

- [1] “ASTM C125-18b Standard Terminology Relating to Concrete and Concrete Aggregates BT - Standard Terminology Relating to Concrete and Concrete Aggregates,” *ASTM Int. West Conshohocken, PA, 2018*.
- [2] M. Adjoudj, K. Ezziane, E. H. Kadri, T. T. Ngo, and A. Kaci, “Evaluation of rheological parameters of mortar containing various amounts of mineral addition with polycarboxylate superplasticizer,” *Constr. Build. Mater.*, vol. 70, pp. 549–559, 2014.
- [3] P. K. Mehta and P. J. Monteiro, *Concrete : microstructure, properties, and materials.*, 3rd ed. New York: McGraw Hill, 2006.
- [4] L. M. Rueschhoff, J. P. Youngblood, R. W. Trice, and R. Bordia, “Stabilizing Highly Loaded Silicon Nitride Aqueous Suspensions Using Comb Polymer Concrete Superplasticizers,” *J. Am. Ceram. Soc.*, vol. 99, no. 12, pp. 3857–3865, 2016.
- [5] K. Sobolev, M. Moini, S. Muzenski, R. Pradoto, M. Kozhukhova, and I. Flores-vivian, “Laboratory Study of Optimized Concrete Pavement Mixtures,” no. 0092, 2015.
- [6] S. Mindess, J. Young, and D. Darwin, *Concrete*, 2nd Editio. Upper Saddle River, NJ: Prentice Hall., 2003.
- [7] L. R. Murray and K. A. Erk, “Jamming rheology of model cementitious suspensions composed of comb-polymer stabilized magnesium oxide particles,” *J. Appl. Polym. Sci.*, vol. 131, no. 12, pp. 1–11, 2014.
- [8] Y. Cao, P. Zavattieri, J. Youngblood, R. Moon, and J. Weiss, “The relationship between cellulose nanocrystal dispersion and strength,” *Constr. Build. Mater.*, vol. 119, pp. 71–79, 2016.
- [9] A. B. Reising, R. J. Moon, and J. P. Youngblood, “Effect of particle alignment on mechanical properties of neat cellulose nanocrystal films,” *J-for*, vol. 2, no. 6, pp. 32–41, 2012.
- [10] R. J. Moon, A. Martini, J. Nairn, J. Simonsen, and J. Youngblood, “Cellulose nanomaterials review: Structure, properties and nanocomposites,” *Chem. Soc. Rev.*, vol. 40, no. 7, pp. 3941–3994, Jul. 2011.
- [11] J. A. Diaz *et al.*, “Thermal Conductivity in Nanostructured Films: From Single Cellulose Nanocrystals to Bulk Films,” 2014.

- [12] J. A. Diaz, X. Wu, A. Martini, J. P. Youngblood, and R. J. Moon, "Thermal expansion of self-organized and shear-oriented cellulose nanocrystal films," *Biomacromolecules*, vol. 14, no. 8, pp. 2900–2908, 2013.
- [13] E. Fortunati *et al.*, "Multifunctional bionanocomposite films of poly ( lactic acid ), cellulose nanocrystals and silver nanoparticles," *Carbohydr. Polym.*, vol. 87, no. 2, pp. 1596–1605, 2012.
- [14] S. X. Peng, R. J. Moon, and J. P. Youngblood, "Design and characterization of cellulose nanocrystal-enhanced epoxy hardeners," *Green Mater.*, vol. 2, no. 4, pp. 193–205, 2014.
- [15] F. Hoeng, A. Denneulin, C. Neuman, and J. Bras, "Charge density modification of carboxylated cellulose nanocrystals for stable silver nanoparticles suspension preparation," *J. Nanoparticle Res.*, vol. 17, no. 6, pp. 1–14, 2015.
- [16] I. Kalashnikova, H. Bizot, B. Cathala, and I. Capron, "Modulation of cellulose nanocrystals amphiphilic properties to stabilize oil/water interface," *Biomacromolecules*, vol. 13, no. 1, pp. 267–275, 2012.
- [17] V. Incani, C. Danumah, and Y. Boluk, "Nanocomposites of nanocrystalline cellulose for enzyme immobilization," *Cellulose*, vol. 20, no. 1, pp. 191–200, 2013.
- [18] Y. C. Ching *et al.*, "Rheological properties of cellulose nanocrystal-embedded polymer composites: a review," *Cellulose*, vol. 23, no. 2, pp. 1011–1030, 2016.
- [19] Y. Cao, P. Zavatierra, J. Youngblood, R. Moon, and J. Weiss, "The influence of cellulose nanocrystal additions on the performance of cement paste," *Cem. Concr. Compos.*, vol. 56, pp. 73–83, 2015.
- [20] S. J. Eichhorn *et al.*, *Review: Current international research into cellulose nanofibres and nanocomposites*, vol. 45, no. 1. 2010.
- [21] W. P. Flauzino Neto, H. A. Silvério, N. O. Dantas, and D. Pasquini, "Extraction and characterization of cellulose nanocrystals from agro-industrial residue – Soy hulls," *Ind. Crops Prod.*, vol. 42, pp. 480–488, 2013.
- [22] M. A. S. Azizi Samir, F. Alloin, A. Dufresne, and M. a S. a Samir, "Review of recent research into cellulosic whiskers, their properties and their application in nanocomposite field," *Biomacromolecules*, vol. 6, no. 2, pp. 612–626, 2005.

- [23] R. R. Devi, P. Dhar, A. Kalamdhad, and V. Katiyar, "Fabrication of Cellulose Nanocrystals from Agricultural Compost," *Compost Sci. Util.*, vol. 23, no. 2, pp. 104–116, 2015.
- [24] S. Elazzouzi-Hafraoui, Y. Nishiyama, J. L. Putaux, L. Heux, F. Dubreuil, and C. Rochas, "The shape and size distribution of crystalline nanoparticles prepared by acid hydrolysis of native cellulose," *Biomacromolecules*, vol. 9, no. 1, pp. 57–65, 2008.
- [25] P. Lu and Y.-L. Hsieh, "Preparation and characterization of cellulose nanocrystals from rice straw," *Carbohydr. Polym.*, vol. 87, no. 1, pp. 564–573, 2012.
- [26] S. Maiti *et al.*, "Preparation and characterization of nano-cellulose with new shape from different precursor," *Carbohydr. Polym.*, vol. 98, no. 1, pp. 562–567, 2013.
- [27] M. Saric-Coric, K. H. Khayat, and A. Tagnit-Hamou, "Performance characteristics of cement grouts made with various combinations of high-range water reducer and cellulose-based viscosity modifier," *Cem. Concr. Res.*, vol. 33, no. 12, pp. 1999–2008, 2003.
- [28] O. A. Hisseine, N. Basic, A. F. Omran, and A. Tagnit-Hamou, "Feasibility of using cellulose filaments as a viscosity modifying agent in self-consolidating concrete," *Cem. Concr. Compos.*, vol. 94, no. September, pp. 327–340, 2018.
- [29] X. Sun, Q. Wu, J. Zhang, Y. Qing, Y. Wu, and S. Lee, "Rheology, curing temperature and mechanical performance of oil well cement: Combined effect of cellulose nanofibers and graphene nano-platelets," *Mater. Des.*, vol. 114, pp. 92–101, 2016.
- [30] A. Govin, M. C. Bartholin, B. Biasotti, M. Giudici, V. Langella, and P. Grosseau, "Modification of water retention and rheological properties of fresh state cement-based mortars by guar gum derivatives," *Constr. Build. Mater.*, vol. 122, pp. 772–780, 2016.
- [31] A. Kamoun, A. Jelidi, and M. Cheebouni, "Evaluation of the performance of sulfonated esparto grass lignin as a plasticizer–water reducer for cement," *Cem. Concr. Res.*, vol. 33, pp. 995–1003, 2003.
- [32] C. Ma, Y. Bu, and B. Chen, "Preparation and performance of a lignosulfonate-AMPS-itaconic acid graft copolymer as retarder for modified phosphoaluminate cement," *Constr. Build. Mater.*, vol. 60, pp. 25–32, 2014.
- [33] T. Fu, F. Montes, P. Suraneni, J. Youngblood, and J. Weiss, "The Influence of Cellulose Nanocrystals on the Hydration and Flexural Strength of Portland Cement Pastes," *Polymers (Basel)*, vol. 9, no. 9, p. 424, 2017.

- [34] R. Moreno, "Colloidal processing of ceramics and composites," *Adv. Appl. Ceram.*, vol. 111, no. 5, pp. 246–253, 2012.
- [35] H. Dong, J. F. Snyder, K. S. Williams, and J. W. Andzelm, "Cation-induced hydrogels of cellulose nanofibrils with tunable moduli," *Biomacromolecules*, vol. 14, no. 9, pp. 3338–3345, 2013.
- [36] W. Kurdowski, *Cement and concrete chemistry*. 2014.
- [37] J. Thomas and H. Jennings, "Informational Web Site on the Science of Cement (TEA-21 Year 8 Final Report)," 2008. [Online]. Available: [http://iti.northwestern.edu/cement/monograph/monograph5\\_1.html](http://iti.northwestern.edu/cement/monograph/monograph5_1.html).
- [38] M. Bishop and A. R. Barron, "Cement hydration inhibition with sucrose, tartaric acid, and lignosulfonate: Analytical and spectroscopic study," *Ind. Eng. Chem. Res.*, vol. 45, no. 21, pp. 7042–7049, 2006.
- [39] G. H. Kirby and J. a. Lewis, "Comb Polymer Architecture Effects on the Rheological Property Evolution of Concentrated Cement Suspensions," *J. Am. Ceram. Soc.*, vol. 87, no. 9, pp. 1643–1652, 2004.
- [40] N. L. Thomas and J. D. Birchall, "The retarding action of sugars on cement hydration," *Cem. Concr. Res.*, vol. 13, no. 6, pp. 830–842, 1983.
- [41] L. Zhang, L. J. J. Catalan, R. J. Balec, A. C. Larsen, H. H. Esmaili, and S. D. Kinrade, "Effects of saccharide set retarders on the hydration of ordinary portland cement and pure tricalcium silicate," *J. Am. Ceram. Soc.*, vol. 93, no. 1, pp. 279–287, 2010.
- [42] D. Bülischen and J. Plank, "Water retention capacity and working mechanism of methyl hydroxypropyl cellulose (MHPC) in gypsum plaster - Which impact has sulfate?," *Cem. Concr. Res.*, vol. 46, pp. 66–72, 2013.
- [43] T. Poinot, A. Govin, and P. Grosseau, "Importance of coil-overlapping for the effectiveness of hydroxypropylguars as water retention agent in cement-based mortars," *Cem. Concr. Res.*, vol. 56, pp. 61–68, 2014.
- [44] S. Guo, Y. Lu, Y. Bu, and B. Li, "Effect of carboxylic group on the compatibility with retarder and the retarding side effect of the fluid loss control additive used in oil well cement," *R. Soc. Open Sci.*, vol. 5, no. 9, 2018.

- [45] O. Chaudhari, J. J. Biernacki, and S. Northrup, "Effect of carboxylic and hydroxycarboxylic acids on cement hydration: experimental and molecular modeling study," *J. Mater. Sci.*, vol. 52, no. 24, pp. 13719–13735, 2017.
- [46] T. Sugama, "Citric acid as a set retarder for calcium aluminate phosphate cements," *Adv. Cem. Res.*, vol. 18, no. 2, pp. 47–57, 2006.
- [47] S. Li *et al.*, "Preparation of Concrete Water Reducer via Fractionation and Modification of Lignin Extracted from Pine Wood by Formic Acid," *ACS Sustain. Chem. Eng.*, vol. 5, no. 5, pp. 4214–4222, 2017.
- [48] R. A. Chowdhury, Md. Nuruddin, C. Clarkson, F. Montes, J. Howarter, and P. Youngblood, "Cellulose Nanocrystal ( CNC ) Coatings with Controlled Anisotropy as High-Performance Gas Barrier Films," *ACS Appl. Mater. Interfaces*, vol. 11, no. 1, pp. 1376–1383, 2019.
- [49] K. Nelson and T. Retsina, "Innovative nanocellulose process breaks the cost barrier," *TAPPI J.*, vol. 13, no. 5, pp. 19–23, 2014.
- [50] M. S. Reid, M. Villalobos, and E. D. Cranston, "Benchmarking Cellulose Nanocrystals: From the Laboratory to Industrial Production," *Langmuir*, vol. 33, no. 7, pp. 1583–1598, 2017.
- [51] C. F. Ferraris, M. Geiker, N. S. Martys, and N. Muzzatti, "Parallel-plate Rheometer Calibration Using Oil and Computer Simulation," *J. Adv. Concr. Technol.*, vol. 5, no. 3, pp. 363–371, 2007.
- [52] C. F. Ferraris, P. E. Stutzman, W. F. Guthrie, and J. Winpigler, "Certification of SRM 2492 : Bingham Paste Mixture for Rheological Measurements," *Spec. Publ. 260-174*, 2012.
- [53] A. Yahia and K. H. Khayat, "Analytical models for estimating yield stress of high-performance pseudoplastic grout," *Cem. Concr. Res.*, vol. 31, no. 5, pp. 731–738, 2001.
- [54] G. Kirby, J. a. Lewis, H. Matsuyama, S. Morissette, and J. F. Young, "Polyelectrolyte effects on the rheological properties of concentrated cement suspensions," *J. Am. Ceram. Soc.*, vol. 83, pp. 1905–1913, 2000.
- [55] Y. Boluk, R. Lahiji, L. Zhao, and M. T. McDermott, "Suspension viscosities and shape parameter of cellulose nanocrystals (CNC)," *Colloids Surfaces A Physicochem. Eng. Asp.*, vol. 377, no. 1–3, pp. 297–303, 2011.

- [56] P. F. G. Banfill, "Rheology of Fresh Cement and Concrete," *Rheol. Rev.*, vol. 2006, pp. 61–130, 2006.
- [57] N. S. Msinjili, W. Schmidt, B. Mota, S. Leinitz, H. C. Kühne, and A. Rogge, "The effect of superplasticizers on rheology and early hydration kinetics of rice husk ash-blended cementitious systems," *Constr. Build. Mater.*, vol. 150, pp. 511–519, 2017.
- [58] H. G. Pedersen and L. Bergström, "Forces Measured between Zirconia Surfaces in Poly ( acrylic acid ) Solutions," *J. Am. Ceram. Soc.*, vol. 82, no. 5, pp. 1137–1145, 1999.
- [59] R. J. Flatt, I. Schober, E. Raphael, C. Plassard, and E. Lesniewska, "Conformation of adsorbed comb copolymer dispersants," *Langmuir*, vol. 25, no. 2, pp. 845–855, 2009.
- [60] J. Plank and C. Hirsch, "Impact of zeta potential of early cement hydration phases on superplasticizer adsorption," *Cem. Concr. Res.*, vol. 37, no. 4, pp. 537–542, 2007.
- [61] Y. He, X. Zhang, and R. D. Hooton, "Effects of organosilane-modified polycarboxylate superplasticizer on the fluidity and hydration properties of cement paste," *Constr. Build. Mater.*, vol. 132, pp. 112–123, 2017.
- [62] H. Soualhi, E.-H. Kadri, T.-T. Ngo, A. Bouvet, F. Cussigh, and B. Benabed, "Rheology of ordinary and low-impact environmental concretes," *J. Adhes. Sci. Technol.*, vol. 29, no. 20, pp. 2160–2175, 2015.
- [63] H. Bessaies-Bey, R. Baumann, M. Schmitz, M. Radler, and N. Roussel, "Effect of polyacrylamide on rheology of fresh cement pastes," *Cem. Concr. Res.*, vol. 76, pp. 98–106, 2015.
- [64] S. Srinivasan, S. A. Barbhuiya, D. Charan, and S. P. Pandey, "Characterising cement-superplasticiser interaction using zeta potential measurements," *Constr. Build. Mater.*, vol. 24, no. 12, pp. 2517–2521, 2010.
- [65] L. Ferrari, J. Kaufmann, F. Winnefeld, and J. Plank, "Interaction of cement model systems with superplasticizers investigated by atomic force microscopy, zeta potential, and adsorption measurements," *J. Colloid Interface Sci.*, vol. 347, no. 1, pp. 15–24, 2010.
- [66] W. Prince, M. Espagne, and P. C. Aitcin, "Ettringite formation: A crucial step in cement superplasticizer compatibility," *Cem. Concr. Res.*, vol. 33, no. 5, pp. 635–641, 2003.
- [67] W. Schmidt, H. J. H. Brouwers, H. C. Kühne, and B. Meng, "Interactions of polysaccharide stabilising agents with early cement hydration without and in the presence of superplasticizers," *Constr. Build. Mater.*, vol. 139, pp. 584–593, 2017.

- [68] J. Pourchez, P. Grosseau, and B. Ruot, "Current understanding of cellulose ethers impact on the hydration of C3A and C3A-sulphate systems," *Cem. Concr. Res.*, vol. 39, no. 8, pp. 664–669, 2009.
- [69] C. Brumaud *et al.*, "Cellulose ethers and water retention," *Cem. Concr. Res.*, vol. 53, pp. 176–184, 2013.
- [70] A. Dufresne, *Nanocellulose: From Nature to High Performance Tailored Material*, De Gruyter., vol. 67, no. 3. ProQuest Ebook Central, 2013.
- [71] G. L. Miller, "Use of Dinitrosalicylic Acid Reagent for Determination of Reducing Sugar," *Anal. Chem.*, vol. 31, no. 3, pp. 426–428, 1959.
- [72] W. Z. Hassid and S. Abraham, "[7] Chemical procedures for analysis of polysaccharides," *Methods Enzymol.*, vol. 3, no. C, pp. 34–50, 1957.
- [73] A. A. Albalasmeh, A. A. Berhe, and T. A. Ghezzehei, "A new method for rapid determination of carbohydrate and total carbon concentrations using UV spectrophotometry," *Carbohydr. Polym.*, vol. 97, no. 2, pp. 253–261, 2013.
- [74] A. Ori and S. Shinkai, "Electrochemical Detection of Saccharides by the Redox Cycle of a Chiral Ferrocenylboronic Acid Derivative: a Novel Method for Sugar Sensing Aiichiro," *J. CHEM. SOC., CHEM. COMMUN.*, vol. 645, no. March, pp. 1771–1772, 1995.
- [75] B. H. Bjorndal, C. G. Hellerqvist, B. Lindberg, and S. S. I, "Gas-Liquid Chromatography and Mass Spectrometry in Methylation Analysis of Polysaccharides," *Angew. Chemie*, vol. 9, no. 8, pp. 610–619, 1970.
- [76] U. Roessner, C. Wagner, J. Kopka, R. N. Trethewey, and L. Willmitzer, "Simultaneous analysis of metabolites in potato tuber by gas chromatography - mass spectrometry," *Plant J.*, vol. 23, no. 1, pp. 131–142, 2000.
- [77] Y. H. P. Zhang and L. R. Lynd, "Determination of the number-average degree of polymerization of cellodextrins and cellulose with application to enzymatic hydrolysis," *Biomacromolecules*, vol. 6, no. 3, pp. 1510–1515, 2005.
- [78] J. C. Barreto, G. S. Smith, N. H. P. Strobel, P. A. McQuillin, and T. A. Miller, "Terephthalic acid: A dosimeter for the detection of hydroxyl radicals in vitro," *Life Sci.*, vol. 56, no. 4, pp. 89–96, 1994.
- [79] M. Karas and F. Hillenkamp, "Laser Desorption Ionization of Proteins with Molecular Masses Exceeding 10 000 Daltons," *Anal. Chem.*, vol. 60, no. 20, pp. 2299–2301, 1988.

- [80] G. A. Grant, S. L. Frison, T. Yeung, T. Vasanthan, and P. Sprons, "Comparison of MALDI-TOF Mass Spectrometric to Enzyme Colorimetric Quantification of Glucose from Enzyme-Hydrolyzed Starch," *Agric. Food Chem.*, vol. 51, pp. 6137–3144, 2003.
- [81] N. Elgrishi, K. J. Rountree, B. D. McCarthy, E. S. Rountree, T. T. Eisenhart, and J. L. Dempsey, "A Practical Beginner's Guide to Cyclic Voltammetry," *J. Chem. Educ.*, vol. 95, no. 2, pp. 197–206, 2018.
- [82] K. J. Wiechelman, R. D. Braun, and J. D. Fitzpatrick, "Investigation of the bicinchoninic acid protein assay: Identification of the groups responsible for color formation," *Anal. Biochem.*, vol. 175, no. 1, pp. 231–237, 1988.
- [83] N. E. Maurer, B. Hatta-Sakoda, G. Pascual-Chagman, and L. E. Rodriguez-Saona, "Characterization and authentication of a novel vegetable source of omega-3 fatty acids, sacha inchi (*Plukenetia volubilis* L.) oil," *Food Chem.*, vol. 134, no. 2, pp. 1173–1180, 2012.
- [84] NIST, "NIST Chemistry WebBook," *Chemistry WebBook*, 2017. [Online]. Available: <http://webbook.nist.gov/chemistry/mw-ser/>. [Accessed: 20-Jun-2017].
- [85] Y. Cao *et al.*, "The influence of cellulose nanocrystals on the microstructure of cement paste," *Cem. Concr. Compos.*, vol. 74, pp. 164–173, 2016.
- [86] L. Wadsö, "Isothermal calorimetry for the study of cement hydration," *Rep. TVBM (Intern 7000-rapport) Div. Build. Mater. LTH, Lund Univ.*, vol. 7166, 2001.
- [87] F. Lagier and K. E. Kurtis, "Influence of Portland cement composition on early age reactions with metakaolin," *Cem. Concr. Res.*, vol. 37, no. 10, pp. 1411–1417, 2007.
- [88] A. C. Jupe, A. P. Wilkinson, K. Luke, and G. P. Funkhouser, "Class H cement hydration at 180°C and high pressure in the presence of added silica," *Cem. Concr. Res.*, vol. 38, no. 5, pp. 660–666, 2008.
- [89] A. C. Jupe, A. P. Wilkinson, K. Luke, and G. P. Funkhouser, "Class H oil well cement hydration at elevated temperatures in the presence of retarding agents: An in situ high-energy X-ray diffraction study," *Ind. Eng. Chem. Res.*, vol. 44, no. 15, pp. 5579–5584, 2005.
- [90] S. Nam, A. D. French, B. D. Condon, and M. Concha, "Segal crystallinity index revisited by the simulation of X-ray diffraction patterns of cotton cellulose I $\beta$  and cellulose II," *Carbohydr. Polym.*, vol. 135, pp. 1–9, 2016.

- [91] R. Sobolev, K., Moini, M., Muzenski, S., Pradoto, “Laboratory Study of Optimized Concrete Pavement Mixtures Laboratory Study of Optimized Concrete Pavement Mixtures,” no. August, 2015.
- [92] N. Bouzoubaa, M. H. Shzng, and V. M. Malhotra, “Mechanical properties and durability of concrete made with high-volume fly ash blended cements using a coarse fly ash,” *Cem. Concr. Res.*, vol. 31, pp. 1393–1402, 2001.
- [93] Y. Qian and S. Kawashima, “Distinguishing dynamic and static yield stress of fresh cement mortars through thixotropy,” *Cem. Concr. Compos.*, vol. 86, pp. 288–296, 2018.

## VITA

Francisco was born in the city of Veracruz, Mexico, in October 1984. He is the oldest of 4 brothers. Being a Navy son, during his childhood, he and his family lived in several cities in the country and abroad, which more than a disadvantage, it was a pleasant adventure.

In August 2003, Francisco began his studies of Bachelor's in Physics and Engineering at the Monterrey Institute of Technology (ITESM), where he became interested in renewable energy and energy management. In January 2008, after getting his B.Sc., Francisco started his Master's studies at the Center of Energy Studies of the same university. During his years as a M.Sc. student, he worked with Dr. Oliver Probst and Dr. Armando Llamas designing statistical models for wind prediction, and blade profiles for small wind turbines.

In 2010, Francisco started a job in his hometown in Tenaristamsa as the Energy Consumptions Regional Specialist of the Central America region. It was in August of 2014 that Francisco obtained the CONACyT scholarship for postgraduate studies abroad. That same month, Francisco arrived in West Lafayette and began his doctoral studies under the supervision of Dr. Jeffrey Youngblood.

Francisco served as Senator for the School of Materials Science in the PGSG, where he later served as a part of the executive board as leader of the Careers team. He was also an Academic Success tutor at the Minority Engineering Program during most of his years at Purdue, helping students to succeed in their early studies as engineers.

Francisco is currently a physics professor at Monterrey Tec *campus* Guadalajara.